UNIVERSIDADE ESTADUAL DE CAMPINAS
Faculdade de Engenharia Mecânica

LUCAS DE CAMPOS BASTOS CAROLO

A study on the influence of wall thickness on the surface quality of Ti-6Al-4V alloy manufactured by electron beam powder bed fusion

Estudo da influência da espessura de parede na qualidade superficial da liga Ti-6Al-4V fabricada por fusão em leito de pó por feixe de elétrons

CAMPINAS
2022

LUCAS DE CAMPOS BASTOS CAROLO

A study on the influence of wall thickness on the surface quality of Ti-6Al-4V alloy manufactured by electron beam powder bed fusion

Estudo da influência da espessura de parede na qualidade superficial da liga Ti-6Al-4V fabricada por fusão em leito de pó por feixe de elétrons

Dissertation presented to the School of Mechanical Engineering of the University of Campinas in partial fulfillment of the requirements for the degree of Master in Mechanical Engineering, in the area of Materials and Manufacturing Processes.

Dissertação apresentada à Faculdade de Engenharia Mecânica da Universidade Estadual de Campinas como parte dos requisitos exigidos para obtenção do título de Mestre em Engenharia Mecânica, na área de Materiais e Processos de Fabricação.

Orientador: Prof. Dr. Robert Eduardo Cooper Ordonez

ESTE TRABALHO CORRESPONDE À VERSÃO FINAL DA DISSERTAÇÃO DEFENDIDA PELO ALUNO LUCAS DE CAMPOS BASTOS CAROLO E ORIENTADA PELO PROF. DR. ROBERT EDUARDO COOPER ORDONEZ.

CAMPINAS
2022

Ficha catalográfica
Universidade Estadual de Campinas
Biblioteca da Área de Engenharia e Arquitetura
Rose Meire da Silva - CRB 8/5974

C221e

Carolo, Lucas de Campos Bastos, 1989-
Estudo da influência da espessura de parede na qualidade superficial da liga Ti-6Al-4V fabricada por fusão em leito de pó por feixe de elétrons / Lucas de Campos Bastos Carolo. – Campinas, SP : [s.n.], 2022.

Orientador: Robert Eduardo Cooper Ordonez.
Dissertação (mestrado) – Universidade Estadual de Campinas, Faculdade de Engenharia Mecânica.

1. Impressão tridimensional. 2. Aspereza de superfície. 3. Feixes de elétrons. 4. Ligas de titânio. I. Cooper Ordonez, Robert Eduardo, 1973-. II. Universidade Estadual de Campinas. Faculdade de Engenharia Mecânica. III. Título.

Informações Complementares

Título em outro idioma: A study on the influence of wall thickness on the surface quality of Ti-6Al-4V alloy
manufactured by electron beam powder bed fusion
Palavras-chave em inglês:
Three-dimensional printing
Surface roughness
Electron beam
Titanium alloys
Área de concentração: Materiais e Processos de Fabricação
Titulação: Mestre em Engenharia Mecânica
Banca examinadora:
Robert Eduardo Cooper Ordonez [Orientador]
Éder Sócrates Najar Lopes
Erik Gustavo Del Conte
Data de defesa: 10-11-2022
Programa de Pós-Graduação: Engenharia Mecânica

Identificação e informações acadêmicas do(a) aluno(a)
- ORCID do autor: https://orcid.org/0000-0002-2835-0016
- Currículo Lattes do autor: http://lattes.cnpq.br/4420397456326609

UNIVERSIDADE ESTADUAL DE CAMPINAS
FACULDADE DE ENGENHARIA MECÂNICA

DISSERTAÇÃO DE MESTRADO ACADÊMICO

A study on the influence of wall thickness on the surface quality of Ti-6Al-4V alloy manufactured by electron beam powder bed fusion

Estudo da influência da espessura de parede na qualidade superficial da liga Ti-6Al-4V fabricada por fusão em leito de pó por feixe de elétrons

Autor: Lucas de Campos Bastos Carolo

Orientador: Prof. Dr. Robert Eduardo Cooper Ordonez

A Banca Examinadora composta pelos membros abaixo aprovou esta Dissertação:

Prof. Dr. Robert Eduardo Cooper Ordonez, Presidente
Faculdade de Engenharia Mecânica - UNICAMP

Prof. Dr. Éder Sócrates Najar Lopes
Faculdade de Engenharia Mecânica - UNICAMP

Prof. Dr. Erik Gustavo Del Conte
Centro de Engenharia, Modelagem e Ciências Sociais Aplicadas - UFABC

A Ata de Defesa com as respectivas assinaturas dos membros encontra-se no SIGA/Sistema de Fluxo de Dissertação/Tese e na Secretaria do Programa da Unidade.

Campinas, 10 de novembro de 2022.

Dedicatória

Dedico esse trabalho à minha família, que sempre acreditou no meu potencial e nunca mediu esforços para minha educação e desenvolvimento pessoal.

À minha esposa, pelo amor, carinho, conselhos e companheirismo ao longo dos anos.

E a todos os bravos cientistas e profissionais da academia brasileira que persistem nesse caminho apesar das crescentes dificuldades em desenvolver pesquisa e ensino no país.

Agradecimentos

Gostaria de agradecer ao Centro de Tecnologia da Informação (CTI) Renato Archer do Ministério da Ciência, Tecnologia e Inovações pela infraestrutura e suporte a essa pesquisa através da fabricação dos corpos-de-prova.

Gostaria também de agradecer aos colegas do CTI Renato Archer: Jorge Vicente Lopes da Silva, Marcelo Fernandes de Oliveira, e Paulo Inforçatti Neto pela disponibilidade e auxílio no desenvolvimento experimental deste trabalho.

Agradeço também à Faculdade de Engenharia Mecânica da UNICAMP, em especial ao Departamento de Engenharia de Manufatura e Materiais, sendo seus laboratórios fundamentais para essa pesquisa.

Ao meu orientador, Robert Eduardo Cooper, pela parceira, pelos aprendizados e pelo irrestrito suporte ao desenvolvimento desse trabalho de mestrado.

À minha esposa Renata, pelo apoio incondicional e por ter estado presente ao meu lado (literalmente) no decorrer destes últimos anos em que este trabalho foi desenvolvido.

This study was financed in part by the Coordenação de Aperfeiçoamento de Pessoal de Nível Superior – Brasil (CAPES) – Finance Code 001

O presente trabalho foi realizado com apoio da Coordenação de Aperfeiçoamento de Pessoal de Nível Superior – Brasil (CAPES) – Código de Financiamento 001.

Resumo

O processo de manufatura aditiva por fusão em leito de pó com feixe de elétrons tem demonstrado enorme potencial para aplicações na indústria aeroespacial e médica, especialmente com a liga Ti-6Al-4V. No entanto, as peças fabricadas por esse inovador processo apresentam superfícies com acabamento considerado grosseiro em comparação com tecnologias de fabricação mais tradicionais como a usinagem. O estudo da qualidade superficial é de grande importância considerando seus efeitos positivos e negativos na funcionalidade e durabilidade de peças mecânicas. A fusão em leito de pó por feixe de elétrons é um processo com grande variabilidade devido aos complexos fenômenos físicos que os materiais são submetidos durante o processamento, e por isso o estudo de variáveis de processo é fundamental para a um maior entendimento e possível melhoria de qualidade do processo. Este trabalho contribui para o estudo do processo em questão ao explorar o tema da qualidade superficial e estabelecer a relação entre a variação de espessura de parede e a rugosidade superficial na liga Ti-6Al-4V.

Palavras-Chave: Manufatura aditiva, Fusão em leito de pó por feixe de elétrons, Rugosidade superficial, Espessura de parede

Abstract

The additive manufacturing process of electron beam powder bed fusion has shown great potential for applications in the aerospace and medical industries, especially with Ti-6Al-4V. However, parts manufactured by this innovative process display surfaces with a rough finish compared to more traditional manufacturing technologies such as machining. The study of surface quality is of great importance considering its positive and negative effects on the functionality and durability of mechanical parts. Electron beam powder bed fusion is a process with great variability due to the complex physical phenomena that the materials undergo during processing, and therefore the study of process variables is fundamental for a better understanding and for improving the process altogether. This work contributes to the study of the process in question by exploring the theme of surface quality and establishing the relationship between build thickness and surface roughness for the Ti-6Al-4V alloy.

Keywords: Additive manufacturing, Electron beam powder bed fusion, Surface roughness, Build thickness

Sumário

1 INTRODUÇÃO

1.1 Contextualização e motivação

Processos de manufatura aditiva (MA) são aqueles cuja fabricação de peças e objetos é feita através da adição de material, em contraste com processos subtrativos (como a usinagem) e conformativos (como forjamento e fundição). A manufatura aditiva é realizada a partir de modelos digitais tridimensionais obtidos através de softwares CAD (*computer-aided manufacturing*) ou por tecnologias de digitalização 3D, sendo preparados para fabricação por softwares de funcionalidade análoga a CAM (*computer-aided manufacturing*) (GIBSON; ROSEN; STUCKER, 2015). Atualmente, são diversas as tecnologias de manufatura aditiva definidas pela norma ISO/ASTM 52900, sendo que todas elas compartilham de vantagens significativas com relação aos processos fabricação considerados mais tradicionais. O fato de a manufatura aditiva ser um processo de natureza digital permite uma maior automação da manufatura, e a não necessidade de ferramental específico como moldes de fundição e fixações para usinagem tornam esse processo flexível o suficiente para permitir fabricação de baixo volume mantendo-se o valor unitário (MOLITCH-HOU, 2018). Isso faz com que processos de manufatura aditiva viabilizem a customização em massa, onde produtos podem ser customizados individualmente dentro sistemas de fabricação de larga escala, como é o caso de aparelhos auditivos intra-auriculares com MA (REEVES; TUCK; HAGUE, 2011). A natureza digital dessas tecnologias também permite uma maior descentralização da manufatura, o que geraria grande impacto nas cadeias logísticas globais (BEN-NER; SIEMSEN, 2017). A manufatura aditiva expande as possibilidades em estratégias de economia circular, principalmente no desenvolvimento de processos que prolongam a vida útil de produtos através de reparos ou *upgrades* (SAUERWEIN *et al.*, 2019). Por fim, a manufatura aditiva possibilita a fabricação de peças com geometrias complexas, que em muitos casos não seriam viáveis ou até possíveis de serem produzidas por outros processos de fabricação, além da liberdade de projeto oferecida que permite a redução de componentes em produtos (DIEGEL; NORDIN; DAMIEN, 2019).

Embora seja uma categoria de processos relativamente novos, tecnologias de manufatura aditiva já se mostraram competitivas no âmbito industrial. Um exemplo recente de como a manufatura aditiva foi integrada a processos de larga-escala vem da General Motors, que devido a uma alteração de projeto de última hora, recorreu ao processo de manufatura aditiva Multi Jet Fusion da HP para a fabricação de cerca de 60.000 componentes poliméricos para o lançamento do veículo Chevrolet Tahoe modelo 2022 (WAKEFIELD, 2022). No caso de aplicações com metais, alguns processos de manufatura aditiva têm se destacado nesta última década, como é o caso da fusão em leito de pó para aplicações no setor aeroespacial. Um caso notável é o da Avio Aero, empresa italiana que utiliza do processo de fusão em leito de pó por feixe de elétrons (EB-PBF) para fabricação de lâminas de turbinas para o motor a jato GE9X utilizado em aeronaves Boeings modelo 777X (GE ADDITIVE, 2022). Esse processo de manufatura aditiva permite que tais peças sejam fabricadas em TiAl, sendo que antes sua fabricação era viável apenas em Inconel 718, uma liga duas vezes mais pesada. A Avio Aero conta com cerca de 62 equipamentos de EB-PBF e está ampliando sua produção para 60.000 peças por ano. Outra aplicação em que fusão em leito de pó com ligas de titânio se destaca é no setor médico. Mesmo com custos mais elevados em comparação com processos tradicionais, seu uso é justificado dada a capacidade de personalização e complexidade geométrica oferecida pela manufatura aditiva, que podem facilitar procedimentos cirúrgicos e acelerar a recuperação de pacientes, aumentando o conforto do paciente e reduzindo cargas em sistemas de saúde privado e públicos (VANMEENSEL *et al.*, 2018).

Mesmo se provando um processo adequado para aplicações industriais em escala, ainda há diversas barreiras que impedem o uso de processos manufatura aditiva de forma mais abrangente. Segundo relatório da Hubs em 2021, cerca de 1.500 profissionais que atuam com manufatura aditiva apontaram o elevado custo de processo e baixa qualidade de peças como as maiores barreiras para uma maior implementação de tecnologias de manufatura aditiva (Figura 1). Esse também é o caso de processos de fusão em leito de pó metálico, que além das questões de custo de equipamento e matéria-prima, ainda apresentam muitos os problemas de confiabilidade, reprodutibilidade e controle de qualidade de peças, sendo ainda mais desfavorável em casos de aplicações em setores aeroespacial e médico, onde o controle da qualidade é mais rígido (BAE; DIGGS; RAMACHANDRAN, 2018).

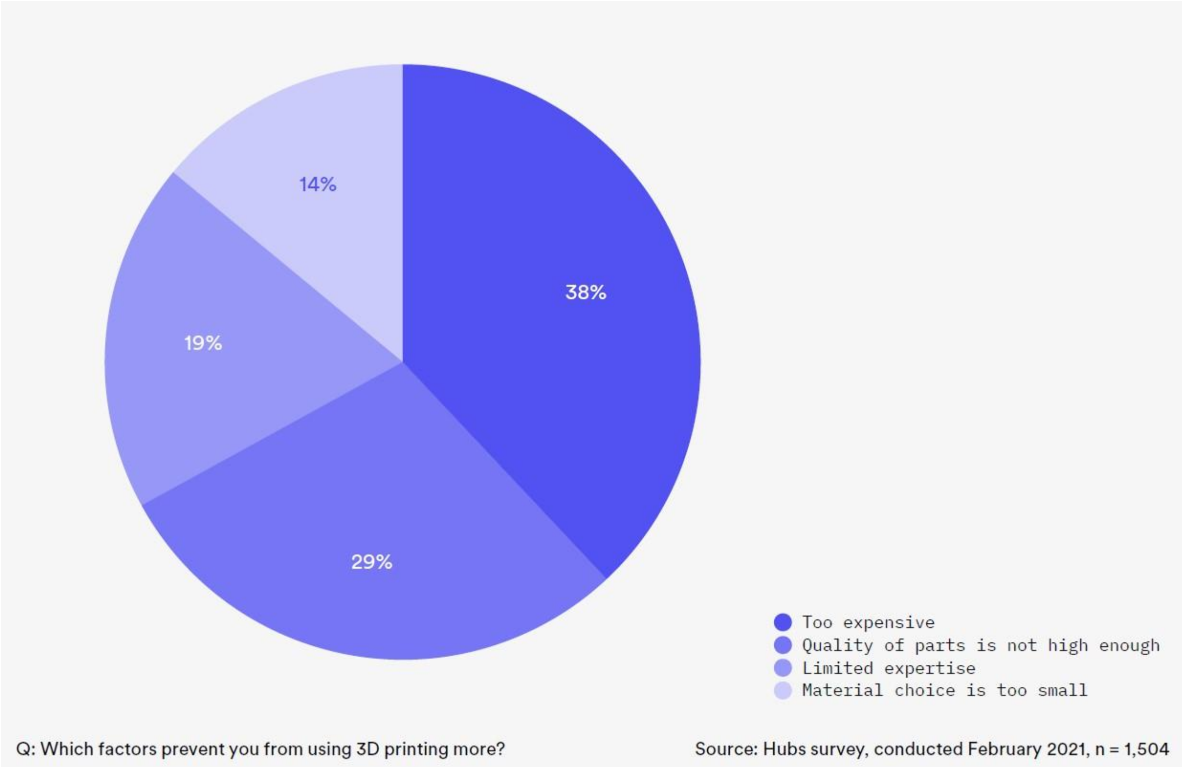

Figura 1. Fatores que impedem o uso mais abrangente de tecnologias de manufatura aditiva segundo pesquisa da Hubs em 2021 (HUBS, 2021).

Isso é ainda pior no caso do processo com feixe de elétrons, que mesmo sendo mais eficiente no processamento de ligas de titânio e ofereça maior produtividade, produz peças com acabamentos superficiais notadamente mais grosseiros do que outros processos que utilizam lasers como fonte de energia (JARDINI *et al.*, 2017). Embora superfícies com níveis de rugosidade superficial elevados segundo padrões da indústria sejam benéficos em alguns casos, elas costumam ser indesejáveis para a maioria das aplicações dado seus efeitos negativos no desagaste e durabilidade de peças. Quando possível de ser realizado, o pós-processamento de peças para acabamento superficial se mostra eficiente no controle da rugosidade, embora adicione ainda mais custos a fabricação, sobretudo considerando processos alternativos de acabamento que devem ser utilizados no caso de peças com geometrias complexas (BAGHERIFARD; GUAGLIANO, 2021). No mais, processos de fusão em leito de pó executam um processamento de material de natureza complexa, introduzindo enorme variabilidade no processo como um todo. Metodologias para a adoção desses processos para fabricação de produtos de uso final envolvem extensa pesquisa para validação e otimização de processo, sendo geralmente baseadas em técnicas de tentativa-e-erro (BAE;

DIGGS; RAMACHANDRAN, 2018; MOLITCH-HOU, 2018), o que eleva ainda mais investimento inicial e a barreira de entrada.

Com isso, o estudo da influência de variáveis de processo e outros aspectos da fabricação na rugosidade superficial em processos de fusão em leito de pó por feixe de elétrons se mostra de grande importância, seja para a avaliação de metodologias para controle dos níveis de rugosidade ou para aumentar a compreensão sobre o processo como um todo, sendo esta última fundamental para o aumento da qualidade e confiabilidade nesses processos (SAMES *et al.*, 2006). O estabelecimento dos efeitos de variáveis de processo na rugosidade também é de grande valor para o desenvolvimento de novas pesquisa área, já que suas influências podem ser consideradas durante o planejamento experimental de novos estudos e evitando assim interferências de fatores externos àqueles investigados. Existe hoje considerável literatura sobre as relações entre variáveis de processo e rugosidade superficial em processos EB-PBF, sobretudo com a liga Ti-6Al-4V visto sua relevância nas aplicações com esse processo. Embora não seja considerada estritamente uma variável de processo, a geometria de peças se mostra relevante no desenvolvimento microestrutural e nas propriedades mecânicas de peças de Ti-6Al-4V por fusão em leito de pó por feixe de elétrons. Entretanto, a literatura sobre a relação entre aspectos geométricos e o acabamento superficial ainda é muito limitada, e embora haja evidencias que a variação na espessura de parede seja fonte de variabilidade na rugosidade superficial de Ti-6Al-4V, não existe nenhuma relação estabelecida de forma concreta na literatura.

1.2 **Objetivos**

1.2.1 **Objetivo geral**

Este trabalho tem como objetivo geral verificar a influência da variação de espessura de parede na qualidade superficial da liga Ti-6Al-4V no processo de fusão em leito de pó por feixe de elétrons uma vez que foi verificada uma lacuna de pesquisa ao explorar o tema.

1.2.2 **Objetivos específicos**

Para atingir o objetivo geral deste trabalho, foram delimitados os seguintes objetivos específicos:

i. Realizar uma análise bibliométrica para validar a motivação desse estudo.
ii. Efetuar uma revisão sistemática da literatura para identificar as variáveis de processo a serem consideradas no estudo.
iii. Estabelecer potenciais efeitos da espessura de parede na qualidade de superfícies fabricadas em diferentes orientações por fusão em leito de pó por feixe de elétrons em Ti-6Al-4V.

1.3 **Procedimentos metodológicos**

Segundo as classificações de tipos de pesquisa de GIL (2017), este trabalho se categoriza como uma pesquisa de caráter descritivo, onde se procura estabelecer relações entre variáveis através da utilização de técnicas padronizadas de coleta de dados. Para se cumprir os objetivos específicos do trabalho, foram utilizados diferentes procedimentos técnicos, entre eles a análise bibliométrica, a revisão sistemática da literatura, e a pesquisa experimental. Os métodos e procedimento empregados estão resumidos na Figura 2.

A análise bibliométrica é uma técnica de pesquisa de caráter quantitativo que avalia o quadro de produção acadêmica através de dados indexados em bases de conhecimento. Essa técnica pode ser utilizada para validação ou confirmação no desenvolvimento de estudos ou para melhor direcionar e hierarquizar a alocação de recursos em projetos de pesquisa. No caso deste trabalho, a análise bibliométrica foi utilizada para validar a motivação do estudo, verificando quantitativamente a relevância do estudo da liga Ti-6Al-4V e da rugosidade superficial em processos de fusão em leito de pó por feixe de elétrons. Por outro lado, a revisão sistemática de literatura, de caráter qualitativo, foi utilizada para maior compreensão do processo de fabricação em questão, das dificuldades e melhores práticas na medição e caracterização de superfícies de peças fabricadas por dito processo, e para identificar as variáveis do processo que afetam a rugosidade superficial da liga Ti-6Al-4V. Os resultados obtidos nesta etapa foram essenciais tanto para o planejamento experimental como para a interpretação dos resultados obtidos nessa última etapa. Finalmente, a pesquisa experimental foi empregada para o avaliar os efeitos da espessura de parede na rugosidade superficial da liga em questão, sendo a coleta e processamento de dados executado estritamente conforme normas técnicas ISO, ABNT e ASTM.

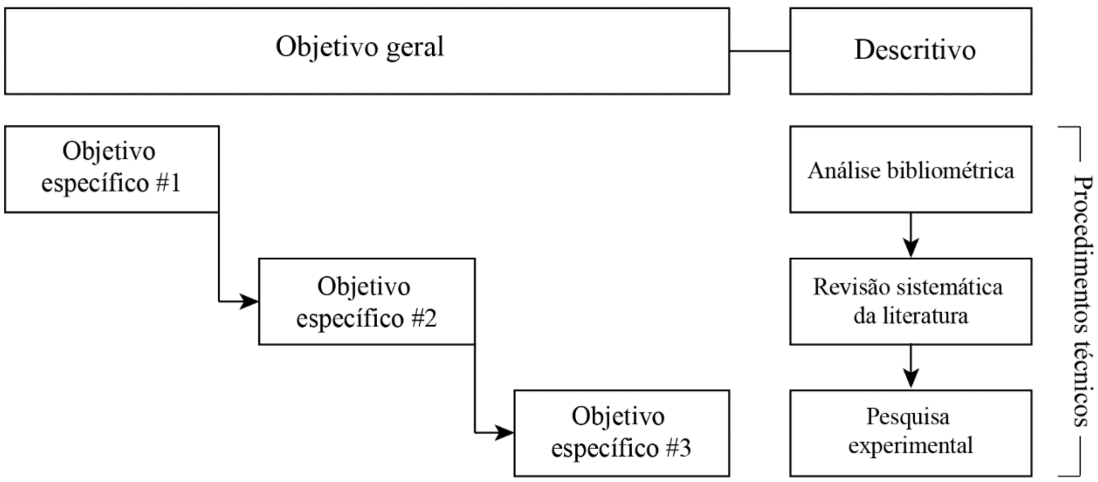

Figura 2. Diagrama dos métodos e procedimentos técnicos utilizados em cada etapa da pesquisa.

1.4 **Limitações do trabalho**

Na etapa de pesquisa experimental, foi utilizado um equipamento táctil (perfilômetro) para medição das superfícies, e isso gerou algumas limitações neste trabalho.

A medição de superfícies com esse tipo de equipamento requer peças com formas relativamente triviais e dimensões pré-estabelecidas conforme a qualidade superficial esperada segundo norma ABNT/ISO 4288. Com isso, foi necessário que a geometria dos corpos-de-prova desenvolvidos para esse experimento fosse simples, contrastando com uma das grandes vantagens de processos de manufatura aditiva: a liberdade geométrica. Entretanto, mesmo com corpos-de-prova com geometrias simples, este trabalho se mantém relevante visto que a literatura carecia de quaisquer estudos que estabelecessem de forma concreta a relação entre as variáveis estudadas. Sendo assim, este trabalho deve servir de base para outras pesquisas que avaliem superfícies curvilíneas ou com geometrias complexas. No mais, alguns casos de aplicação de manufatura aditiva de metais podem teoricamente se beneficiar deste estudo, como no caso de fabricação de peças com aletas retas, cuja geometria pode se assemelhar com as dos corpos-de-prova deste estudo e onde rugosidade superficial possui efeitos relevantes em fenômenos de transferência de calor.

Outra limitação imposta pelo tipo de equipamento utilizado é a sua capacidade de avaliação de superfícies. Equipamentos de medição de superfície tácteis possuem uma menor sensibilidade a pequenos detalhes topológicos quando comparados com equipamentos com tecnologias sem contato. Equipamentos como o perfilômetro utilizado neste trabalho também são capazes de registrar apenas perfis de superfície em linha reta. Embora a medição de rugosidade de perfil ainda seja o padrão na indústria metalmecânica, eles são considerados por alguns autores insuficientes para avaliação das superfícies geradas por processos de fusão em leito de pó metálico. Todavia, a medição de superfícies com equipamentos tácteis e parâmetros de rugosidade de perfil continuam sendo as mais frequentes em estudos com ligas metálicas por fusão em leito de pó, como será descrito neste trabalho.

1.5 **Organização do trabalho**

Este texto foi estruturado no formato alternativo de dissertação conforme estabelecido pela Comissão Central de Pós-Graduação (CCPG) da UNICAMP no parecer CCPG Nº 001/2019. O texto está dividido em quatro capítulos:

- No Capítulo 1 são dados o contexto e a motivação do trabalho, assim como os objetivos, os métodos de pesquisa empregados e as limitações do trabalho.
- No Capítulo 2 são apresentados três artigos que compõem a pesquisa deste trabalho, sendo dois deles já publicados e um submetido para revista internacional.
- No Capítulo 3 é realizada uma discussão visando uma análise dos resultados dos artigos como um todo.
- No Capítulo 4 são apresentadas as conclusões gerais deste trabalho, além de trazer recomendações para pesquisas futuras.

- O Anexo A traz informações a respeito da reutilização dos artigos publicados em trabalho acadêmico conforme estabelecido no parecer CCPG Nº 001/2019 da Comissão Central de Pós-Graduação (CCPG) da UNICAMP.

2 ARTIGOS DESENVOLVIDOS

O corpo deste trabalho é composto por três artigos científicos que foram concebidos durante o desenvolvimento dessa pesquisa. O primeiro deles foi publicado no I Congresso Brasileiro de Manufatura Aditiva (ISBN 978-65-86861-62-4) em novembro de 2020 e traz uma visão geral da pesquisa acadêmica em processos de EB-PBF e defeitos de qualidade associados. O segundo artigo, publicado na revista *Additive Manufacturing* (ISSN 2214-8604) em novembro de 2022, faz uma profunda revisão da literatura a respeito da rugosidade superficial da liga Ti-6Al-4V processada por fusão em leito de pó por feixe de elétrons. Além dos mecanismos por traz da geração de rugosidade, foram também revisadas as técnicas de medição e caracterização de superfícies, os processos de acabamento superficial, e as variáveis de processos que foram verificadas afetar a rugosidade final de peças. O terceiro artigo, submetido para a mesma revista *Additive Manufacturing* em outubro de 2022, reporta da pesquisa experimental realizada para estabelecer a relação entre a variação de espessura de parede e rugosidade superficial em corpos-de-prova de Ti-6Al-4V. Todos os artigos estão na língua inglesa segundo requisitos do congresso e da revista em questão.

This is the accepted manuscript of the article published in the proceedings of Congresso Brasileiro de Manufatura Aditiva (ISBN 978-65-86861-62-4), 1st Edition, on November 2020, available at: https://eventos.congresse.me/cbmadi/edicoes/247-i-cbmadi---1-edicao/anais

Defects in Electron Beam Melting: a bibliometric analysis

Lucas de Campos Bastos Carolo[a], Robert Eduardo Cooper Ordoñez[b]

[a] University of Campinas, School of Mechanical Engineering, Department of Manufacturing Engineering and Materials - Campinas, São Paulo, Brazil.

[b] University of Campinas, School of Mechanical Engineering, Department of Manufacturing Engineering and Materials - Campinas, São Paulo, Brazil. E-mail. E-mail: recooper@unicamp.br

Abstract

Metal Powder Bed Fusion technologies have been increasingly applied for end-use part production over the last years, with important contributions to the medical and aerospace sectors. Despite the rapid and constant improvement, additively manufactured parts still cannot fully comply with the strict quality standards associated with these industries, being a major barrier to the broader adoption of such technologies. This study aimed to identify the trends and main research topics on defects in Electron Beam Melting (EBM) through bibliometric analysis. Bibliometrics is a quantitative statistical analysis of scientific publications that provides an overview of the structured knowledge in a given research topic. The results reveal a worldwide growing interest in the topic over the last ten years, mostly focused on Titanium alloys and defects such as internal porosity and elevated surface roughness. Influences of such defects in the mechanical performance of parts are extensively studied by the scientific community, including post-processing treatments such as Hot Isostatic Pressing (HIP) and surface finishing. The findings obtained by this study should enhance the understanding of how this research field is evolving and the way it is structured worldwide.

Keywords

Additive Manufacturing; Electron Beam Melting; EBM; Bibliometric Analysis; Quality; Defects;

1. Introduction

Until very recently, additive manufacturing (AM) processes were commonly referred to as rapid prototyping (RP), which reflects what is still, to date, the main application of these technologies. However, the last ten years have seen exponential growth in expenditure for end-use parts production by AM processes, as shown in Figure 1 [1]. Layer-by-layer additive methods allow the creation of complex shapes that are usually impossible to achieve through traditional manufacturing techniques while eliminating the need for specific tooling and enabling mass-customization at low costs [2]. AM would also positively impact the environment through localized production and higher efficiency in raw material processing [3].

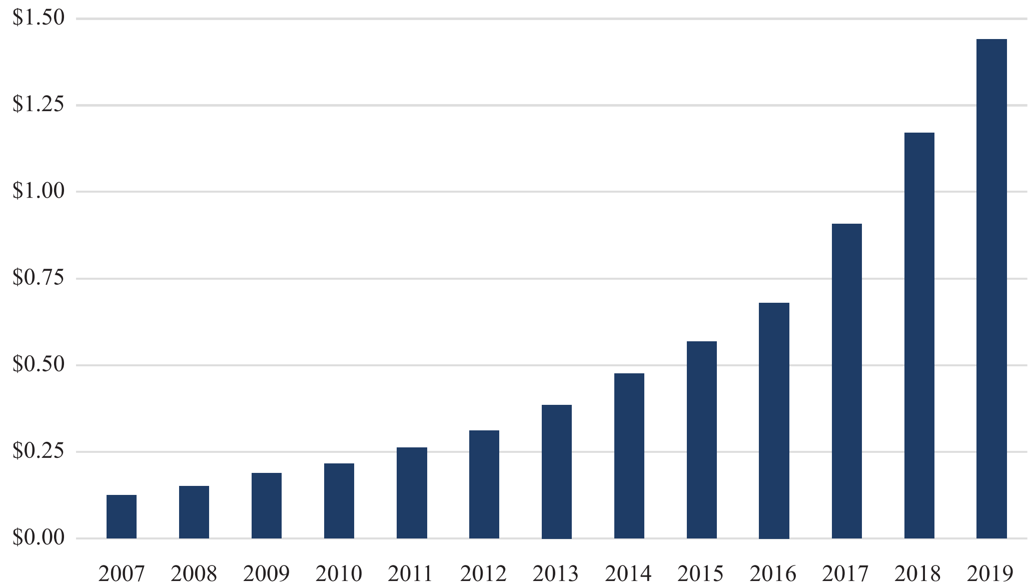

Figure 1. Annual expenditure on final part production by AM worldwide, in billions of dollars (US$). Adapted from [1].

Electron Beam Melting (EBM) is a powder bed fusion (PBF) process defined by ISO/ASTM 52900 as a “process in which thermal energy selectively fuses regions of a powder bed”. EBM differs from other PBF processes by using a high-energy electron beam rather than a laser to melt metallic powder material. EBM is known for processing titanium alloys more efficiently than other PBF processes due to the higher absorption capacity of electron beams in these materials and for the higher scanning speeds provided by its electromagnetic control [4]. The metallic parts produced are free of residual stresses as the manufacturing chamber is kept at high temperatures (650°C to 1000 °C) and, as such, eliminates the need for thermal post-processing. EBM technology is often applied by the aerospace industry, most noticeably for manufacturing high-performance jet engine blades for the new Boeing 777X [5]. The medical area also benefits from the flexibility offered by additive manufacturing techniques, and by the end of 2018, over 100,000 hip cup implants were successfully produced by EBM [6].

Unfortunately, PBF processes are notoriously known for problems of repeatability and reproducibility, partially due to the high complexity associated with these processes and the difficulties that remain in understanding and controlling them [7]. In addition, parts manufactured specifically by EBM display a level of quality that is insufficient for many industrial applications [8]. In truth, Vo et al. [9] attribute poor part quality and repeatability as the most significant barriers to the broader adoption of PBF processes in the industry. Most of the quality issues associated with EBM originate from defects classified by Cooke and Soons [10] into four distinct groups: (1) geometric and dimensional defects, (2) surface defects, (3) microstructure, and (4) mechanical properties. The many potential causes of quality-related defects in EBM are a constant object of study by many authors who aim to identify and analyze the phenomena behind its occurrence. Grasso and Colosimo [11] categorize the sources of errors in metallic PBF processes into three distinct groups, with Sames et al. [12] adding a fourth:

1. Equipment-induced defects, such as those generated by failures in the electron beam scanning system, in the raw material deposition system, optical aberrations due to lack of calibration, disturbances in the manufacturing chamber environment, among others.
2. Process-induced defects, such as the thermal expansion of the material, instabilities in the melt pool, warping, electrostatic repulsion, vaporization of the metallic material, among many others.
3. Defects originated from the 3D digital model, including those generated during the conversion and approximation of CAD files onto triangular meshes surfaces.
4. Powder-induced defects, directly related to the metallic feedstock material quality.

Sames et al. [12] also emphasize the importance of understanding quality-related issues and the mechanisms associated with them as they contribute to a better understanding of the physical phenomena and consequently help to improve the quality and reliability of the process as a whole. This is a crucial milestone for a breakthrough of EBM in the industry as an end-use part manufacturing method. With this in mind, the present study focuses on exploring the research trends on defects associated with EBM using bibliometric tools and indicators. The most cited publications were closely analyzed to identify the main research topics and the lines of studies developed. While there have been review articles on process-related defects in EBM, none has used such an exploratory approach and methodology as of this work.

2. Materials and Methods

Bibliometric analysis is a quantitative research method that evaluates measurable data from academic publications through mathematical and statistical techniques. It relies on large publication databases and provides an overview of a scientific field from which a deeper analysis can be performed. This study was based on data acquired from books, journals, and proceedings indexed on the Web of Science (WoS) database. The data collection was performed at the WoS online search platform and was done iteratively to obtain the most relevant dataset within the target subject area. The search terms that were revealed to be most suitable are displayed in Table 1. These terms were searched in titles, abstracts, and keywords of indexed papers published between 2011 and 2020, with the data collection performed in October 2020.

Table 1. Search terms used for dataset collection at the Web of Science database.

Topic	**Operator**	**Term**
1	-	"*Additive Manufacturing*", "*AM*"
2	*AND*	"*Electron Beam*", "*Electron Beam Melting*", "*Selective Electron Beam Melting*", "*EBM*", "*SEBM*"
3	*AND*	"*Defect*"

The initial dataset of publications was exported and analyzed one by one to verify the compatibility and relevance to the present study. Around 35% of all publications were discarded for being related to other manufacturing processes, such as laser PBF and other electron beam processes (wire feed, welding), as well as EBM publications unrelated to defects altogether. By such, the final dataset was guaranteed to have only specific and relevant data for the subsequential processing and analysis. Most data were processed using Microsoft Excel, with the exception of the keyword analysis which was performed by the VOSviewer software. This analysis examines the occurrence of keywords in a database and evaluates their relationships according to their correlation. A keyword co-occurrence network (KCN) is a graphical representation of the most outstanding keywords in a database and how they relate with each other, thus providing meaningful insights into the knowledge patterns of a research area [13]. Both the author's keywords and those generated by the WoS database (Keywords Plus®) were considered for this analysis. Some keywords had to be standardized so that they were counted correctly. For example, "Ti-6Al-4V" and "Ti6Al4V", although spelled differently, have the same meaning and were considered equivalent. The KCN was created with keywords with a minimum occurrence of 7 times. Finally, the 20 most cited publications from the dataset were further studied as they are considered the most valuable and important publications in the area [14].

3. Results

The final dataset comprised 156 research papers published between January 2011 and October 2020. There has been a gradual increase in the number of articles published in the period, as shown in Figure 2. This considerable growth reveals the importance and current relevance this subject has gained over the last years, confirming the premise of this study and its initial motivation. The dataset is mainly composed of research articles published in journals (82%), with the remaining being proceedings papers (13%) and reviews (5%). Table 2 shows the ten journals with the most publications on the topic, accounting for more than half (55%) of all articles and reviews from the dataset. By far, the most studied material in the dataset is Ti-6Al-4V (72%), followed by Inconel 718 (17%) and Ti-48Al-2Cr-2Nb (4%). Other materials include Stainless Steel (316L), Co-Cr-Mo, and other Titanium alloys.

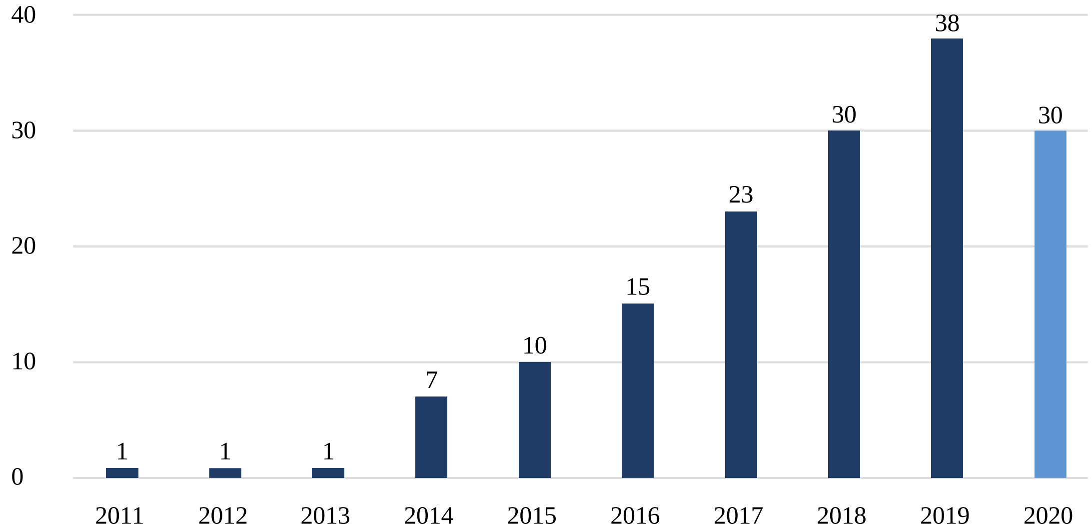

Figure 2. Number of publications per year (from January 2011 through October 2020).

Table 2. Top 10 journals in number of publications on the topic.

Source	**Number of Publications**
Additive Manufacturing	13
International Journal of Fatigue	11
Materials Science and Engineering	10
Materials	9
Materials Characterization	7
Acta Materialia	5
Journal of the Minerals, Metals & Materials Society (JOM)	5
Journal of Alloys and Compounds	5
Journal of Materials Engineering and Performance	5
Journal of Materials Processing Technology	5

The analysis performed by the VOSviewer software showed a total of 26 different keywords with a minimum frequency of 7 occurrences each. The correspondent KCN of this analysis is seen in Figure 3 as a density map, which highlights the most critical regions within the bibliometric study [13]. The map follows a thermal color palette, in which the color intensity assigned to each item refers to the total number of occurrences of that keyword while their positions on the map reveal the strength of the correlations among them. The central cluster with warmer colors is composed of the following keywords: “Microstructure”, “Mechanical Properties”, “Fatigue”, “Surface roughness” and “Ti-6Al-4V”, together with the ones directly related to the search terms such as “Additive manufacturing” and “EBM”. Other keywords with high occurrence include “Porosity”, “Heat treatment”, “Titanium Alloy” and “Laser”.

The 20 most cited publications are responsible for 64% of all the 5021 citations from the 156 publications in the dataset. More than half of these articles are experimental works focused on either (1) characterizing and understanding defect generation in EBM, (2) verifying the influence of defects on mechanical performance, or (3) analyzing the effectiveness of post-processing treatments and mitigation strategies for avoiding defects. The remaining are bibliographic reviews and articles presenting mathematical simulation models of the EBM process concerning defect generation. Out of the 20 most cited publications, the defects analyzed were mostly porosity and elevated surface roughness, sometimes simultaneously and often presenting solutions for mitigation or post-processing.

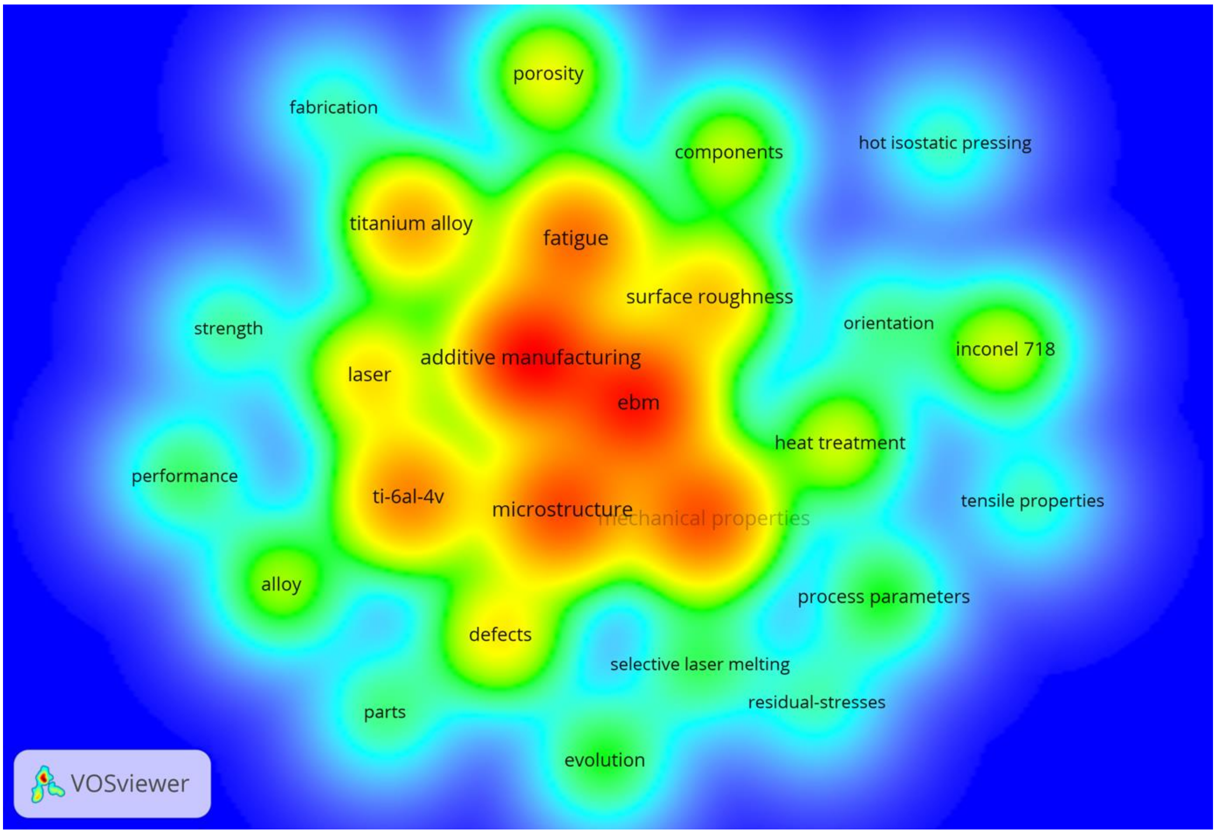

Figure 3. Density keyword co-occurrence network (KCN) based on the dataset collected.

4. Discussion

The growing interest in EBM process defects by the academic community is illustrated by the increasing number of publications covering the topic over the last years (Figure 2). This growth pattern is similar to the annual expenditure on end-part production by AM shown in Figure 1, which is very coherent since current fabrication standards are very strict concerning the overall part's quality.

Moreover, both the KCN (Figure 3) and the analysis of the most cited publications showed great concern with the mechanical performance of as-built parts produced by EBM, specifically those related to fatigue. In fact, the International Journal of Fatigue is the second journal in number of publications within the dataset, with 11 articles. Although mechanical properties are determined mainly by their microstructure, they are also strongly influenced by micro and macroscopic physical defects. Internal porosity and surface roughness are notoriously known for their negative influences on static and dynamic performance [15, 16].

The concern with mechanical properties and fatigue life could be explained partially due to the great interest of both aerospace and medical industries in EBM, where components are frequently subjected to cyclical efforts. This hypothesis is also supported by the materials studied by the publications, in which Ti-6Al-4V is predominant. This alloy is best known for its low density and superb mechanical properties, being developed specifically for aircraft structural applications. Ti-6Al-4V is also widely used for producing medical implants as it presents high biocompatibility and corrosion resistance. The most prominent post-processes used in EBM parts are hot isostatic pressing (HIP) and surface finishing processes such as machining and shot peening. These are often applied for addressing internal porosity and surface roughness, respectively, and both their effectiveness and influences on overall mechanical properties are the main subject of many publications within the dataset. Mitigation strategies such as process parameter optimization are also often proposed, usually verified through experimental methods or computer simulation. Finally, different non-destructive inspection methods like micro XCT are extensively applied and studied by publications within the dataset to access internal integrity of EBM manufactured parts, mostly regarding porosity and crack initiation. Many publications have also proposed *in-situ* monitoring and control systems, where both hardware and software systems are developed.

5. Conclusions

This study has provided an overview of research activities and trends in process defects in EBM via a bibliometric analysis of scientific publications from the last ten years. A total of 156 publications composed the final dataset used for the analysis, which led to the following conclusions:

- Most studied materials in regard to EBM process defects are Ti-6Al-4V (72%), Inconel 718 (17%) and Ti-48Al-2Cr-2Nb (4%).
- Internal porosity and surface roughness are the most common defects addressed by the publications.
- The influence of process defects on mechanical properties is extensively explored, especially for fatigue performance.
- Post-processing techniques such as HIP and surface finishing processes are largely applied for addressing the afore-mentioned defects, and their effects on mechanical properties and microstructure are the focus of numerous publications within the dataset.
- Defect mitigation strategies such as process parameter optimization are widely studied, either through experimental studies or mathematical simulations.
- Micro XCT is the main non-destructive inspection method for checking and measuring internal defects such as porosity. *In-situ* monitoring is also a popular solution proposed to assess the internal integrity of parts during the manufacturing process.

References

[1] WOHLERS, T, et al. Wohlers Report 2020. 2020.

[2] FORD, S; DESPEISSE, M. Additive manufacturing and sustainability: an exploratory study of the advantages and challenges. Journal of Cleaner Production 2016;137:1573–87.

[3] PRIARONE, P. C, et al. Assessment of Cost and Energy Requirements of Electron Beam Melting (EBM) and Machining Processes, 2017, p. 723–35.

[4] ZHANG, L. C. et al. Additive Manufacturing of Titanium Alloys by Electron Beam Melting: A Review. Advanced Engineering Materials 2018;20.

[5] KELLNER, T. The Blade Runners: This Factory Is 3D Printing Turbine Parts For The World's Largest Jet Engine 2018. https://www.ge.com/news/reports/future-manufacturing-take-look-inside-factory-3d-printing-jet-engine-parts (accessed September 16, 2020).

[6] OLSON, P.D. 100,000 Patients Later, the 3D-Printed Hip Is A Decade Old and Going Strong 2018. https://www.ge.com/news/reports/100000-patients-later-3d-printed-hip-decade-old-going-strong (accessed August 16, 2020).

[7] DOWNLING, L. et al. A review of critical repeatability and reproducibility issues in powder bed fusion. Materials and Design 2020;186.

[8] SHARRATT, B.M. Non-Destructive Techniques and Technologies for Qualification of Additive Manufactured Parts and Processes: A Literature Review. 2015.

[9] VO, T.H. et al. Typology of geometrical defects in Electron Beam Melting. Procedia CIRP, vol. 75, Elsevier B.V.; 2018, p. 92–7.

[10] COOKE, A.L; SOONS, J.A. Variability in the Geometric Accuracy of Additively Manufactured Test Parts. National Institute of Standards and Technology 2010:1–12.

[11] GRASSO, M; COLOSIMO, B.M. Process defects and *in situ* monitoring methods in metal powder bed fusion: a review. Measurement Science and Technology 2017;28:044005.

[12] SAMES, W.J. et al. The metallurgy and processing science of metal additive manufacturing. International Materials Reviews 2016;61:315–60.

[13] VAN ECK, N.J.; WALTMAN, L. Software survey: VOSviewer, a computer program for bibliometric mapping. Scientometrics 2010;84:523–38.

[14] OSAREH, F. Bibliometrics, citation analysis and co-citation analysis: A review of literature I. Libri 1996;46:149–58.

[15] GAO, Y.X. et al. The effect of porosity on the fatigue life of cast aluminium-silicon alloys. Fatigue & Fracture of Engineering Materials & Structures 2004;27:559–70.

[16] XIAO, W.L. et al. Effects of surface roughness on the fatigue life of alloy steel. Key Engineering Materials, vol. 525–526, Trans Tech Publications Ltd; 2012, p. 417–20.

This is the accepted manuscript of the article published by Elsevier in Additive Manufacturing Volume 59, Part A, on November 2022, available at:
https://doi.org/10.1016/j.addma.2022.103103

A review on the influence of process variables on the surface roughness of Ti-6Al-4V by electron beam powder bed fusion

Lucas de Campos Bastos Carolo[a], Robert Eduardo Cooper Ordoñez[b]

[a] University of Campinas, School of Mechanical Engineering, Department of Manufacturing Engineering and Materials - Campinas, São Paulo, Brazil.

[b] *Corresponding author*. University of Campinas, School of Mechanical Engineering, Department of Manufacturing Engineering and Materials - Campinas, São Paulo, Brazil. E-mail. E-mail: recooper@unicamp.br

Abstract

Electron beam powder bed fusion (EB-PBF) has been given much attention in recent years for its potential in the aerospace and medical industries, particularly with Ti-6Al-4V. However, these processes produce parts with inherent rough surface finishes, impacting the performance and generating additional challenges and costs with surface post-processing. This review examines the primary mechanisms responsible for surface roughness generation in EB-PBF and the process variables that have been verified to influence the surface quality of Ti-6Al-4V parts. The challenges in surface metrology of metallic PBF parts are also discussed, as are new perspectives and guidelines for future research.

Keywords

Additive manufacturing; electron beam powder bed fusion; surface roughness; process variables; process parameters; process optimization

1. Introduction

The use of additive manufacturing (AM) processes for end-use parts have been steadily growing over the past decade. Powder bed fusion (PBF) processes were one of the first AM processes to be used in industrial activities with polymers and eventually with metals, being employed today by various distinct sectors. These processes utilize an energy source for selectively sintering or fusing successive layers of a fine powder feedstock material. Laser PBF processes (L-PBF) [1] use one or more laser beams as energy sources and are currently the most common AM technology for processing metals. Other energy sources for PBF processes include the electron beam (EB), in which kinetic energy from accelerated electrons is converted to thermal energy upon impact into the powder bed [2]. This particular process is known commercially as Electron Beam Melting, and while detailed explanations of this process can be found elsewhere [3], it is worth highlighting the main distinctions with laser processes. For instance, the electron beam is controlled by electromagnetic lenses instead of the mirror deflecting mechanism of laser systems, allowing faster scanning speeds as there are no moving parts [4]. Parts produced by electron beam powder bed fusion processes (EB-PBF) [1] are also not affected by the adverse effects of the different laser beam incidence angles that are known to affect the final quality of parts [5]. Moreover, electron beams are also more homogenously absorbed by metallic powders than lasers and can reach farther into the material powder bed [6]. However, EB-PBF also differs from laser processes in aspects beyond the energy source. EB-based processes happen in a near-vacuum chamber to avoid the deflection of electrons by air molecules, with a small amount of Helium gas to secure the chemical stability of reactive metals [4]. The lack of a constant inert gas flow as it is required in L-PBF is also beneficial for EB-PBF since the mechanical properties and quality of parts are influenced by the gas inlet's position and flow direction [7]. Another noteworthy difference between EB and laser PBF processes is that the powder bed and build chamber are kept at high temperatures throughout the entire EB-PBF process, producing parts free of residual stresses [8]. The high internal temperatures in EB-PBF are achieved through preheating stages performed at each newly deposited layer, heating the material to around 60% of its melting point to sinter the feedstock powder particles [9]. Besides elevating the temperatures, the powder sintering is required to avoid particle repulsion and create conductivity paths for the incident electrons on the powder bed [10,11]. A sintered powder bed also provides a more solid base for building overhang structures and allows the production of stacked parts for increased productivity, a strategy known as nesting [12].

Most applications involving EB-PBF rely on high-performance alloys such as Inconel 718 and Ti-6Al-4V. The latter offers excellent mechanical performance and high corrosion resistance, being initially developed by the aerospace industry, where the strength-to-weight ratio is of utmost importance [13], while AM's geometric freedom creates opportunities for further mass reductions in aerospace components [14]. The superior corrosion resistance and biocompatibility of Ti-6Al-4V make this alloy also suitable for medical implants. In this case, AM's design freedom was already proven valuable, with Ti-6Al-4V EB-PBF manufactured acetabular cup implants passing the mark of 100,000 implanted patients in 2018 [15]. Ti-6Al-4V is also one the most investigated materials with EB-PBF in academia, being in almost 70% of all papers and publications in the reviewed literature for this study on surface roughness, followed by Inconel 718 (Figure 1).

Though EB-PBF has proven suitable for processing Ti-6Al-4V for high-demand applications, it is not without its challenges. Besides issues related to internal porosity and anisotropy, the surface quality of EB-PBF parts is considered poor compared to other fabrication methods such as machining. The additive layer-stacking method of PBF processes generates significantly different surfaces within the same part. Surfaces strictly parallel to the build platform, like the top and bottom surfaces, are formed by one single layer, whereas the side or lateral surfaces are made by several stacked layers, creating a superficial stepping effect. The processing phenomena experienced by the top and lateral surfaces during manufacturing also contribute to the notably different surface appearance and texture [16,17], as seen in Figure 2. Top surfaces generally display a significantly better surface quality compared to lateral ones. For Ti-6Al-4V parts produced by EB-PBF, the Ra roughness values for top surfaces usually range from 1 to 13 µm [18–20], and its topology is dominated by weld tracks left by the electron beam scanning paths [19,21]. The lateral surfaces, on the other hand, display Ra values that range between 15 to 50 µm [20,22–26], constituting a roughness level comparable to rough manufacturing processes like sand casting, sawing, hot rolling, and forging [27]. The topology of lateral surfaces is characterized by a rippled structure caused by successive layer stacking and the presence of partially melted powder particles attached to them (Figure 2) [28–32].

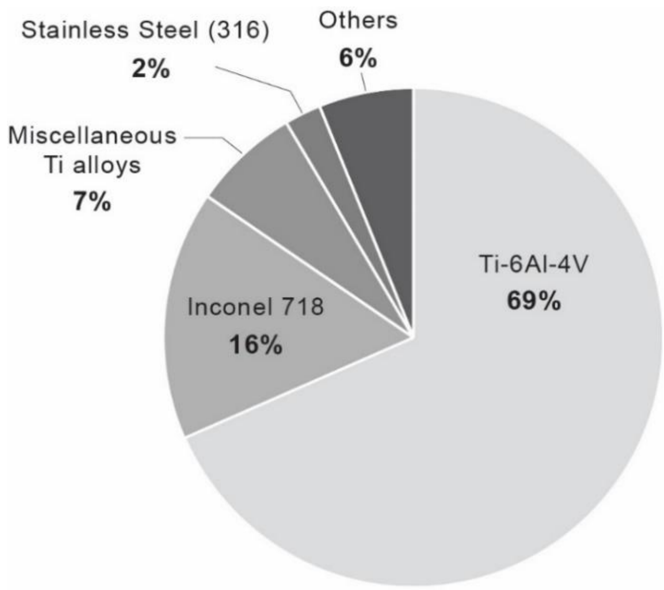

Figure 1. Summary of studied materials for EB-PBF in papers and publications in the reviewed literature.

Surface quality affects the functionality and performance of mechanical components in diverse ways. According to Thomas [33], it influences the static contact of surfaces, being an critical factor in calculating limits and fits, as well as in thermal and electrical contact conductance. The author also emphasizes the impacts of surface finish in tribology, having profound effects on friction, lubrication, and wear, being particularly relevant in automotive components such as engines and transmissions [33]. It also influences the aesthetic perception of products [34], and its optical properties [35]. Leary et al. [36] highlight a few metal PBF applications with "roughness-critical functional requirements," including those that involve dynamic loads, medical implants, and thermofluidics applications.

For EB-PBF processes specifically, the adverse effects of the associated surface roughness in fatigue are very established [37]. EB processes generate distinct surface structures that will be detailed in Section 4, but they act as stress concentration points that stimulate fatigue cracking [38,39]. Fractography analyses show that fatigue cracks in EB-PBF with Ti-6Al-4V start from micro-notches on the surface and then propagate [23,40–42], being directly correlated to its higher surface roughness levels. In fact, surface roughness was verified to be the most critical aspect regarding fatigue performance in EB-PBF, even more impactful than porosity defects [41–44]. Still, proper surface finishing processes have shown promising results in improving the fatigue life of EB-PBF parts. Kahlin et al. [38] showed that machined and polished specimens of Ti-6Al-4V had fatigue limits 75% higher than those in the as-built condition. Vayssette et al. [45] compared the multiaxial high cycle fatigue performance of Ti-6Al-4V specimens by EB-PBF in the as-built condition and with chemical polishing, with the latter showing an improved fatigue limit of around 46%. Though proven beneficial to increasing fatigue performance, both traditional or alternative surface finishing processes can be particularly challenging with PBF parts, as will be detailed in Section 3.

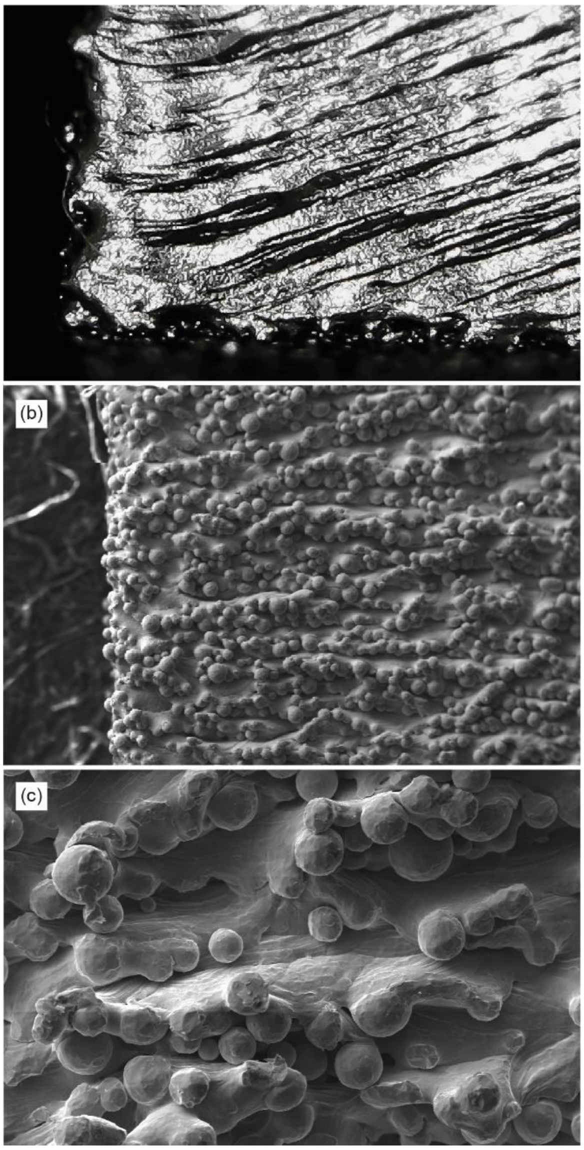

Figure 2. The visual appearance of EB-PBF Ti-6Al-4V (a) top and (b)(c) lateral surfaces obtained via optical (a) and SEM (b)(c) microscopy.

Surface roughness is known to positively influence living cell attachment [46,47], therefore the surface roughness in EB-PBF parts for medical applications such as implants is also proficiently studied. The particular topology of EB-PBF surfaces creates a more extensive contact surface between implant and organism, promoting better adhesion levels according to experiments by Thomsen et al. [48] with Ti-6Al-4V. The same phenomenon was confirmed in later studies [49–51] with the same alloy and process, though the optimal levels of surface roughness for enhanced cell attachment are still debatable. Nevertheless, the roughness levels of as-built EB-PBF with Ti-6Al-4V were found beneficial to blood coagulation processes that favor healing in implants as well [22]. Another positive effect of the roughness levels of EB-PBF in the medical sector was verified by Lindsay et al. [52] for transcutaneous implants. Traditionally machined and EB-PBF Ti-6Al-4V parts were compared in terms of osseointegration and contamination by external agents. The AM specimens in the as-built condition consistently outperformed the machined parts in both the mechanical and microbiological barrier tests [52].

The effects of surface roughness in fluid systems such as heat exchangers or in conformal cooling channels of dies are also worth noting since these are identified as suitable applications for PBF processes [36]. Surface roughness can profoundly affect the performance and service life of these systems, either positively or negatively. The as-built roughness levels of EB-PBF can enhance the convective heat transfer through surfaces [53], though in cooling channels, it can cause severe pressure drops and create difficulties for unprocessed powder removal after manufacturing [54].

The correlation between process variables and the parts' resulting properties is crucial, especially for sensitive manufacturing processes like EB-PBF, in which materials undergo a series of heating cycles and rapid melting [55]. While the influence of process variables on the surface roughness of EB-PBF parts has been investigated, any definitive correlations are challenging to establish primarily due to this process's complexity and novelty. This work aims to explore the literature regarding the influence of process variables on surface roughness of Ti-6Al-4V by EB-PBF to provide insights valuable for new experimental research in related fields and to access the potential of controlling the surface quality through process optimization.

This review starts by discussing the various surface metrology methods utilized for evaluating metal PBF surfaces (Section 2). Section 3 describes some surface finishing processes reported with this alloy and process, while the main mechanisms behind the distinct topology and roughness of EB-PBF surfaces are introduced in Section 4. Section 5 details the process variables known to influence the surface roughness of Ti-6Al-4V specifically, whereas Section 6 mentions other process-related factors contributing to surface roughness in EB-PBF and provides recommendations for future works.

2. Surface metrology of metal PBF parts

Every manufactured surface deviates from its intended ideal, and the geometric divergences affect many functional aspects as already mentioned. Whitehouse [56] characterized the surface deviations according to their causes and wavelength scale:

- Roughness: superficial irregularities associated with the manufacturing process, like tool marks from machining processes and impressions left by grinding or polishing.
- Waviness: superficial irregularities caused by improper manufacturing, including machinery's poor performance or miscalibration, with longer wavelengths than roughness.
- Form error: dimensional and geometrical deviations of greater wavelengths, caused by inaccuracies in machinery's slides or guideways, or by thermal distortion.

Figure 3 illustrates a typical surface profile comparing its roughness and waviness components. Surface profiles have two main domains: the amplitude or height of the profile, and its wavelength [33]. The amplitude and wavelength scale of roughness and waviness differ significantly, and these surface features are usually evaluated independently as they are generated from separate mechanisms and affect the function of parts differently. This study focuses on the roughness component and the microphysical irregularities that characterize the surface texture of EB-PBF. There are two complementary approaches to surface roughness: one is concerned with its influence on functional aspects, while the other utilizes surface measurements to gauge and control manufacturing processes [57]. Since the roughness is highly susceptible to changes in the process, any noticeable variation in roughness parameters can indicate process deviations, making surface metrology a powerful tool for quality control [58].

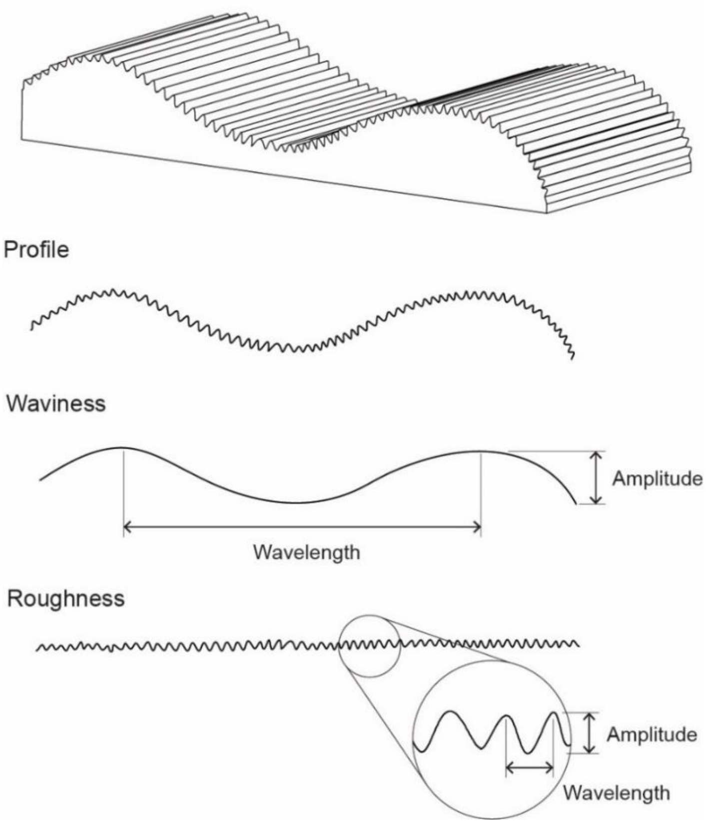

Figure 3. A typical surface profile and its waviness and roughness components.

2.1 Surface roughness measurement

Different surface measurement techniques can extract the topography information from a sampled surface. The instruments involved in surface metrology predominantly consist of tactile devices with a stylus or non-contact instruments based on optical instruments [29]. EB-PBF processes produce naturally rough surfaces for reasons that will be further explored in Section 4, but its inherent surface characteristics, such as sharp protrusions, deep recesses, and undercuts, present several challenges for measurement regardless of the type of instrument [31].

Tactile-based methods with stylus remain the industry's most used surface measurement methods due to their operational simplicity, low-cost equipment, and good repeatability [59,60]. However, contact-based methods can underperform depending on the scale of interest. Figure 4a illustrates a surface profile measurement with a probing stylus. The amount of topographic details registered by the stylus depends on its tip cone's size and shape, sometimes acting as a low-pass filter for small-scale features [60]. There are also concerns when measuring low hardness materials since the stylus can cause irreversible damage to the surfaces. Besides these operational challenges, tactile methods face additional obstacles when measuring EB-PBF surfaces. These methods can usually register only one-dimensional profiles, being intrinsically limited for assessing the heterogeneous and anisotropic surfaces created by metal PBF processes [61]. Nevertheless, contact methods with stylus probing are well-established and highly reproducible, being verified as the most common method used for surface evaluation of metal AM parts [59].

A wide variety of optical-based devices can be utilized for surface metrology through various measurement techniques. Contactless surface measurement excludes the risk of surface damage and has fewer accessibility limitations compared to stylus instruments (Figure 4b). For metallic PBF parts, typical measuring techniques with optical instruments include focus variation microscopy, confocal microscopy, and coherence scanning interferometry [59]. All these methods are used for areal surface evaluation, in which three-dimensional data is acquired from a sampling area instead of a linear profile [62]. For this reason, optical-based methods are seen as a more complete way of assessing the roughness of metallic PBF parts [16,63,64], although not without limitations. According to Leach et al. [61], the abrupt alternation of dark and bright regions of deep recesses and sharp protrusions, plus non-uniform optical properties due to surface oxidization, are among the biggest challenges for optical measurement with PBF. Moreover, every optical system depends on materials' reflective properties, and some contactless methods have been reported to be inadequate for measuring the highly reflective top surfaces of metallic PBF parts [18]. It is also worth noting that optical instruments cannot effectively capture undercut surface features like in tactile methods (Figure 4b).

In such cases, inspection technologies such as x-ray computer tomography (XCT) were reported to capture and measure reentrant and undercut surface features of metallic PBF parts [65,66]. These technologies have been used in elaborate measurement procedures that extract topographic information from XCT data of inspected surfaces [67]. However, XCT usually lacks the appropriate spatial resolutions for capturing the smallest surface details of metallic PBF parts, although increasingly investigated as an alternative surface measurement method [68]. 2D imaging devices such as scanning electron microscope (SEM) are also commonly used for qualitative analysis of metal PBF surfaces as they cannot measure topographic height information directly [58,62].

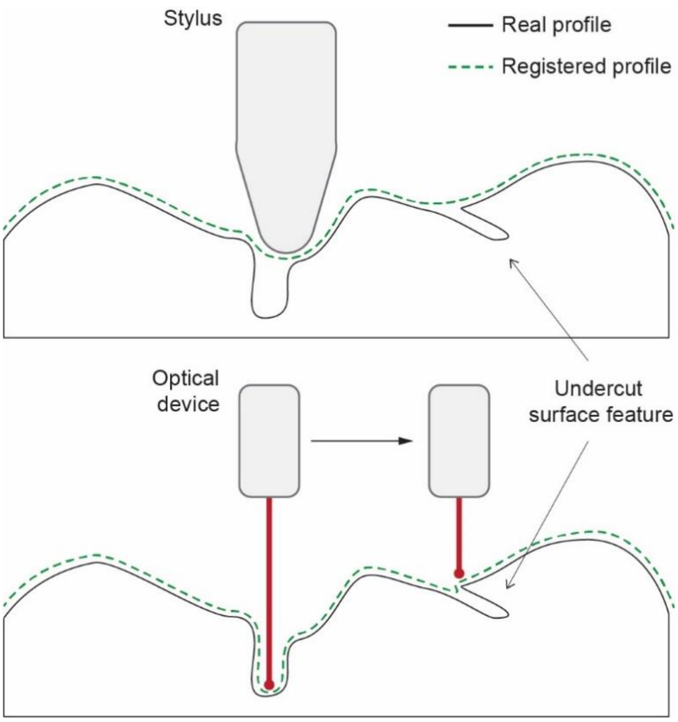

Figure 4. Schematics of surface profile measurements and the registered profile with (a) stylus probing and (b) optical device.

No single surface measurement instrument or technique can accurately capture the exact topographies of metal PBF surfaces on their own. Several authors [59–61] point toward using a combination of methods for more precisely accessing all the surface features and the roughness of PBF parts. The ultimate goal of the surface measurement and the subsequent planned analysis should also be considered when selecting instruments and measurement methods.

2.2 Test artifacts for surface evaluation of AM processes

Test or benchmark artifacts are tools used for quantitative performance evaluations of capabilities and limitations of manufacturing systems or processes [69]. For AM processes, Mahesh [70] has classified the benchmark artifacts into three categories according to their final purposes:

- Geometric benchmark parts for evaluating the geometric and dimensional accuracy
- Mechanical benchmark parts for mechanical properties characterization
- Process benchmarking parts used for process parameters optimization

Geometric test artifacts designed explicitly for AM processes usually come with a diversity of features to evaluate not only the process's geometrical and dimensional accuracy but also its repeatability, minimum feature size, and surface texture [71]. Townsend et al. [59] state that most test artifacts designed solely for surface assessments focus on the relationship between roughness and surface orientation. The truncheon [72] (Figure 5a) was one of the first surface test artifacts for AM, initially designed for stereolithography processes but also used for metal PBF processes [73]. It comprises a series of tilted flat surfaces with 5-degree increments to analyze different orientations in relation to the build platform. ISO/ASTM 52902 [74] proposes a series of geometric test artifacts for AM processes, including those specific for surface texture evaluation. These artifacts are composed of six labeled plates tilted in 15-degree increments (from 0° to 90°) that can be individually detached for tactile and optical measurements (Figure 5b). Overall, the experiments in the reviewed literature followed a similar approach to that of the ISO/ASTM standard, relying on test artifacts comprised of flat plates or disks manufactured in different orientations and slopping angles. Some studies have also measured the surfaces of mechanical test parts to evaluate the roughness before testing.

Figure 5. Different test artifacts used for surface evaluation in AM processes based on (a) Reeves [73], (b) ISO/ASTM 52903, and Galati et al. [76].

A few considerations must be deemed when selecting or designing artifacts for surface measurement with metal PBF processes. Besides the concerns with build time, material consumption, and accessibility, test parts should be appropriately sized for measurement according to the techniques that will be employed. Moreover, support structures must be avoided in regions that will be measured since they leave witness marks on the interface with the part, thus altering the original surface topology. In addition, Galati et al. [75] recently verified the need to maintain a constant wall cross-section in surface test artifacts as the dissimilar thermal behavior caused by varying thickness affected the final surface roughness in a past study [76]. With that in mind, the authors developed a new test artifact (Figure 5c) that can be built without support structures and allow measuring all surfaces (external and internal) while maintaining a constant cross-section throughout the build.

2.3 Surface roughness characterization

To be able to quantify and compare surface roughness information, the measured topographic data is converted to standardized parameters in a process known as surface characterization [59]. This process is described by international standards such as ISO 4287 [77] for profile surface characterization and ISO 25178-2 [78] for areal characterization and involves filtering stages to separate waviness from roughness and the selection of appropriate roughness parameters. Regardless of the type of measured data (profile or areal), the standardized parameters for roughness are mainly divided into amplitude, spatial, and hybrid parameters. Amplitude and spatial parameters quantify the two primary domains of surface topographies: height and wavelength, respectively, whereas hybrid parameters combine the two [79]. Amplitude parameters used to be considered more relevant as they were thought to better relate to function [56], although few amplitude or spatial parameters can be directly correlated to functional properties. Moreover, there has been a historical preference by the industry to utilize average amplitude parameters, which reflects the primary use of surface metrology as a quality control tool for manufacturing [33].

The heterogeneous surface structures produced by AM processes also pose significant challenges for surface characterization. Lou et al. [64] state that the current characterization methods are inadequate for the complex topology of AM parts and even more so for metal PBF processes. According to the authors, new roughness parameters should be developed to better describe the unique characteristics of AM surfaces, along with new filtering and characterization methods. Even with considerable challenges in surface metrology for metal

PBF processes, there are no standardized procedures for inspection and characterization, although ISO/ASTM 52902 [74] recommends the use of some roughness parameters for evaluating AM surfaces in general. These suggested parameters include the profile arithmetic mean deviation (Ra), maximum height of profile (Rz), the skewness (Rsk), and the kurtosis (Rku) of the height distribution, as well as their correspondent areal parameters – Sa, Sz, Ssk, and Sku, respectively. The Ra average parameter is defined by ISO 4287 [77] and computes the arithmetic mean deviation in microns (µm) from peaks and valleys about the mean line (Figure 6). The skewness and kurtosis (Rsk and Rku) parameters describe the relationship between the height distribution of the sampled profile and a Gaussian distribution, with the first providing indications of a predominance of peaks or valleys and the second the sharpness of the profile [59].

The lack of established surface inspection procedures for metal PBF processes leads to a very dispersed environment in academia, often making the comparison of results across studies impractical. For the reviewed literature, the arithmetic mean height (Ra or Sa) is by far the most common parameter used for quantifying the surface roughness of EB-PBF parts, regardless of the measurement method, followed by the root mean square deviation (Rq/Sq) and the maximum height of the profile (Rz/Sz). The same trend was observed by other studies [18,19,59,60], for metal PBF processes in general. According to Triantaphyllou et al. [18], the Ra profile parameter is how several metal PBF equipment manufacturers characterize and control their own processes, even though it is considered a poor parameter for AM surface evaluation [80]. Due to the prevalence of this parameter in the literature, the discussion of surface roughness in this review will be done mainly around Ra values.

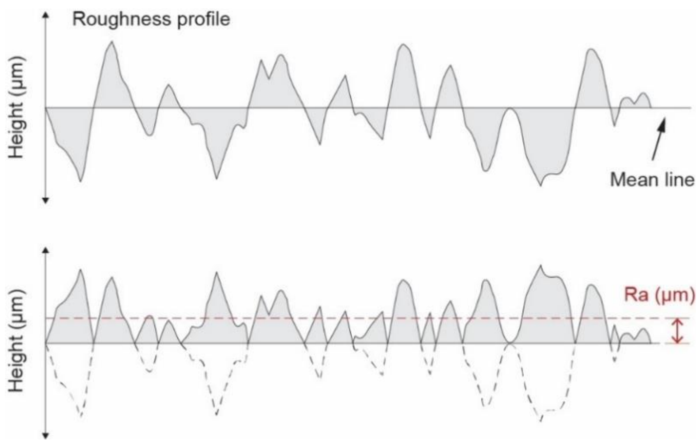

Figure 6. Representation of the arithmetic mean deviation (Ra) roughness parameter in an actual stylus-measured EB-PBF surface.

3. Surface finishing processes

Given the relatively high surface roughness and irregular topology of metallic PBF parts, surface finishing processes are very often required to make parts comply with dimensional and structural requirements. New and existing surface finishing processes have been adapted to more efficiently post-process metal PBF surfaces and their unique characteristics. Bagherifard and Guagliano [81] categorized the different finishing processes used in AM in general based on their intrinsic characteristics:

- Mechanical surface finishing processes, with methods that remove material from surfaces, like machining and grinding, and methods that induce plastic deformation to homogenize surfaces, such as peening and sand blasting.
- Chemical and electrochemical surface finishing processes, in which chemical solutions are used to remove material from surfaces in a controlled manner, including processes such as chemical etching and electrochemical polishing.
- Laser-based surface finishing processes, where material can be either removed from surfaces, such as in laser ablation methods, or altered by local re-melting as in laser polishing processes.

The authors [81] include a fourth category - surface coating processes - although it relates more to inducing specific surface functions than controlling dimensional or roughness aspects. A few factors must be considered for selecting the appropriate finishing processes for EB-PBF, such as the final surface quality requirements, the properties of the treated material, the part geometry, and its final application [82].

Mechanical finishing processes were the most typical methods utilized within the reviewed literature. These processes are regarded as the most effective in enhancing the mechanical properties of metallic AM parts, regardless of the inherent mechanism (material removal or deformation) [82]. Among the mechanical finishing processes, conventional machining remains the most common for metallic PBF parts, being reported to reduce the surface roughness of Ti-6Al-4V parts by EB-PBF to Ra levels as low as 0.05 µm [83]. Machining operations can also achieve the desired dimensional accuracy of parts and remove near-surface defects such as pores depending on the depth of cut [30], both of which are highly beneficial to fatigue. However, Ti-6Al-4V can be particularly tough to machine due to its high chemical reactivity, low thermal conductivity, and relatively low modulus of elasticity [84,85]. Mechanical finishing techniques based on plastic deformation have also become widespread with metallic PBF parts. Although the finished surfaces might not be as smooth as in material removal processes, these methods can improve the mechanical properties by inducing compressive residual stresses on the surface, promoting near-surface pore closure, and refining surface grain [86]. Soyama and Takeo [87] analyzed the effects of various peening surface treatments on the roughness and fatigue performance of Ti-6Al-4V specimens by both L-PBF and EB-PBF. Shot peening was by far the most effective, reducing Ra values from 19.3 µm to around 5 µm in EB-PBF specimens, while cavitation peening only showed a marginal reduction. However, the observed effects on fatigue were very significant for both treatments since they introduced similar levels of compressive residual stresses on the surfaces, with a 75% increase in fatigue strength at N=10^7 for cavitation peening and 95% for shot peening in EB-PBF parts [87].

While peeing techniques can be more flexible in dealing with highly complex structures than conventional machining, mechanical surface finishing processes are limited to accessible regions. For treating internal surfaces and channels in EB-PBF, or even intricate structures like lattice and cellular geometries, chemical and electrochemical surface finishing processes can be very effective [82]. These processes work the entire geometry of parts as they are completely submerged, and the amount of material removed is usually controlled by the composition of the solution, exposure times, temperature, and electrical voltage and current in the latter case [88]. Lhuissier et al. [31] showed that a chemical etching process with a Hydrofluoric acid (HF) and Nitric Acid (HNO3) solution could uniformly reduce the Ra roughness of Ti-6Al-4V struts by EB-PBF from around 35 to 20 µm in 60 minutes. The authors observed a more rapid roughness reduction in the first 20 minutes of the process, when the partially melted powder particles were preferably removed. The underlying surface irregularities were smoothed in the remaining 40 minutes at a much slower pace [31]. Electrochemical polishing processes are faster than chemical etching, though restricted to conductive materials, and could lead to dimensional issues in the treated parts if not properly controlled [88]. Wu et al. [89] showed that, with proper solution and parameters, the Ra roughness of Ti-6Al-4V specimens by EB-PBF could be reduced from around 24 to 4.5 µm in only 20 minutes.

Lastly, laser-based finishing processes are also viable options for post-processing metallic PBF parts. The most usual techniques include laser polishing, in which pulsed lasers re-melt micrometer-thin layers of material on surfaces, and laser ablation, where higher energy lasers vaporize the irregular surface structures. For Ti-6Al-4V by EB-PBF, laser polishing techniques were reported to reduce the Sa roughness values by 75 to 90% [90,91]. However, it was also verified that significant effects on the surface microstructure were induced, along with high levels of tensile residual stresses, local oxidation, and a small agglomeration of re-melted material on the edges of polished surfaces [90,91]. Laser ablation, on the other hand, has shown the potential to reduce Ra roughness values by 80% without the issues reported with laser polishing, to levels as low as 5 µm, according to Genna and Rubino [92], although the results are known to be highly dependent on the process parameters [93].

4. Causes of surface roughness in EB-PBF

Although often linked to the layer-stacking building technique of AM, the high roughness levels in EB-PBF parts are due to various causes. Three main mechanisms behind roughness generation in these surfaces were identified when reviewing the present literature on the subject, and they will be detailed in this section.

4.1 The staircase effect

The stepping pattern observed in lateral surfaces of EB-PBF parts is known as the staircase effect [73,94,95]. It is a topographical defect inherent to all AM technologies that produce geometrical and dimensional variations between the digital 3D model and the manufactured part, illustrated in Figure 7. Naturally, surfaces strictly parallel to the build platform, like top surfaces, are not affected [62].

The staircase effect is characterized by a directional peak-and-valley topographical pattern along the Z direction that contributes to the total surface roughness of lateral surfaces [28,96]. The international standard for surface profile measurement (ISO 4287 [77]) clearly indicates that the measurement direction must be perpendicular to the direction of the lay, which is the predominant surface pattern generated during the manufacturing process [97]. For AM processes, the lay corresponds to the stepping pattern produced by the staircase effect, and so all surface profile measurements should be performed along the build direction (Z). However, for EB-PBF with Ti-6Al-4V, the reported Ra values obtained from profile measurements performed both along and across the build direction showed little difference - only up to 4 μm on average [18,19,98]. While this can be considered a small contribution considering the level of roughness in lateral surfaces, the severity of the staircase effect on the surface quality of EB-PBF parts relies on factors detailed in Section 5.

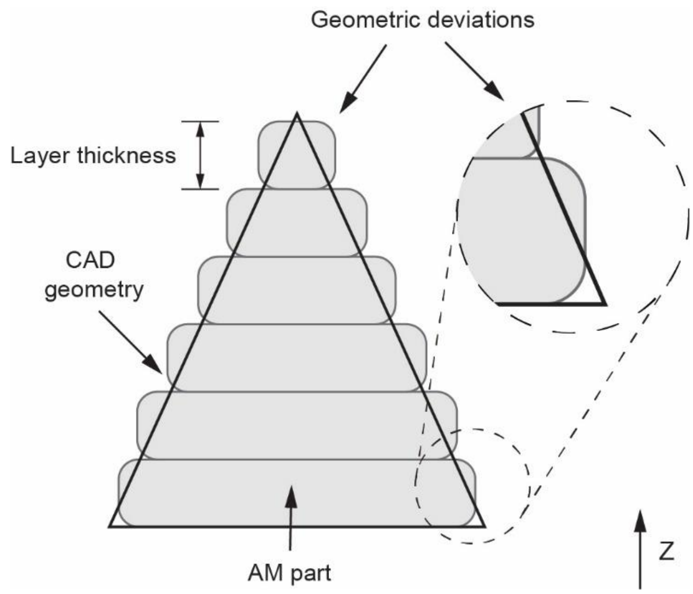

Figure 7. The staircase effect and its inherent geometrical deviation from the CAD model

4.2 Partially melted powder particles adhesion

Another mechanism known to contribute to the highly irregular surface topology in EB-PBF is the adhesion of unprocessed feedstock powder particles to the solid surfaces [30,93,99–101]. This phenomenon is caused by high-heat diffusion from the solid part to the surrounding feedstock powder, which is enough to partially melt powder particles. These particles then attach to solid surfaces and create the many round protuberances observed in Figure 8 [41]. The resulting irregularities are believed to contribute the most to the surface roughness of EB-PBF, and as such, this phenomenon is considered the dominant mechanism of roughness generation by some authors [102,103]. While particle adhesion is known to affect all surfaces, it seems to be more evident in overhang and down-facing surfaces [63]. The adhesion of powder particles is more severe in EB-based processes than in laser processes due to higher thermal radiation by the electron beam [17] and the preheating stages that sinter the powdered material around the solid part.

4.3 Process deviation

EB-PBF processes involve complex multi-physics interactions caused by the high-speed scanning and rapid material phase change [2,24]. As such, the melt pool experiences different hydrodynamic effects throughout the melting and solidifying stages, giving shape to irregular surface structures of stochastic nature that contribute to the overall roughness [104].

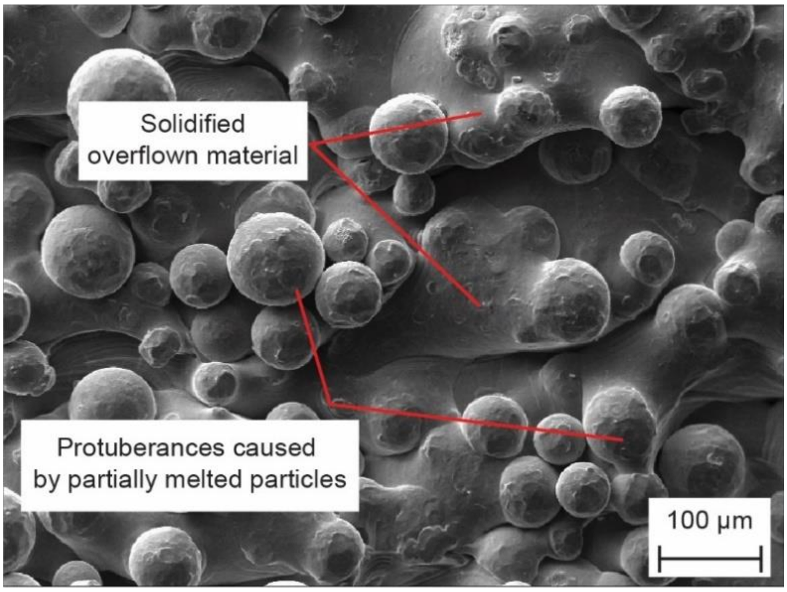

Figure 8. Partially melted feedstock particles and overflown material on lateral surfaces of Ti-6Al-4V by EB-PBF

Thermocapillary effects such as the Marangoni flow [105], can promote horizontal movement in the material inside the melt pool, and during the electron beam scanning, material tends to flow toward the edges of the scanned track, leading to the formation of wavy structures on top surfaces [106]. The turbulent hydrodynamic effects can be severe enough to make the melt pool overflow into the edges of the solid part [104]. creating surface protrusions on lateral surfaces of EB-PBF parts as indicated in Figure 8. These structures from overflow material have been identified by several authors in Ti-6Al-4V specimens, being sometimes referred to as "plate-pile" stacking irregularities [31,41,107,108].

Other anomalies caused by melt pool instabilities and unoptimized process parameters can also produce surface defects that add to the irregular topology of EB-PBF parts. Porosity is a common defect in metal PBF processes and can be observed both in bulk and on the surfaces of parts, with the latter constituting deep recesses on the surface [109]. Porosity in EB-PBF is attributed to lack-of-fusion phenomenon and to process deviations such as balling and particle spatter. Lack-of-fusion occurs when an insufficient energy density is provided to the powder bed during the electron beam scanning, leading to unmelted regions that form pores and voids [9,110]. However, if too much energy is provided, Plateau–Rayleigh instabilities can break the melt pool to reduce its surface energy, ejecting small sphere-like particles and creating voids in EB-PBF parts [111–113].

It is worth mentioning that the irregularities and defects caused by hydrodynamic effects and process deviations are believed to be the main responsible for crack initiation on surfaces in EB-PBF with Ti-6Al-4V [19,114].

5. Influence of process variables on the surface roughness of Ti-6Al-4V

Gibson et al. [99], categorized the process parameters of metal PBF processes into four groups: (1) laser or EB-related parameters, (2) scan-related parameters, (3) powder-related parameters, and (4) temperature-related parameters. In order to discuss the surface roughness of EB-PBF parts, two additional process variables must be considered: the internal arrangement of parts and their build orientation inside the chamber. The fishbone diagram in Figure 9 shows all the process variables verified to affect the surface roughness of Ti-6Al-4V by EB-PBF in the reviewed literature, while Table 1 highlights the most relevant experimental studies on the subject. This section will detail each process variable in Figure 9 through a slightly different categorization scheme.

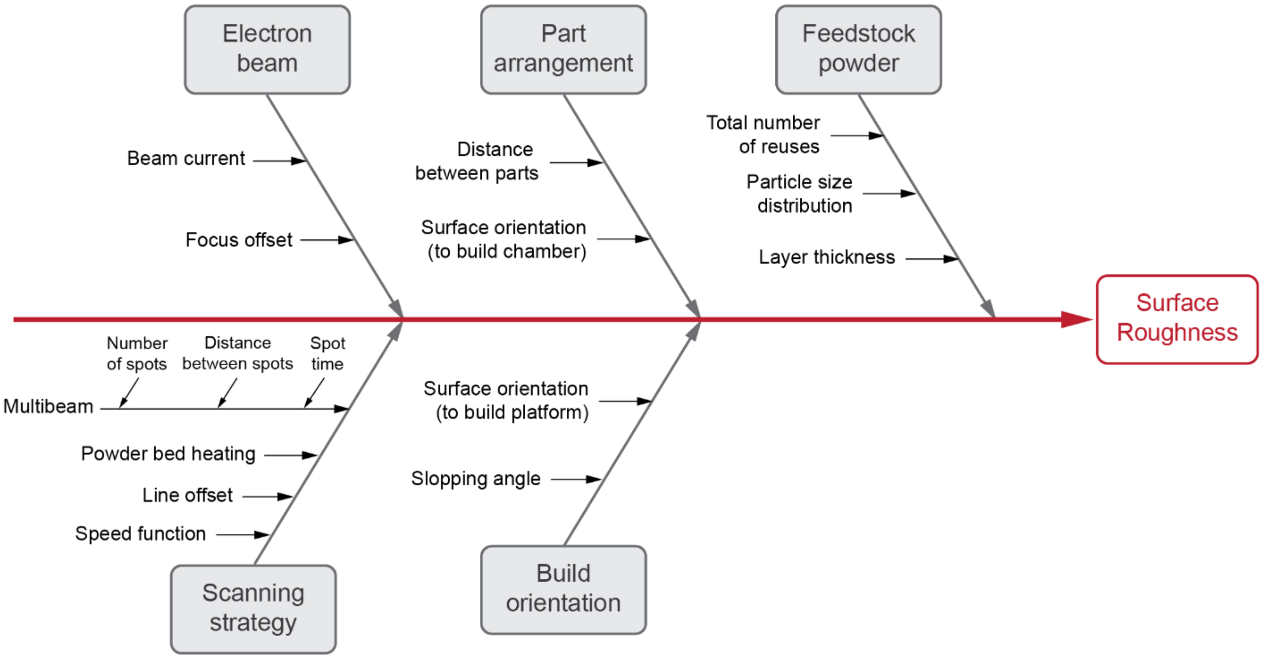

Figure 9. Fishbone diagram of process variables verified to influence the surface roughness of Ti-6Al-4V parts produced by EB-PBF processes.

Table 1. Summary of experimental studies regarding process variables and surface roughness of Ti-6Al-4V by EB-PBF.

Category	**Reference**	**Process variables**	**Surfaces evaluated**	**Measurement instruments**	**Roughness parameters**
Feedstock powder related	Karlsson et al. [115]	Powder size distribution, Layer thickness	Lateral (vertical)	Scanning Electron Microscope	-
	Karlsson et al. [116]	Layer thickness	Lateral (vertical)	Optical	Ra
Build orientation and part arrangement	Sidambe et al. [95]	Surface orientation (to build platform)	Top and lateral (vertical, upskin)	Optical	Sa, Sq, Sku, Ssk, Sp, Sv, Sz
	Persenot et al. [108]	Surface orientation (to build platform)	Top and lateral (vertical, upskin, downskin)	X-ray tomography	Ra, Rt
	Galati et al. [76]	Slopping angle	Top and lateral (vertical, upskin, downskin)	Tactile	Ra
	Galati et al. [75]	Slopping angle	Lateral (vertical, upskin, downskin)	Tactile and optical	Ra, Rq, Rz, Sa, Sq, Sz

	Borrelli et al. [98]	Surface orientation (to build chamber)	Lateral (vertical)	Tactile	Ra
	Kotzem et al. [117]	Surface orientation (to build chamber)	Lateral (vertical)	Tactile and X-ray tomography	Ra
	Jamshidinia and Kovacevic [118]	Distance between parts	Lateral (vertical)	Optical	Sa
Electron beam and scanning strategy	Safdar et al. [102]	Beam current, Focus offset, Scanning speed	Lateral (vertical)	Optical	Ra, Rq
	Scharowsky et al. [119]	Beam current, Line offset, Scanning speed	Top	Optical	Ra
	Silvestri et al. [120]	Beam current, Line offset, Scanning speed	Top	Optical	Sa
	Wang et al. [121]	Beam current, Focus offset, Speed function, Multibeam	Lateral (vertical)	Tactile and optical	Ra
	Prisco et al. [122]	Focus offset, Line offset, Scanning speed	Top and lateral (not specified)	Tactile	Ra
	Klingvall et al. [123]	Line offset, Number of contours	Lateral (vertical)	Tactile	Ra
	Shrestha and Chou [106]	Speed function	Top	Optical	Ra, Rq, Rt

5.1 Feedstock powder

The metallic powder used as feedstock material by metal PBF processes can be produced by various methods[124,125] and is comprised of particles that vary in size and shape. According to Dowling et al. [96], the powder's morphology, which includes the particle size distribution and shape characteristics, is an essential process variable for the repeatability and reproducibility of metal PBF processes. The morphology determines the flowability and the packing density of the powder bed, which in turn affects its thermal conductivity and optical penetration, thus also affecting parts' microstructure, porosity, and surface quality [96,124,126–129].

EB-PBF processes, in particular, require larger-sized powder particles to help counteract powder spreading effects due to electrostatic repulsion [130]. The powder size distribution is defined in terms of particle diameter, and the most common size distribution found in reviewed literature for EB-PBF is in the range of 45 - 105 µm for Ti-6Al-4V. A significant amount of authors attribute the rougher surface finish of EB-PBF parts to its larger powder particles, especially when compared to L-PBF processes that utilize finer powder [25,26,41,103,131]. Smaller-sized powder particles have indeed been verified to produce better surface finishes on top and lateral surfaces in L-PBF [127,132]. Sinico et al. [129], in particular, showed that very fine powder (10 – 30 µm) of Maraging steel resulted in a significant decrease of Ra values in lateral surfaces, even when compared to a slightly coarser powder (15 – 45 µm). Since powder particle adhesion is considered by many authors the primary mechanism behind roughness generation in EB-PBF, it should be expected that powders with smaller size distributions would positively impact the surface quality. However, for EB-PBF with Ti-6Al-4V, Karlsson et al. [115] concluded that finer powder particles are more likely to adhere to surfaces. In this study, a visual comparison through SEM micrographs was performed in parts produced by powder size distributions of 25 – 45 µm and 45 – 100 µm using the same layer thickness. The authors also mention that the underlying peaks and valleys of parts produced with finer powder appeared more regular and smoother, presumably due to the more densely packed powder layers. Nonetheless, it should be noted that no surface measurement and characterization were performed, and the process parameters for the builds with finer powder were not optimized since this material is not officially supported by the EB-PBF equipment manufacturer [115].

The overall quality of the powder can also lead to higher surface roughness in EB-PBF. The unprocessed powder of each build can be reutilized up to a limited number of times and is usually mixed with new fresh powder [125]. he number of reuse times can directly affect the powder's chemical composition, particle morphology, and microstructure [133,134]. Tang et al. [135] believe that the changes in particle morphology could potentially affect part's surface quality in EB-PBF. After each reuse, Ti-6Al-4V powder particles became less spherical and more naturally rougher, becoming significantly distorted after the 16th and 21st reuses [136–138]. he particles also tend to cluster as they are repeatedly sintered together, and the recovery process with pressurized air can fracture these clustered particles, increasing the distortions that can affect the final roughness of parts [135]. Yet, no surface roughness assessment has been made to verify the possible effect of highly reused Ti-6Al-4V powder.

The particle size distribution also determines the minimum layer thickness that can be used in a specific build [64,139], which affects the surface roughness in its own way, as will be described next.

5.2 Layer thickness

Layer thickness, or layer height, is a process parameter common to all AM processes that define the physical thickness of each layer created at a time. Typical values for layer thickness in EB-PBF processes are 50 and 70 µm [115], above the 20 – 50 µm range of L-PBF processes [140,141]. It is a major process parameter in metal PBF processes that affects many process variables, including build time, detail resolution in Z , and generation of defects like porosity [140], and the surface quality. Regarding surface quality, layer thickness impacts the severity of the geometric deviations caused by the staircase effect: the thicker the layers, the more parts deviate from the original CAD geometry (Figure 7).

Many authors associate the coarser surface finish of EB-PBF parts relative to L-PBF with the thicker layers used in EB processes [25,28,29,95,131]. Körner et al. [104] verified through numerical simulations that increased layer thickness might also contribute to the surface roughness of EB-PBF as it facilitates melt pool movement and material overflow. Still, only a few studies experimentally investigated the influence of layer thickness on the roughness of lateral surfaces of Ti-6Al-4V parts. In a first study, Karlsson et al. [115] found no differences in the surface quality of builds with layer thicknesses of 50 and 70 µm, although no measurement or characterization was performed - only comparison through SEM images. Later, Karlsson et al. [142] evaluated the roughness of lateral surfaces of Ti-6Al-4V specimens produced with 25 and 50 µm layer thicknesses. The specimens showed a similar level of Ra roughness, although the authors claim that the overall surface quality of the lower layer thickness parts looked better in SEM micrographs.

5.3 Build orientation

In AM processes, build orientation refers to how parts are oriented inside the manufacturing chamber in relation to the build platform [1]. The build orientation of parts is defined prior to the manufacturing job and directly influences the total number of parts that can be fitted inside the build chamber. It also sets the maximum build height of each manufacturing run and, consequently, their build times [123]. The build orientation was also verified to affect the part's microstructure and mechanical properties [101,108,143], its dimensional accuracy [98,144], the manufacturability of small-scale features [145], and the generation of lack-of-fusion defects [146]. The build orientation evidently defines how each surface of a part will be produced, either as a top or lateral surface - and for the latter, whether they will be facing upwards (upskin surfaces) or downwards (downskin surfaces), as illustrated in Figure 10a. It also determines the location, quantity, or even the necessity of support structures, thus having a substantial influence on the surface quality [95]. It was mentioned that the roughness of top and lateral surfaces differ significantly, but upskin and downskin lateral surfaces also show distinct topologies and roughness levels. Table 2 summarizes some studies that analyzed the roughness of Ti-6Al-4V with EB-PBF in different orientations. Relatively large dispersion of Ra values can be noted across different studies for one specific surface orientation, and that is due to various factors, including the surface measurement methods utilized and process parameters. Still, by comparing the results within same studies, it is possible to notice a discrepancy in Ra values between vertical, upskin, and downskin lateral surfaces.

According to Galati et al. [75], the topology of upskin surfaces is dominated by the staircase effect and process deviation roughness. In terms of sloping angle, the authors verified a positive linear relationship between Ra/Sa roughness values and sloping angles for upskin surfaces. This means the roughness worsens with the increasing of sloping angles between upskin surfaces and the build platform. This outcome was explained by the different heat transfer effects the material experience during solidification. In upskin surfaces with low sloping angles, the just melted material has a larger surface area in contact with previous solid layers, and the solid body underneath acts as a heat sink that inhibit heat transfer to the surrounding powder particles [75].

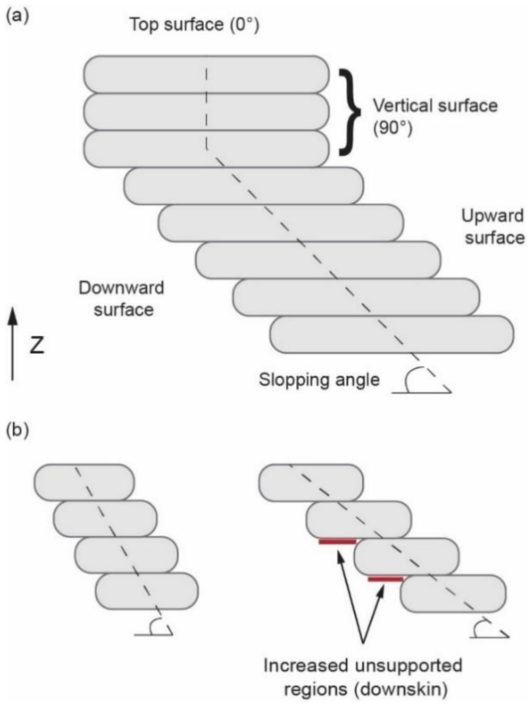

Figure 10. (a) Surface orientation of PBF parts and (b) surfaces with different sloping angles.

Table 2. Summary of Ra roughness values obtained from surfaces with different orientation in EB-PBF with Ti-6Al-4V.

Surface orientation	**Powder size distribution (µm)**	**Layer height (µm)**	**Ra (µm)**	**Reference**
Top	49 – 98	70	1 – 6	Triantaphyllou et al. [18]
	25 – 45	50	4 – 10	Nicoletto et al. [19]
	45 – 105	50	3 – 11	Galati et al. [76]
Lateral vertical (90°)	49 – 98	70	30 – 40	Triantaphyllou et al. [18]
	25 – 45	50	17 – 25	Nicoletto et al. [19]
	45 – 105	50	26	Borrelli et al. [98]
	45 – 105	50	26 – 28	Greitemeier et al. [43]
Lateral upskin (60°)	49 – 98	70	44 – 48	Triantaphyllou et al. [18]
	45 – 105	50	18 – 33	Galati et al. [76]
Lateral downskin (60°)	49 – 98	70	32 – 50	Triantaphyllou et al. [18]
	45 – 105	50	17 – 20	Galati et al. [76]

Downskin surfaces are often considered to be rougher than upskin, with surfaces dominated by partially melted particles adhered instead [40,63]. These surfaces are built on unsupported regions, as shown in the diagram in Figure 10. The effect of gravity on the melt pool in these unsupported areas can cause the melted material to sag into the powder bed below and create protrusions when the overflown material is solidified [18,147,148]. Layer building over these unsupported regions also favors the heat transfer towards the sintered powder bed right below, causing more particles to partially melt and attach to the downskin surfaces [75]. Regarding the inclination of downskin surfaces, Galati et al. [75] verified a negative linear relationship between Ra/Sa roughness and the sloping angle instead, with the more tilted surfaces showing the highest values. The lower the angle, the larger the unsupported regions and the heat transfer toward the powder bed below (Figure 10b).

5.4 Position on build chamber

Besides build orientation, the way parts are positioned and manufactured inside the build chamber can also affect the roughness generation in EB-PBF processes. The arrangement inside the build chamber can determine the total number of parts that can be fitted, ultimately impacting batch production times and unit cost. The position of parts in L-PBF processes has been proven to affect their final roughness due to the laser incidence spot deformation [149,150] the direction of inert gas flow and recoater movement [151–153].

Although these factors are not applicable to EB-PBF processes, there is evidence that the position of parts can influence the surface finish of Ti-6Al-4V parts. Borrelli et al. [98] noticed that parts produced at the four corners of the build platform consistently displayed slightly higher Ra values than other parts, even more so in the surfaces facing the outward directions. These corner parts were built very close to the limits of the build platform, and the authors attribute this adverse behavior towards roughness to the less efficient heat dissipation of these regions. Their hypothesis was that heat was trapped in the narrow space between the solid part and the boundaries of the build chamber, inducing more powder particles to attach to the outward-facing surfaces [98]. Galati et al. [76] and Kotzem et al. [117], also observed a similar tendency, especially in parts positioned closer to the EB-PBF equipment door. It is worth noting that the position of parts along the Z direction had no significant influence on surface roughness [98].

Yet, the relative position between Ti-6Al-4V parts inside the EB-PBF build chamber has been proven to affect their surface quality. Jamshidinia and Kovacevic [118] verified an inverse relationship between the spacing distance of thin-walled parts and their surface roughness: the closer two distinct surfaces were positioned, the higher their Sa roughness values were. Similar to Borrelli et al. [98], the authors explain this behavior as being due to the increased accumulation of thermal energy in the regions between parts with shorter spacing distance, which ultimately favors the adhesion of partially melted particles.

5.5 Energy Density

The size and shape of the melt pool are determined, among other aspects [154], by the total amount of energy supplied by the energy source and absorbed by the powder bed, which in turn depends on interdependent and mutually interacting process parameters of the PBF process [99,141]. For EB-PBF, in particular, the process parameters are dynamically controlled by a proprietary algorithm, making the study of individual parameters very challenging. For this reason, researchers rely on theoretical variables for calculating the total energy input levels. Among the most usual variables are the linear energy density [122,155] and the volumetric energy density, the latter of which is defined as:

$$E_v = \frac{P}{V_S \times H_S \times t} \tag{1}$$

For EB-PBF specifically, P (W) is the power of the electron beam, (mm/s) the scanning speed of the electron beam, (mm) the hatching space between scan lines, and (mm) the layer thickness of the build. The electron beam power is a function of both the accelerating voltage and the current, though it is controlled by the current (in mA) alone since the accelerating voltage is kept constant in EB-PBF equipment [155,156]. The hatching space is the physical distance between two adjacent tracks, and for EB-PBF processes, it is determined by the line offset parameter [9,130]. The scanning speed is the actual translational velocity of the electron beam and can be either dynamically controlled by the speed function parameter or be assigned a fixed value in manual control operation [120]. The layer thickness was already discussed in 5.2, and all these parameters are illustrated in Figure 11.

Another parameter closely related to the energy density input is the focus of the electron beam. The focus is controlled by a process parameter called focus offset, which is the current (in mA) that defocuses the electron beam from the sharpest calibrated position [155,157]. Defocusing the electron beam can sometimes enlarge the EB spot size up to a point but at the expense of producing shallower melt pools [158]. It is worth noting that the EB spot size is ultimately controlled by a combination of the beam current and focus offset parameters through a non-linear relationship that is not disclosed by the EB-PBF equipment manufacturer [159]. The energy density affects many aspects of EB-PBF parts since the size and temperature of the melt pool is known to influence the microstructure [123,160], the chemical composition [119], and the porosity of Ti-6Al-4V parts [24,156].

The energy density also significantly affects the surface quality of top surfaces in EB-PBF with Ti-6Al-4V. Guo et al. [156] observed that lower energy density levels, achieved by reduced beam current and higher scanning speeds, lead to top surfaces dominated by cavities and lack-of-fusion pores. The authors claim that there was not enough energy to melt the whole powder region properly, and a gradual increase of the energy density with higher beam current values and slower scanning speeds produced much denser and smoother surfaces. Similar results were observed by Shrestha and Chou [106], in which the higher energy density levels obtained by only reducing the scan speed produced denser and flatter surfaces.

The energy density also significantly affects the surface quality of top surfaces in EB-PBF with Ti-6Al-4V. Guo et al. [163] observed that lower energy density levels, achieved by reduced beam current and higher scanning speeds, lead to top surfaces dominated by cavities and lack-of-fusion pores. The authors claim that there was not enough energy to melt the whole powder region properly, and a gradual increase of the energy density with higher beam current values and slower scanning speeds produced much denser and smoother surfaces. Similar results were observed by Shrestha and Chou [109], in which the higher energy density levels obtained by only reducing the scan speed produced denser and flatter surfaces.

As mentioned in Section 4.3, the topology of top surfaces is dominated by wavy structures located at the edges of each melted track. Employing larger melt pools can re-melt some of these structures from adjacent scan tracks and improve these surfaces. Higher energy density levels elevate the melt pool's temperature and reduce its surface tension, increasing the width of the melt track [120] and benefiting the surface quality, but only up to a point. Excessive energy density can cause intense hydrodynamic instabilities in the melt pool, producing highly distorted structures on top surfaces [156] or, in extreme cases, leading to material vaporization that produces highly damaged top surfaces [8,110].

Still, using higher energy density levels can be a suitable strategy for roughness control on top surfaces, as verified by Prisco et al. [122] with Ti-6Al-4V specimens. According to the authors, besides reducing the scanning speed, increasing the focus offset values created a defocused beam spot large enough to re-melt the ridges of adjacent scan tracks. Another way of achieving these results is by reducing the distance between adjacent melting tracks through the line offset parameter [119,122,130]. This strategy induces scan tracks to overlap more while increasing the energy density as per (1).

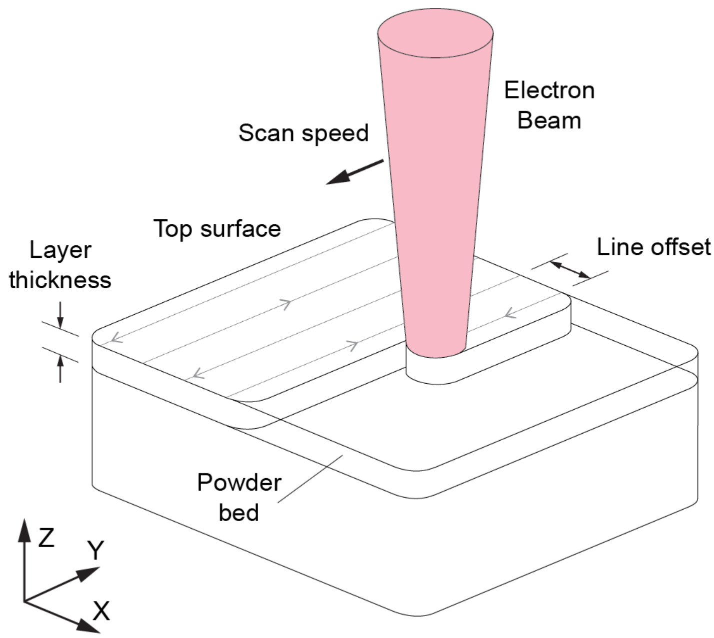

Figure 11. Schematic of the electron beam and scanning strategy process variables.

It is also worth mentioning the individual influence of parameters when the energy density is kept constant during the top surface melting. Silvestri et al. [120] verified that using higher levels of beam current and scanning speeds individually while maintaining the total energy density constant produced top surfaces with lower Sa roughness in Ti-6Al-4V specimens by EB-PBF. According to the authors, although the total amount of energy input is maintained, the thermal diffusion times are lower at higher scanning speeds, which results in higher temperatures in the melt pool that are beneficial to surface roughness.

As for the lateral surfaces, the energy density also plays a central role in the surface quality EB-PBF with Ti-6Al-4V, but mostly due to partially melted particles. Increased energy density levels lead to thermal accumulation in parts and high-temperature gradients towards the surrounding powder bed region, thus enabling more particles to partially melt and adhere to surfaces [102,159]. This seems to be the case as either increasing the beam current and reducing the scan speeds [102,121] or reducing the scanning speeds only [122]. resulted in rougher lateral surfaces in Ti-6Al-4V. On the other hand, the influence of the focus offset in the roughness of lateral surfaces showed mixed results with EB-PBF with Ti-6Al-4V. For Safdar et al. [102], decreasing the focus offset from 25 mA to 10 mA produced lateral surfaces with much higher roughness, which according to the authors, is due to the concentrated electron beam that leads to higher energy densities. Prisco et al. [122] on the other hand, tested three different levels of focus offset – 4, 10, and 20 mA – that showed no influence on the surface roughness of lateral surfaces.

It is also important to highlight the impact of energy density in the process deviation roughness by anomalies like balling. Yan et al [161] verified through multi-physics modeling that the energy density from the electron beam must be sufficient enough to melt solid substrate below the powder bed. Suppose the energy provided is only enough for the powder particles to melt or the melt pool is not as deep as to reach the layer below. The melted material would cluster into isolated agglomerates (balls) to reduce the surface energy, but according to the authors, a properly melted substrate should avoid the balling effect as the melted particles can spread to reduce the surface energy [161].

5.6 Scanning Strategy

The scanning strategy in EB-PBF comprehends both the powder bed heating stages and the melting process [159]. The powder bed heating is done by a defocused electron beam and consists of 3 separate stages: (1) preheating of the entire build platform, (2) preheating regions closer to the where melting process will take place, and (3) a post-heating stage performed after the melting process to either heat up or cool down the layer [10,162]. However, a sintered powder bed favors the thermal conductivity between the solid part and surrounding powder [163], which in turn contribute to the melting and adhesion of particles to the surfaces [164], even more so considering the already elevated temperature of the surrounding powder in EB-PBF processes [8]. As such, it would be expected that the role of the preheating stages in the roughness generation had been investigated, but no experimental studies were found in the reviewed literature.

The scanning strategy of the melting process relates to individual paths that the electron beam follows to purposely melt the powder and create solid layers. Figure 12 exemplifies the melting of a single layer. This process is divided into two separate stages: the first involves melting the perimeters, which can be up to 5 concentric contour lines [10]. This stage is also known as contouring, and for EB-PBF processes, the default themes perform it with a spot melting strategy called Multibeam [3,123,165,166]. This function is specific to EB-PBF processes since the translational speeds of electron beams are much higher when compared to lases, allowing several melt pools to be simultaneously active. Unlike typical continuous fusion, in the Multibeam strategy, the electron beam rapidly shifts between several points along a scanned track, promoting faster scanning and increasing productivity [167]. It is also claimed that the smaller melt pools created by this strategy reduce the thermal gradient toward the surrounding powder and leads to better surface finishes [123,167]. However, a comparison between Multibeam and a continuous melting strategy for the contours performed by Wang et al. [121] showed that the non-multispot strategy was able to produce surfaces with lower Ra values for Ti-6Al-4V, though with the worst dimensional accuracy. The authors also verified that the parameters of the Multibeam function had some impact on the surface roughness on lateral surfaces of Ti-6Al-4V by EB-PBF, among them the number of beam spots, the spot time, and the distance between two consecutive spots. The number of spots determines the total number of active melt pools [55], and was the dominating factor in affecting roughness according to the authors, with a higher number of spots producing better-finished surfaces. A combination of shorter spot time, which is the total amount of time that the electron beam melts each spot, and reduced distances between spots also produced better results in terms of Ra roughness [121].

The second melting stage involves melting the bulk of the part, as illustrated in Figure 12. This is known as rastering or hatching since continuous parallel tracks are melted in varying patterns to produce the inner regions of the parts. The direction and the pattern of the hatching are altered between consecutive layers to avoid anisotropy [159]. It is worth mentioning that EB-PBF parts can be produced by hatching strategies only - without contours

- yielding faster build times although producing extremely rough surfaces as verified by Mallipeddi et al. [168] with Ti-6Al-4V.

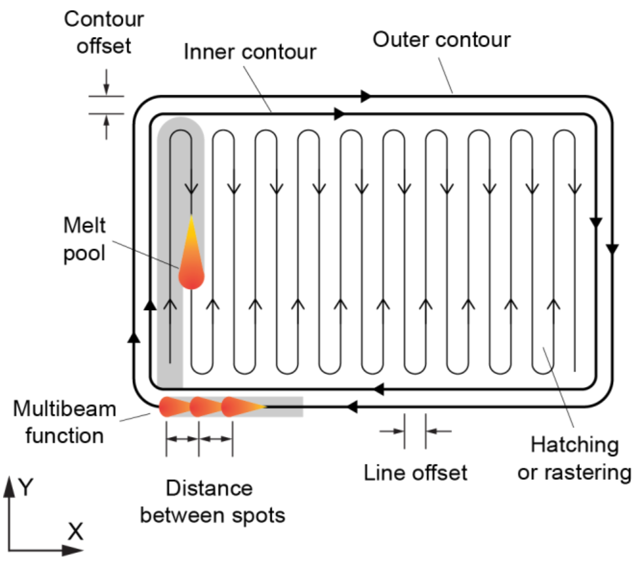

Figure 12. Diagram of the scanning strategy for the contour and fill pattern.

The scanning speed and line offset parameters are also linked to the scanning strategy, although their influences on surface roughness were already discussed in the context of energy density (Section 5.5). Still, the effects of the line offset for the contours (contour offset) along with the number of perimeters also showed some influence on the side surfaces of EB-PBF with Ti-6Al-4V, although practical results were not obtained by Klingvall et al. [123].

6. Future research and outlook

Another factor contributing to surface roughness in EB-PBF processes is the geometry of parts. The effect of geometrical features and attributes, such as wall-thickness of parts, have also been investigated in terms of surface roughness, although not extensively. Safdar et al. state that thicker walls produced higher levels of Ra roughness in Ti-6Al-4V by EB-PBF. The authors claim that the increased energy required to melt these bulkier structures promoted more particles to partially melt and adhere to lateral surfaces partially. The results later observed by Razavi et al. [40] and Karlsson et al. [116] contradict these findings, with the thin-walled specimens displaying the worst Ra roughness levels compared to the thicker ones, though with different thickness levels. Yet, more recent studies by Segersäll et al. [169]

showed that the part's thickness did not influence the roughness of Ti-6Al-4V specimens. More research on the matter is required to investigate further the role of geometry and wall-thickness in the surface roughness of EB-PBF parts. The influence of the powder size distribution and the layer thickness, although claimed by many authors as the main drivers of surface roughness generation in EB-PBF, still demand additional experimental evidence for the actual influence of these parameters to be established. The effects of the preheating stages should also be explored due to their role in surface roughness, as explored in this review. With that said, the high costs associated with the EB-PBF equipment operation and the feedstock material can hinder experimental studies in the field. Numerical simulations have gained much traction over the past decade, including those to predict surface roughness [9].

It is also worth mentioning some guidelines for future research in the area. A deep understanding of the subject is often made impractical by how experiments are conducted and the results are published. Though properly established procedures for the surface measurement of metallic PBF parts are still to be conceived, ISO/ASTM 52902 [74] provides a good starting point, and its guidelines should be followed when designing an experiment. As a general recommendation, all the evaluated surfaces must be duly identified when publishing results, along with all the methods and parameters used for measurement and characterization. In addition, the feedstock material information, the EB-PBF equipment model, the final orientation and disposition of parts inside the build chamber, and the relevant process parameters described in Section 5 should also be clearly stated.

7. Conclusion

This study reveals the growing effort by the academic community to better understand and correlate EB-PBF process variables with the surface roughness of Ti-6Al-4V parts, which also indicates the relevancy of this field of study. EB-PBF has already shown a great potential for industrial applications, and its inherent rough surface quality plays a central role, both positively and negatively. Yet, surface metrology for metallic PBF parts remains a very challenging task with the present measurement and characterization methods and techniques.

Practical and experimental correlations are very challenging to establish in EB-PBF processes due to the highly interrelated process parameters and differences between measurement and characterization methods. Still, the main mechanisms behind surface roughness generation in EB-PBF were reviewed, as well as the process variables and experimental correlations obtained for Ti-6Al-4V specifically. The opportunities for future research in the area were also covered, along with recommendations and guidelines that would allow the community to better interpret the results.

Overall, the relationship between process variables and surface roughness of EB-PBF can better serve the purpose of comprehending the process rather than controlling the roughness entirely. To that end, surface finishing processes still present the best solution for fine roughness control, despite their many limitations regarding AM parts.

Funding

This study was financed in part by the Coordenação de Aperfeiçoamento de Pessoal de Nível Superior – Brasil (CAPES) – Finance Code 001.

References

[1] ISO/ASTM 52900:2015 Additive Manufacturing - General Principles - Terminology, ASTM and International Organization for Standardization ISO, 2015.

[2] E. Attar, Simulation of Selective Electron Beam Melting Processes, Doctoral dissertation, University of Erlangen-Nuremberg (2011). https://d-nb.info/1013101472/34.

[3] M. Markl, M. Lodes, M. Franke, C. Körner, Additive manufacturing using selective electron beam melting, Welding and Cutting, Vol. 16 (2017) 177–184. https://www.researchgate.net/publication/317955281_Additive_manufacturing_using_selective_electron_beam_melting.

[4] L.C. Zhang, Y. Liu, S. Li, Y. Hao, Additive Manufacturing of Titanium Alloys by Electron Beam Melting: A Review, Adv. Eng. Mater. 20 (2018) 1–16. https://doi.org/10.1002/adem.201700842.

[5] P. Fathi-Hafshejani, A. Soltani-Tehrani, N. Shamsaei, M. Mahjouri-Samani, Laser incidence angle influence on energy density variations, surface roughness, and porosity of additively manufactured parts, Addit. Manuf. 50 (2022) 102572. https://doi.org/10.1016/j.addma.2021.102572.

[6] GE Additive, Inside Electron Beam Melting, White Paper. https://www.ge.com/additive/download-ebm-white-paper (accessed 17 February 2022).

[7] A. Mussatto, R. Groarke, R.K. Vijayaraghavan, C. Hughes, M.A. Obeidi, M.N. Doğu, M.A. Yalçin, P.J. McNally, Y. Delaure, D. Brabazon, Assessing dependency of part properties on the printing location in laser-powder bed fusion metal additive manufacturing, Mater. Today Commun. 30 (2022). https://doi.org/10.1016/j.mtcomm.2022.103209.

[8] W.J. Sames, F.A. List, S. Pannala, R.R. Dehoff, S.S. Babu, The metallurgy and processing science of metal additive manufacturing, Int. Mater. Rev. 61 (2016) 315–360. https://doi.org/10.1080/09506608.2015.1116649.

[9] M. Galati, O. Di Mauro, L. Iuliano, Finite element simulation of multilayer electron beam melting for the improvement of build quality, Crystals. 10 (2020) 1–18. https://doi.org/10.3390/cryst10060532.

[10] T.R Mahale, Electron Beam Melting of Advanced Materials and Structures, Doctoral dissertation, NC State University, (2019). http://www.lib.ncsu.edu/resolver/1840.16/4943.

[11] J. Milberg, M. Sigl, Electron beam sintering of metal powder, Prod. Eng. 2 (2008) 117–122. https://doi.org/10.1007/s11740-008-0088-2.

[12] P. Wanjara, D. Backman, F. Sikan, J. Gholipour, R. Amos, P. Patnaik, M. Brochu, Microstructure and Mechanical Properties of Ti-6Al-4V Additively Manufactured by Electron Beam Melting with 3D Part Nesting and Powder Reuse Influences, J. Manuf.

Mater. Process. 2022, 6, 21. https://doi.org/10.3390/jmmp6010021.

[13] D. Manfredi, F. Calignano, M. Krishnan, R. Canali, E. Paola, S. Biamino, D. Ugues, M. Pavese, P. Fino, Additive Manufacturing of Al Alloys and Aluminium Matrix Composites (AMCs), Light Met. Alloy. Appl. (2014) 2–34. https://doi.org/10.5772/58534.

[14] S. Rosso, F. Uriati, L. Grigolato, R. Meneghello, G. Concheri, G. Savio, An optimization workflow in design for additive manufacturing, Appl. Sci. 11 (2021). https://doi.org/10.3390/app11062572.

[15] P.D. Olson, General Electric. https://www.ge.com/news/reports/100000-patients-later-3d-printed-hip-decade-old-going-strong, 2018 (accessed 02 February 2022).

[16] T. Grimm, G. Wiora, G. Witt, Characterization of typical surface effects in additive manufacturing with confocal microscopy, Surf. Topogr. Metrol. Prop. 3 (2015). https://doi.org/10.1088/2051-672X/3/1/014001.

[17] S. Liu, Y.C. Shin, Additive manufacturing of Ti6Al4V alloy: A review, Mater. Des. 164 (2019) 107552. https://doi.org/10.1016/j.matdes.2018.107552.

[18] A. Triantaphyllou, C.L. Giusca, G.D. Macaulay, F. Roerig, M. Hoebel, R.K. Leach, B. Tomita, K.A. Milne, Surface texture measurement for additive manufacturing, Surf. Topogr. Metrol. Prop. 3 (2015). https://doi.org/10.1088/2051-672X/3/2/024002.

[19] G. Nicoletto, R. Konečná, M. Frkáň, E. Riva, Surface roughness and directional fatigue behavior of as-built EBM and DMLS Ti6Al4V, Int. J. Fatigue. 116 (2018) 140–148. https://doi.org/10.1016/j.ijfatigue.2018.06.011.

[20] W. Liu, C. Chen, S. Shuai, R. Zhao, L. Liu, X. Wang, T. Hu, W. Xuan, C. Li, J. Yu, J. Wang, Z. Ren, Study of pore defect and mechanical properties in selective laser melted Ti6Al4V alloy based on X-ray computed tomography, Materials Science and

Engineering: A (2020), Vol. 797, 139981, https://doi.org/10.1016/j.msea.2020.139981.

[21] N. Senin, A. Thompson, R.K. Leach, Characterisation of the topography of metal additive surface features with different measurement technologies, Meas. Sci. Technol. 28 (2017). https://doi.org/10.1088/1361-6501/aa7ce2.

[22] R. Klingvall Ek, J. Hong, A. Thor, M. Bäckström, L.-E. Rännar, Micro- to Macroroughness of Additively Manufactured Titanium Implants in Terms of Coagulation and Contact Activation, Int. J. Oral Maxillofac. Implants. 32 (2017) 565–574. https://doi.org/10.11607/jomi.5357.

[23] V. Chastand, P. Quaegebeur, W. Maia, E. Charkaluk, Comparative study of fatigue properties of Ti-6Al-4V specimens built by electron beam melting (EBM) and selective laser melting (SLM), Mater. Charact. 143 (2018) 76–81. https://doi.org/10.1016/j.matchar.2018.03.028.

[24] P. Aliprandi, F. Giudice, E. Guglielmino, A. Sili, Tensile and Creep Properties Improvement of Ti-6Al-4V Alloy Specimens Produced by Electron Beam Powder Bed Fusion Additive Manufacturing, Metals (Basel). 9 (2019). https://doi.org/10.3390/met9111207.

[25] A.A. Al-Tamimi, M.A. Hernandez, A. Omar, D.F. Morales-Aldana, C. Peach, P. Bartolo, Mechanical, biological and tribological behaviour of fixation plates 3D printed by electron beam and selective laser melting, Int. J. Adv. Manuf. Technol. 109 (2020) 673–688. https://doi.org/10.1007/s00170-020-05676-1.

[26] M.J. Mian, J. Razmi, L. Ladani, Defect analysis and fatigue strength prediction of as-built Ti6Al4V parts, produced using electron beam melting (EBM) AM technology, Materialia, 16 (2021). https://doi.org/10.1016/j.mtla.2021.101041.

[27] T.V. Vorbuguer, Surface finish metrology tutorial, Natl. Inst. Stand. Technol. (1990) 1–159. https://www.nist.gov/system/files/documents/calibrations/89-4088.pdf.

[28] H. Khalid Rafi., N. V. Karthik, T.L. Starr, B.E. Stucker, Mechanical property evaluation of Ti-6Al-4V parts made using Electron Beam Melting, 23rd Annu. Int. Solid Free. Fabr. Symp. - An Addit. Manuf. Conf. SFF 2012. (2012) 526–535. http://dx.doi.org/10.26153/tsw/15371.

[29] K.S. Chan, M. Koike, R.L. Mason, T. Okabe, Fatigue life of titanium alloys fabricated by additive layer manufacturing techniques for dental implants, Metall. Mater. Trans. A Phys. Metall. Mater. Sci. 44 (2013) 1010–1022. https://doi.org/10.1007/s11661-012-1470-4.

[30] Y.Y. Sun, S. Gulizia, C.H. Oh, D. Fraser, M. Leary, Y.F. Yang, M. Qian, The Influence of As-Built Surface Conditions on Mechanical Properties of Ti-6Al-4V Additively Manufactured by Selective Electron Beam Melting, Jom. 68 (2016) 791–798. https://doi.org/10.1007/s11837-015-1768-y.

[31] P. Lhuissier, C. de Formanoir, G. Martin, R. Dendievel, S. Godet, Geometrical control of lattice structures produced by EBM through chemical etching: Investigations at the scale of individual struts, Mater. & Des. 110 (2016) 485–493. https://doi.org/10.1016/j.matdes.2016.08.029.

[32] A. Acquesta, T. Monetta, As-built EBM and DMLS Ti-6Al-4V parts: Topography–corrosion resistance relationship in a simulated body fluid, Metals (Basel). 10 (2020) 1–15. https://doi.org/10.3390/met10081015.

[33] T.R. Thomas, Roughness and function, Surf. Topogr. Metrol. Prop. 2 (2014). https://doi.org/10.1088/2051-672X/2/1/014001.

[34] B.G. Rosen, L. Eriksson, M. Bergman, Kansei, surfaces and perception engineering, Surf. Topogr. Metrol. Prop. 4 (2016). https://doi.org/10.1088/2051-672X/4/3/033001.

[35] J. M. Bennett, L. Mattsson, Introduction to Surface Roughness and Scattering, Optical

Society of America, Washington, D.C. (1989). https://dx.doi.org/10.1364/1557521085.

[36] M. Leary, M. Khorasani, A. Sarker, J. Tran, K. Fox, D. Downing, A. Du Plessis, Surface roughness, Elsevier Inc., 2021. https://doi.org/10.1016/B978-0-12-824090-8.00023-8.

[37] N. Sanaei, A. Fatemi, Analysis of the effect of surface roughness on fatigue performance of powder bed fusion additive manufactured metals, Theor. Appl. Fract. Mech. 108 (2020). https://doi.org/10.1016/j.tafmec.2020.102638.

[38] M. Kahlin, H. Ansell, J.J. Moverare, Fatigue behaviour of notched additive manufactured Ti6Al4V with as-built surfaces, Int. J. Fatigue. 101 (2017) 51–60. https://doi.org/10.1016/j.ijfatigue.2017.04.009.

[39] R. Schur, S. Ghods, E. Schultz, C. Wisdom, R. Pahuja, A. Montelione, D. Arola, M. Ramulu, A Fractographic Analysis of Additively Manufactured Ti6Al4V by Electron Beam Melting: Effects of Powder Reuse, J. Fail. Anal. Prev. 20 (2020) 794–803. https://doi.org/10.1007/s11668-020-00875-0.

[40] S.M.J. Razavi, B. Van Hooreweder, F. Berto, Effect of build thickness and geometry on quasi-static and fatigue behavior of Ti-6Al-4V produced by Electron Beam Melting, Addit. Manuf. 36 (2020). https://doi.org/10.1016/j.addma.2020.101426.

[41] M. Fousová, D. Vojtěch, K. Doubrava, M. Daniel, C.F. Lin, Influence of inherent surface and internal defects on mechanical properties of additively manufactured Ti6Al4V alloy: Comparison between selective laser melting and electron beam melting, Materials (Basel). 11 (2018). https://doi.org/10.3390/ma11040537.

[42] K.S. Chan, Characterization and analysis of surface notches on Ti-alloy plates fabricated by additive manufacturing techniques, Surf. Topogr. Metrol. Prop. 3 (2015). https://doi.org/10.1088/2051-672X/3/4/044006.

[43] D. Greitemeier, C. Dalle Donne, F. Syassen, J. Eufinger, T. Melz, Effect of surface roughness on fatigue performance of additive manufactured Ti–6Al–4V, Mater. Sci. Technol. (United Kingdom). 32 (2016) 629–634. https://doi.org/10.1179/1743284715Y.0000000053.

[44] R. Jones, J.G. Michopoulos, A.P. Iliopoulos, R.K. Singh Raman, N. Phan, T. Nguyen, Representing crack growth in additively manufactured Ti-6Al-4V, Int. J. Fatigue. 116 (2018) 610–622. https://doi.org/10.1016/j.ijfatigue.2018.07.019.

[45] B. Vayssette, N. Saintier, C. Brugger, M. El May, Surface roughness effect of SLM and EBM Ti-6Al-4V on multiaxial high cycle fatigue, Theor. Appl. Fract. Mech. 108 (2020) 102581. https://doi.org/10.1016/j.tafmec.2020.102581.

[46] P.K.C. Venkatsurya, B. Girase, R.D.K. Misra, T.C. Pesacreta, M.C. Somani, L.P. Karjalainen, The interplay between osteoblast functions and the degree of nanoscale roughness induced by grain boundary grooving of nanograined materials, Mater. Sci. Eng. C. 32 (2012) 330–340. https://doi.org/10.1016/j.msec.2011.10.036.

[47] P.A. Kokkinos, P.G. Koutsoukos, D.D. Deligianni, Detachment strength of human osteoblasts cultured on hydroxyapatite with various surface roughness. Contribution of integrin subunits, J. Mater. Sci. Mater. Med. 23 (2012) 1489–1498. https://doi.org/10.1007/s10856-012-4628-0.

[48] P. Thomsen, J. Malmström, L. Emanuelsson, M. René, A. Snis, Electron beam-melted, free-form-fabricated titanium alloy implants: Material surface characterization and early bone response in rabbits, J. Biomed. Mater. Res. - Part B Appl. Biomater. 90 B (2009) 35–44. https://doi.org/10.1002/jbm.b.31250.

[49] V. Weissmann, P. Drescher, H. Seitz, H. Hansmann, R. Bader, A. Seyfarth, A. Klinder, A. Jonitz-Heincke, Effects of Build Orientation on Surface Morphology and Bone Cell Activity of Additively Manufactured Ti6Al4V Specimens, Materials (Basel). 11 (2018). https://doi.org/10.3390/ma11060915.

[50] B.S. Lee, H.J. Lee, K.S. Lee, H.G. Kim, G.H. Kim, C.W. Lee, Enhanced osseointegration of Ti6Al4V ELI screws built-up by electron beam additive manufacturing: An experimental study in rabbits, Appl. Surf. Sci. 508 (2020) 145160. https://doi.org/10.1016/j.apsusc.2019.145160.

[51] D.S. Ruppert, O.L.A. Harrysson, D.J. Marcellin-Little, S. Abumoussa, L.E. Dahners, P.S. Weinhold, Osseointegration of Coarse and Fine Textured Implants Manufactured by Electron Beam Melting and Direct Metal Laser Sintering, 3D Print. Addit. Manuf. 4 (2017) 91–97. https://doi.org/10.1089/3dp.2017.0008.

[52] C. Lindsay, D. Ruppert, S. Abumoussa, L. Dahners, P. Weinhold, Benefits of additive manufacturing and micro and nano surface texture modifications on mechanical strength and infection resistance of skin–implant interfaces in rats, J. Biomater. Appl. 34 (2020) 1193–1200. https://doi.org/10.1177/0885328220903961.

[53] I. Kaur, P. Singh, State-of-the-art in heat exchanger additive manufacturing, Int. J. Heat Mass Transf. 178 (2021) 121600. https://doi.org/10.1016/j.ijheatmasstransfer.2021.121600.

[54] S. Han, F. Salvatore, J. Rech, J. Bajolet, Abrasive flow machining (AFM) finishing of conformal cooling channels created by selective laser melting (SLM), Precis. Eng. 64 (2020) 20–33. https://doi.org/10.1016/j.precisioneng.2020.03.006.

[55] M. Galati, L. Iuliano, A literature review of powder-based electron beam melting focusing on numerical simulations, Addit. Manuf. 19 (2018) 1–20. https://doi.org/10.1016/j.addma.2017.11.001.

[56] D.J. Whitehouse, Handbook of Surface and Nanometrology (1st ed.), Taylor & Francis (2002). https://doi.org/10.1201/9781420034196.

[57] D.J. Whitehouse, Surface Characterization and Roughness Measurement in

Engineering. In: Rastogi, P.K. (eds) Photomechanics. Topics in Applied Physics, vol 77. Springer, Berlin, Heidelberg (2000). https://doi.org/10.1007/3-540-48800-6_12.

[58] D.J. Whitehouse, Surface metrology, Meas. Sci. Technol. 8 (1997) 955–972. https://doi.org/10.1088/0957-0233/8/9/002.

[59] A. Townsend, N. Senin, L. Blunt, R.K. Leach, J.S. Taylor, Surface texture metrology for metal additive manufacturing: a review, Precis. Eng. 46 (2016) 34–47. https://doi.org/10.1016/j.precisioneng.2016.06.001.

[60] M. Heinl, M. Heinl, S. Greiner, K. Wudy, C. Pobel, M. Rasch, M. Rasch, F. Huber, F. Huber, T. Papke, M. Merklein, M. Schmidt, M. Schmidt, C. Körner, D. Drummer, T. Hausotte, Measuring procedures for surface evaluation of additively manufactured powder bed-based polymer and metal parts, Meas. Sci. Technol. 31 (2020). https://doi.org/10.1088/1361-6501/ab89e2.

[61] R.K. Leach, D. Bourell, S. Carmignato, A. Donmez, N. Senin, W. Dewulf, Geometrical metrology for metal additive manufacturing, CIRP Ann. 68 (2019) 677–700. https://doi.org/10.1016/j.cirp.2019.05.004.

[62] R. Leach, Optical Measurement of Surface Topography, Springer Berlin, Heidelberg (2018), 323. https://doi.org/10.1007/978-3-642-12012-1.

[63] F. Cabanettes, A. Joubert, G. Chardon, V. Dumas, J. Rech, C. Grosjean, Z. Dimkovski, Topography of as built surfaces generated in metal additive manufacturing: A multi scale analysis from form to roughness, Precis. Eng. 52 (2018) 249–265. https://doi.org/10.1016/j.precisioneng.2018.01.002.

[64] S. Lou, X. Jiang, W. Sun, W. Zeng, L. Pagani, P.J. Scott, Characterisation methods for powder bed fusion processed surface topography, Precis. Eng. Int. Soc. Precis. Eng. Nanotechnol. 57 (2019) 1–15. https://doi.org/10.1016/j.precisioneng.2018.09.007.

[65] A. Thompson, N. Senin, I. Maskery, L. Korner, S. Lawes, R. Leach, Internal surface measurement of metal powder bed fusion parts, Addit. Manuf. 20 (2018) 126–133. https://doi.org/10.1016/j.addma.2018.01.003.

[66] G. Pyka, G. Kerckhofs, I. Papantoniou, M. Speirs, J. Schrooten, M. Wevers, Surface roughness and morphology customization of additive manufactured open porous Ti6Al4V structures, Materials (Basel). 6 (2013) 4737–4757. https://doi.org/10.3390/ma6104737.

[67] G. Kerckhofs, G. Pyka, M. Moesen, S. Van Bael, J. Schrooten, M. Wevers, High-resolution microfocus X-ray computed tomography for 3d surface roughness measurements of additive manufactured porous materials, Adv. Eng. Mater. 15 (2013) 153–158. https://doi.org/10.1002/adem.201200156.

[68] A. Thompson, I. Maskery, R.K. Leach, X-ray computed tomography for additive manufacturing: A review, Meas. Sci. Technol. 27 (2016). https://doi.org/10.1088/0957-0233/27/7/072001.

[69] S. Moylan, A. Cooke, K. Jurrens, J. Slotwinski, M.A. Donmez, A Review of test artifacts for additive Manufacturing (Report Number: NISTIR 7858), Natl. Inst. Stand. Technol. (2012). https://doi.org/10.6028/NIST.IR.7858.

[70] M. Mahesh, Rapid prototyping and manufacturing benchmarking, Doctoral dissertation, National University of Singapore (2002), 57–94. http://scholarbank.nus.edu.sg/handle/10635/14697.

[71] L. Rebaioli, I. Fassi, A review on benchmark artifacts for evaluating the geometrical performance of additive manufacturing processes, Int. J. Adv. Manuf. Technol. 93 (2017) 2571–2598. https://doi.org/10.1007/s00170-017-0570-0.

[72] P.E. Reeves, Reducing the surface deviation of Stereolithography components,

Doctoral dissertation, University of Nottingham (1998). http://eprints.nottingham.ac.uk/13191/1/263458.pdf.

[73] G. Strano, L. Hao, R.M. Everson, K.E. Evans, Surface roughness analysis, modelling and prediction in selective laser melting, J. Mater. Process. Technol. 213 (2013) 589–597. https://doi.org/10.1016/j.jmatprotec.2012.11.011.

[74] ISO/ASTM 52902:2019 Additive manufacturing - Test artifacts - Geometric capability assessment of additive manufacturing systems, ASTM and International Organization for Standardization ISO, 2019.

[75] M. Galati, G. Rizza, S. Defanti, L. Denti, Surface roughness prediction model for Electron Beam Melting (EBM) processing Ti6Al4V, Precis. Eng. 69 (2021) 19–28. https://doi.org/https://doi.org/10.1016/j.precisioneng.2021.01.002.

[76] M. Galati, P. Minetola, G. Rizza, Surface Roughness Characterisation and Analysis of the Electron Beam Melting (EBM) Process, Materials (Basel). 12 (2019). https://doi.org/10.3390/ma12132211.

[77] ISO 4287:1997 Geometrical Product Specifications (GPS) — Surface texture: Profile method — Terms, definitions and surface texture parameters, International Organization for Standardization ISO, 1997.

[78] ISO 25178-2:2012 Geometrical product specifications (GPS) — Surface texture: Areal — Part 2: Terms, definitions and surface texture parameters, International Organization for Standardization ISO, 2012.

[79] D.J. Whitehouse, Surfaces and their measurements, Butterworth-Heinemann (2002). https://doi.org/10.1016/B978-1-903996-01-0.X5000-2.

[80] J.C. Fox, S.P. Moylan, B.M. Lane, Effect of process parameters on the surface roughness of overhanging structures in laser powder bed fusion additive manufacturing,

in: Davies, MA and MSaoubi, R (Ed.), 3RD CIRP Conf. Surf. Integr., 2016: pp. 131–134. https://doi.org/10.1016/j.procir.2016.02.347.

[81] S. Bagherifard, M. Guagliano, 12 - Post-processing, In Additive Manufacturing Materials and Technologies, Fundamentals of Laser Powder Bed Fusion of Metals, Elsevier, 2021, pp. 327-348, Elsevier Inc. (2021). https://doi.org/10.1016/B978-0-12-824090-8.00001-9.

[82] E. Maleki, S. Bagherifard, M. Bandini, M. Guagliano, Surface post-treatments for metal additive manufacturing: Progress, challenges, and opportunities, Addit. Manuf. 37 (2021) 101619. https://doi.org/10.1016/j.addma.2020.101619.

[83] Y.Y. Sun, S.L. Lu, S. Gulizia, C.H. Oh, D. Fraser, M. Leary, M. Qian, Fatigue Performance of Additively Manufactured Ti-6Al-4V: Surface Condition vs. Internal Defects, Jom. 72 (2020) 1022–1030. https://doi.org/10.1007/s11837-020-04025-7.

[84] A.S. Patil, S. V. Ingle, Y.S. More, M.S. Mathe, Machining Challenges in Ti-6Al-4V . - A Review, Int. J. Innov. Eng. Technol. 5 (2015) 6–23. ijiet.com/wp-content/uploads/2015/08/2.pdf.

[85] S. Pradhan, S. Singh, C. Prakash, G. Królczyk, A. Pramanik, C.I. Pruncu, Investigation of machining characteristics of hard-to-machine Ti-6Al-4V-ELI alloy for biomedical applications, J. Mater. Res. Technol. 8 (2019) 4849–4862. https://doi.org/10.1016/j.jmrt.2019.08.033.

[86] S. Bagheri Fard, M. Guagliano, Effects of surfaces nanocrystallization induced by shot peening on material properties : a Review, Frat. Ed Integrità Strutt. 3 (2009) 3–16. https://doi.org/10.3221/igf-esis.07.01.

[87] H. Soyama, F. Takeo, Effect of Various Peening Methods on the Fatigue Properties of Titanium Alloy Ti6Al4V Manufactured by Direct Metal Laser Sintering and Electron Beam Melting, Materials (Basel). 13 (2020). https://doi.org/10.3390/ma13102216.

[88] M.M. Basha, S.M. Basha, V.K. Jain, M.R. Sankar, State of the art on chemical and electrochemical based finishing processes for additive manufactured features, Additive Manufacturing, Volume 58 (2022), 103028. https://doi.org/10.1016/j.addma.2022.103028.

[89] Y.-C. Wu, C.-N. Kuo, Y.-C. Chung, C.-H. Ng, J.C. Huang, Effects of Electropolishing on Mechanical Properties and Bio-Corrosion of Ti6Al4V Fabricated by Electron Beam Melting Additive Manufacturing, Materials (Basel). 12 (2019). https://doi.org/10.3390/ma12091466.

[90] S. Nesli, O. Yilmaz, Surface characteristics of laser polished Ti-6Al-4V parts produced by electron beam melting additive manufacturing process, Int. J. Adv. Manuf. Technol. 114 (2021) 271–289. https://doi.org/10.1007/s00170-021-06861-6.

[91] Y. Tian, W.S. Gora, A.P. Cabo, L.L. Parimi, D.P. Hand I, S. Tammas-Williams, P.B. Prangnell, Material interactions in laser polishing powder bed additive manufactured Ti6Al4V components, Addit. Manuf. 20 (2018) 11–22. https://doi.org/10.1016/j.addma.2017.12.010.

[92] S. Genna, G. Rubino, Laser Finishing of Ti6Al4V Additive Manufactured Parts by Electron Beam Melting, Appl. Sci. 10 (2020). https://doi.org/10.3390/app10010183.

[93] A. Mohammad, M.K. Mohammed, A.M. Alahmari, Effect of laser ablation parameters on surface improvement of electron beam melted parts, Int. J. Adv. Manuf. Technol. 87 (2016) 1033–1044. https://doi.org/10.1007/s00170-016-8533-4.

[94] S. Taylor, J.B. Wright, E.C. Forrest, B. Jared, J. Koepke, J. Beaman, Investigating relationship between surface topography and emissivity of metallic additively manufactured parts, Int. Commun. HEAT MASS Transf. 115 (2020). https://doi.org/10.1016/j.icheatmasstransfer.2020.104614.

[95] A.T. Sidambe, Three dimensional surface topography characterization of the electron beam melted Ti6Al4V, Met. Powder Rep. 72 (2017) 200–205. https://doi.org/10.1016/j.mprp.2017.02.003.

[96] L. Dowling, J. Kennedy, S. O'Shaughnessy, D. Trimble, A review of critical repeatability and reproducibility issues in powder bed fusion, Mater. Des. 186 (2020). https://doi.org/10.1016/j.matdes.2019.108346.

[97] R. Leach, Characterisation of areal surface texture, Springer Berlin, Heidelberg (2013), 353. https://doi.org/10.1007/978-3-642-36458-7.

[98] R. Borrelli, S. Franchitti, C. Pirozzi, L. Carrino, L. Nele, W. Polini, L. Sorrentino, A. Corrado, Ti6Al4V Parts Produced by Electron Beam Melting: Analysis of Dimensional Accuracy and Surface Roughness, J. Adv. Manuf. Syst. 19 (2020) 107–130. https://doi.org/10.1142/S0219686720500067.

[99] O. Diegel, A. Nordin, D. Motte, Additive Manufacturing Technologies. In: A Practical Guide to Design for Additive Manufacturing. Springer Series in Advanced Manufacturing. Springer, Singapore (2019). https://doi.org/10.1007/978-981-13-8281-9_2.

[100] R.K. Leach, D. Bourell, S. Carmignato, A. Donmez, N. Senin, W. Dewulf, Geometrical metrology for metal additive manufacturing, CIRP Ann. Technol. 68 (2019) 677–700. https://doi.org/10.1016/j.cirp.2019.05.004.

[101] Z. Liu, Z. Zhao, J. Liu, Q. Wang, Z. Guo, J. Wang, G. Yang, S. Gong, Anisotropy in microstructure and tensile properties of Ti-5Al-5Mo-5V-1Cr-1Fe produced via additive manufacturing, Mater. Sci. Eng. A-STRUCTURAL Mater. Prop. Microstruct. Process. 798 (2020). https://doi.org/10.1016/j.msea.2020.140093.

[102] A. Safdar, H.Z. He, L.Y. Wei, A. Snis, L.E. Chavez De Paz, Effect of process parameters settings and thickness on surface roughness of EBM produced Ti-6Al-4V,

Rapid Prototyp. J. 18 (2012) 401–408. https://doi.org/10.1108/13552541211250391.

[103] W. Everhart, E. Sawyer, T. Neidt, J. Dinardo, B. Brown, The effect of surface finish on tensile behavior of additively manufactured tensile bars, J. Mater. Sci. 51 (2016) 3836–3845. https://doi.org/10.1007/s10853-015-9702-9.

[104] C. Körner, A. Bauereiß, E. Attar, Fundamental consolidation mechanisms during selective beam melting of powders, Model. Simul. Mater. Sci. Eng. 21 (2013). https://doi.org/10.1088/0965-0393/21/8/085011.

[105] T. Hibiya, S. Ozawa, Marangoni Flow and Surface Tension of High Temperature Melts. In: Fukuyama, H., Waseda, Y. (eds) High-Temperature Measurements of Materials. Advances in Materials Research, Vol. 11 (2009). Springer, Berlin, Heidelberg. https://doi.org/10.1007/978-3-540-85918-5_3.

[106] S. Shrestha, Y.K. Chou, Process effect on part surface roughness in powder-bed electron beam additive manufacturing, ASME 2017 12th Int. Manuf. Sci. Eng. Conf. MSEC 2017 Collocated with JSME/ASME 2017 6th Int. Conf. Mater. Process. 2 (2017). https://doi.org/10.1115/MSEC2017-3015.

[107] M. Suard, G. Martin, P. Lhuissier, R. Dendievel, F. Vignat, J.J. Blandin, F. Villeneuve, Mechanical equivalent diameter of single struts for the stiffness prediction of lattice structures produced by Electron Beam Melting, Addit. Manuf. 8 (2015) 124–131. https://doi.org/10.1016/j.addma.2015.10.002.

[108] T. Persenot, A. Burr, G. Martin, J.Y. Buffiere, R. Dendievel, E. Maire, Effect of build orientation on the fatigue properties of as-built Electron Beam Melted Ti-6Al-4V alloy, Int. J. Fatigue. 118 (2019) 65–76. https://doi.org/10.1016/j.ijfatigue.2018.08.006.

[109] H. Gong, H. Gu, K. Zeng, J.J.S. Dilip, D. Pal, B. Stucker, D. Christiansen, J. Beuth, J.J. Lewandowski, Melt pool characterization for selective laser melting of Ti-6Al-4V pre-alloyed powder, International Solid Freeform Fabrication Symposium (2014), 256–267.

http://dx.doi.org/10.26153/tsw/15682.

[110] N. Sanaei, A. Fatemi, Defects in additive manufactured metals and their effect on fatigue performance: A state-of-the-art review, Prog. Mater. Sci. 117 (2021). https://doi.org/10.1016/j.pmatsci.2020.100724.

[111] J.P. Kruth, L. Froyen, J. Van Vaerenbergh, P. Mercelis, M. Rombouts, B. Lauwers, Selective laser melting of iron-based powder, J. Mater. Process. Technol. 149 (2004) 616–622. https://doi.org/10.1016/j.jmatprotec.2003.11.051.

[112] M.F. Zäh, S. Lutzmann, Modelling and simulation of electron beam melting, Prod. Eng. 4 (2010) 15–23. https://doi.org/10.1007/s11740-009-0197-6.

[113] A. V. Gusarov, I. Yadroitsev, P. Bertrand, I. Smurov, Heat transfer modelling and stability analysis of selective laser melting, Appl. Surf. Sci. 254 (2007) 975–979. https://doi.org/10.1016/j.apsusc.2007.08.074.

[114] K.S. Chan, Characterization and analysis of surface notches on Ti-alloy plates fabricated by additive manufacturing techniques, Surf. Topogr. Prop. 3 (2015). https://doi.org/10.1088/2051-672X/3/4/044006.

[115] J. Karlsson, A. Snis, H. Engqvist, J. Lausmaa, Characterization and comparison of materials produced by Electron Beam Melting (EBM) of two different Ti-6Al-4V powder fractions, J. Mater. Process. Technol. 213 (2013) 2109–2118. https://doi.org/10.1016/j.jmatprotec.2013.06.010.

[116] J.K. Algardh, T. Horn, H. West, R. Aman, A. Snis, H. Engqvist, J. Lausmaa, O. Harrysson, Thickness dependency of mechanical properties for thin-walled titanium parts manufactured by Electron Beam Melting (EBM) ®, Addit. Manuf. 12 (2016) 45–50. https://doi.org/10.1016/j.addma.2016.06.009.

[117] D. Kotzem, A. Höffgen, R. Raveendran, F. Stern, K. Möhring, F. Walther, Position-

dependent mechanical characterization of the PBF-EB-manufactured Ti6Al4V alloy. Prog Addit Manuf 7, 249–260 (2022). https://doi.org/10.1007/s40964-021-00228-9.

[118] M. Jamshidinia, R. Kovacevic, The influence of heat accumulation on the surface roughness in powder-bed additive manufacturing, Surf. Topogr. Prop. 3 (2015). https://doi.org/10.1088/2051-672X/3/1/014003.

[119] T. Scharowsky, A. Bauereiss, C. Koerner, Influence of the hatching strategy on consolidation during selective electron beam melting of Ti-6Al-4V, Int. J. Adv. Manuf. Technol. 92 (2017) 2809–2818. https://doi.org/10.1007/s00170-017-0375-1.

[120] A.T. Silvestri, S. Foglia, R. Borrelli, S. Franchitti, C. Pirozzi, A. Astarita, Electron beam melting of Ti6Al4V: Role of the process parameters under the same energy density, J. Manuf. Process. 60 (2020) 162–179. https://doi.org/10.1016/j.jmapro.2020.10.065.

[121] P. Wang, W.J. Sin, M.L.S. Nai, J. Wei, Effects of processing parameters on surface roughness of additive manufactured Ti-6Al-4V via electron beam melting, Materials (Basel). 10 (2017) 8–14. https://doi.org/10.3390/ma10101121.

[122] U. Prisco, A. Astarita, A. El Hassanin, S. Franchitti, Influence of processing parameters on microstructure and roughness of electron beam melted Ti-6Al-4V titanium alloy, Mater. Manuf. Process. 34 (2019) 1753–1760. https://doi.org/10.1080/10426914.2019.1683576.

[123] R.K. Ek, L.-E. Rannar, M. Backstom, P. Carlsson, The effect of EBM process parameters upon surface roughness, Rapid Prototyping Journal, Vol. 22 No. 3, pp. 495-503, (2016). https://doi.org/10.1108/RPJ-10-2013-0102.

[124] A. Neira-Arce, Thermal Modeling and Simulation of Electron Beam Melting for Rapid Prototyping on Ti6Al4V Alloys, Doctoral dissertation, North Carolina State University, Raleigh, North Carolina (2012). http://www.lib.ncsu.edu/resolver/1840.16/8202.

[125] P. Moghimian, T. Poirie, M. Habibnejad-Korayem, J.A. Zavala, J. Kroeger, F. Marion, F. Larouche, Metal powders in additive manufacturing: A review on reusability and recyclability of common titanium, nickel and aluminum alloys, Addit. Manuf. 43 (2021). https://doi.org/10.1016/j.addma.2021.102017.

[126] B. Liu, R. Wildman, C. Tuck, I. Ashcroft, R. Hague, Investigation the Effect of Particle Size Distribution on Processing Parameters Optimisation in Selective Laser Melting Process, International Solid Freeform Fabrication Symposium (2011) 227–238. http://dx.doi.org/10.26153/tsw/15290.

[127] M.N. Ahsan, A.J. Pinkerton, R.J. Moat, J. Shackleton, A comparative study of laser direct metal deposition characteristics using gas and plasma-atomized Ti-6Al-4V powders, Mater. Sci. Eng. A. 528 (2011) 7648–7657. https://doi.org/10.1016/j.msea.2011.06.074.

[128] A.M. Rausch, V.E. Kueng, C. Pobel, M. Markl, C. Koerner, Predictive Simulation of Process Windows for Powder Bed Fusion Additive Manufacturing: Influence of the Powder Bulk Density, Materials (Basel). 10 (2017). https://doi.org/10.3390/ma10101117.\

[129] M. Sinico, A. Witvrouw, W. Dewulf, Influence of the particle size distribution on surface quality of Maraging 300 parts produced by Laser Powder Bed Fusion, Proceedings of the Special Interest Group meeting on Advancing Precision in Additive Manufacturing, pp. 31 (2019) 31–34. https://www.euspen.eu/knowledge-base/AM19115.pdf.

[130] H. Gong, K. Rafi, T. Starr, B. Stucker, The effects of processing parameters on defect regularity in Ti-6Al-4V parts fabricated by Selective Laser Melting and Electron Beam Melting, International Solid Freeform Fabrication Symposium (2013) 424–439. https://repositories.lib.utexas.edu/handle/2152/88631.

[131] M. Nakatani, H. Masuo, Y. Tanaka, Y. Murakami, Effect of Surface Roughness on Fatigue Strength of Ti-6Al-4V Alloy Manufactured by Additive Manufacturing, Procedia Struct. Integr. 19 (2019) 294–301. https://doi.org/10.1016/j.prostr.2019.12.032.

[132] A.B. Spierings, N. Herres, G. Levy, Influence of the particle size distribution on surface quality and mechanical properties in AM steel parts, Rapid Prototyp. J. 17 (2011) 195–202. https://doi.org/10.1108/13552541111124770.

[133] Y. Cao, M. Delin, F. Kullenberg, L. Nyborg, Surface modification of Ti-6Al-4V powder during recycling in EBM process, Surf. Interface Anal. 52 (2020) 1066–1070. https://doi.org/10.1002/sia.6847.

[134] A. Montelione, S. Ghods, R. Schur, C. Wisdom, D. Arola, M. Ramulu, Powder Reuse in Electron Beam Melting Additive Manufacturing of Ti6Al4V: Particle Microstructure, Oxygen Content and Mechanical Properties, Addit. Manuf. 35 (2020) 101216. https://doi.org/10.1016/j.addma.2020.101216.

[135] H.P. Tang, M. Qian, N. Liu, X.Z. Zhang, G.Y. Yang, J. Wang, Effect of Powder Reuse Times on Additive Manufacturing of Ti-6Al-4V by Selective Electron Beam Melting, Jom. 67 (2015) 555–563. https://doi.org/10.1007/s11837-015-1300-4.

[136] V. Petrovic, R. Niñerola, Powder recyclability in electron beam melting for aeronautical use, Aircr. Eng. Aerosp. Technol. 87 (2015) 147–155. https://doi.org/10.1108/AEAT-11-2013-0212.

[137] G. Shanbhag, M. Vlasea, The effect of reuse cycles on Ti-6Al-4V powder properties processed by electron beam powder bed fusion, Manuf. Lett. 25 (2020) 60–63. https://doi.org/10.1016/j.mfglet.2020.07.007.

[138] S. Ghods, E. Schultz, C. Wisdom, R. Schur, R. Pahuja, A. Montelione, D. Arola, M. Ramulu, Electron beam additive manufacturing of Ti6Al4V: Evolution of powder

morphology and part microstructure with powder reuse, Materialia. 9 (2020) 100631. https://doi.org/10.1016/j.mtla.2020.100631.

[139] H. Li, M. Wang, D. Lou, W. Xia, X. Fang, Microstructural features of biomedical cobalt-chromium-molybdenum (CoCrMo) alloy from powder bed fusion to aging heat treatment, J. Mater. Sci. & Technol. 45 (2020) 146–156. https://doi.org/10.1016/j.jmst.2019.11.031.

[140] C. Qiu, C. Panwisawas, M. Ward, H.C. Basoalto, J.W. Brooks, M.M. Attallah, On the role of melt flow into the surface structure and porosity development during selective laser melting, Acta Mater. 96 (2015) 72–79. https://doi.org/10.1016/j.actamat.2015.06.004.

[141] T. Majumdar, T. Bazin, E.M.C. Ribeiro, J.E. Frith, N. Birbilis, Understanding the effects of PBF process parameter interplay on Ti-6Al-4V surface properties, PLoS One. 14 (2019) 1–24. https://doi.org/10.1371/journal.pone.0221198.

[142] J.K. Algardh, T. Horn, H. West, R. Aman, A. Snis, H. Engqvist, J. Lausmaa, O. Harrysson, Thickness dependency of mechanical properties for thin-walled titanium parts manufactured by Electron Beam Melting (EBM) ®, Addit. Manuf. 12 (2016) 45–50. https://doi.org/10.1016/j.addma.2016.06.009.

[143] J.J. Lewandowski, M. Seifi, Metal Additive Manufacturing: A Review of Mechanical Properties, in: Clarke, DR (Ed.), Annu. Rev. Mater. Res. VOL 46, 2016: pp. 151–186. https://doi.org/10.1146/annurev-matsci-070115-032024.

[144] S. Franchitti, R. Borrelli, C. Pirozzi, L. Carrino, W. Polini, L. Sorrentino, A. Gazzerro, Investigation on Electron Beam Melting: Dimensional accuracy and process repeatability, Vacuum. 157 (2018) 340–348. https://doi.org/10.1016/j.vacuum.2018.09.007.

[145] X.Z. Zhang, H.P. Tang, M. Leary, T. Song, L. Jia, M. Qian, Toward Manufacturing Quality Ti-6Al-4V Lattice Struts by Selective Electron Beam Melting (SEBM) for

Lattice Design, Jom. 70 (2018) 1870–1876. https://doi.org/10.1007/s11837-018-3030-x.

[146] C. de Formanoir, S. Michotte, O. Rigo, L. Germain, S. Godet, Electron beam melted Ti-6Al-4V: Microstructure, texture and mechanical behavior of the as-built and heat-treated material, Mater. Sci. Eng. A. 652 (2016) 105–119. https://doi.org/10.1016/j.msea.2015.11.052.

[147] A. Charles, A. Elkaseer, U. Paggi, L. Thijs, V. Hagenmeyer, S. Scholz, Down-facing surfaces in laser powder bed fusion of Ti6Al4V: Effect of dross formation on dimensional accuracy and surface texture, Addit. Manuf. 46 (2021) 102148. https://doi.org/10.1016/j.addma.2021.102148.

[148] S. Evsevleev, T. Mishurova, D. Khrapov, A. Paveleva, D. Meinel, R. Surmenev, M. Surmeneva, A. Koptyug, G. Bruno, X-ray Computed Tomography Procedures to Quantitatively Characterize the Morphological Features of Triply Periodic Minimal Surface Structures, Materials (Basel). 14 (2021). https://doi.org/10.3390/ma14113002.

[149] S. Sendino, M. Gardon, F. Lartategui, S. Martinez, A. Lamikiz, The effect of the laser incidence angle in the surface of l-pbf processed parts, Coatings. 10 (2020) 1–12. https://doi.org/10.3390/coatings10111024.

[150] S. Kleszczynski, A. Ladewig, K. Friedberger, J. zur Jacobsmühlen, D. Merhof, G. Witt, Position dependency of surface roughness in parts from laser beam melting systems, International Solid Freeform Fabrication Symposium (2015) 360–370. https://repositories.lib.utexas.edu/handle/2152/89333.

[151] B.Q. Li, Z. Li, P. Bai, B. Liu, Z. Kuai, Research on surface roughness of AlSi10Mg parts fabricated by laser powder bed fusion, Metals (Basel). 8 (2018) 1–10. https://doi.org/10.3390/met8070524.

[152] X. Chen, J. Zhang, X. Chen, X. Cheng, Z. Huang, Electron beam welding of laser

additive manufacturing Ti-6.5Al-3.5Mo-1.5Zr-0.3Si titanium alloy thick plate, Vacuum. 151 (2018) 116–121. https://doi.org/10.1016/j.vacuum.2018.02.011.

[153] F. Calignano, Investigation of the accuracy and roughness in the laser powder bed fusion process, Virtual Phys. Prototyp. 13 (2018) 97–104. https://doi.org/10.1080/17452759.2018.1426368.

[154] M. Grasso, B.M. Colosimo, Process defects and in situ monitoring methods in metal powder bed fusion: A review, Meas. Sci. Technol. 28 (2017) 1–40. https://doi.org/10.1088/1361-6501/aa5c4f.

[155] D.H. Abdeen, B.R. Palmer, Corrosion evaluation of Ti-6Al-4V parts produced with electron beam melting machine, RAPID Prototyp. J. 22 (2016) 322–329. https://doi.org/10.1108/RPJ-09-2014-0104.

[156] C. Guo, W. Ge, F. Lin, Effects of scanning parameters on material deposition during Electron Beam Selective Melting of Ti-6Al-4V powder, J. Mater. Process. Technol. 217 (2015) 148–157. https://doi.org/10.1016/j.jmatprotec.2014.11.010.

[157] J. Schwerdtfeger, R.F. Singer, C. Körner, In situ flaw detection by IR-imaging during electron beam melting, Rapid Prototyp. J. 18 (2012) 259–263. https://doi.org/10.1108/13552541211231572.

[158] S.S. Al-Bermani, An investigation into microstructure and microstructural control of additive layer manufactured Ti-6Al-4V by electron beam melting, Doctoral dissertation, Univiversity of Sheffield, UK, (2011) 258. http://ethos.bl.uk/OrderDetails.do?uin=uk.bl.ethos.555712.

[159] M. Galati, Chapter 8 - Electron beam melting process: a general overview, In Handbooks in Advanced Manufacturing, Additive Manufacturing, Elsevier (2021), pp. 277-301,ISBN 9780128184110. https://doi.org/10.1016/B978-0-12-818411-0.00014-8.

[160] N. Hrabe, T. Quinn, Effects of processing on microstructure and mechanical properties of a titanium alloy (Ti-6Al-4V) fabricated using electron beam melting (EBM), Part 2: Energy input, orientation, and location, Mater. Sci. Eng. A-STRUCTURAL Mater. Prop. Microstruct. Process. 573 (2013) 271–277. https://doi.org/10.1016/j.msea.2013.02.065.

[161] W. Yan, W. Ge, Y. Qian, S. Lin, B. Zhou, W.K. Liu, F. Lin, G.J. Wagner, Multi-physics modeling of single/multiple-track defect mechanisms in electron beam selective melting, Acta Mater. 134 (2017) 324–333. https://doi.org/10.1016/j.actamat.2017.05.061.

[162] M. Galati, A. Snis, L. Iuliano, Powder bed properties modelling and 3D thermo-mechanical simulation of the additive manufacturing Electron Beam Melting process, Addit. Manuf. 30 (2019) 100897. https://doi.org/10.1016/j.addma.2019.100897.

[163] B. Cheng, S. Price, J. Lydon, K. Cooper, K. Chou, On Process Temperature in Powder-Bed Electron Beam Additive Manufacturing: Model Development and Validation, J. Manuf. Sci. Eng. Trans. ASME. 136 (2014) 1–12. https://doi.org/10.1115/1.4028484.

[164] M. Sigl, S. Lutzmann, M.F. Zaeh, Transient physical effects in electron beam sintering, 17th International Solid Freeform Fabrication Symposium (2006) 464–477. https://repositories.lib.utexas.edu/handle/2152/80133.

[165] P. Karimi, C. Schnur, E. Sadeghi, J. Andersson, Contour design to improve topographical and microstructural characteristics of Alloy 718 manufactured by electron beam-powder bed fusion technique, Addit. Manuf. 32 (2020). https://doi.org/10.1016/j.addma.2019.101014.

[166] M. Galati, A. Snis, L. Iuliano, Experimental validation of a numerical thermal model of the EBM process for Ti6Al4V, Comput. Math. with Appl. 78 (2019) 2417–2427. https://doi.org/10.1016/j.camwa.2018.07.020.

[167] M. Svensson, U. Ackelid, Additive manufacturing with multibeam technology, Aeromat 21 Conf. Expo. Am. Soc. Met. (2010). https://asm.confex.com/asm/aero10/webprogram/Paper26575.html.

[168] D. Mallipeddi, T. Hajali, L.E. Rännar, A. Bergström, S. Hernandez, E. Strandh, L. Nyborg, P. Krajnik, Surface Integrity of Machined Electron Beam Melted Ti6Al4V Alloy Manufactured with Different Contour Settings and Heat Treatment, Procedia CIRP. 87 (2020) 327–332. https://doi.org/10.1016/j.procir.2020.02.091.

[169] M. Segersall, A. Kerwin, A. Hardaker, M. Kahlin, J. Moverare, Fatigue response dependence of thickness measurement methods for additively manufactured E-PBF Ti-6Al-4 V, FATIGUE \& Fract. Eng. Mater. \& Struct. 44 (2021) 1931–1943. https://doi.org/10.1111/ffe.13461.

This manuscript was submitted to the Additive Manufacturing journal in October 2022.

The effects of varying build thickness on the surface roughness of Ti-6Al-4V by electron beam powder bed fusion

Lucas C. B. Carolo[a], Marcelo F. de Oliveira[b], Jorge V. L. da Silva[c], Robert E. Cooper O.[d]

[a] University of Campinas, School of Mechanical Engineering, Department of Manufacturing Engineering and Materials - Campinas, São Paulo, Brazil.

[b] Three-Dimensional Research Group, Renato Archer Information Technology Center - CTI, Campinas, São Paulo, Brazil. E-mail: marcelo.oliveira@cti.gov.br

[c] Three-Dimensional Research Group, Renato Archer Information Technology Center - CTI, Campinas, São Paulo, Brazil. E-mail: jorge.silva@cti.gov.br

[d] University of Campinas, School of Mechanical Engineering, Department of Manufacturing Engineering and Materials - Campinas, São Paulo, Brazil. E-mail. E-mail: recooper@unicamp.br

Abstract

Electron beam powder bed fusion (EB-PBF) is an additive manufacturing technology (AM) that can efficiently process high-performance alloys such as Inconel 718 and Ti-6Al-4V for aerospace and medical applications. However, EB-PBF produces parts with relatively high surface roughness levels, which can be either a negative aspect in terms of wear and fatigue or a positive one for the osseointegration of medical implants. For this reason, a deeper understanding of surface roughness generation in this manufacturing process is crucial. In this work, a full factorial Design of Experiments (DoE) was designed to evaluate the effects of the build (or wall) thickness in the surface roughness of Ti-6Al-4V by EB-PBF. The profiles of surfaces built in three orientations (vertical, upskin, and downskin) were collected by a tactile profilometer and characterized. The results show that the build thickness affects not only the surface roughness but also in ways that differ according to the surface orientation.

Keywords

Additive manufacturing; electron beam powder bed fusion; surface roughness; build thickness; wall-thickness.

1. Introduction

In general, Titanium alloys are known for exhibiting high heat resistance, superior mechanical performance, and biocompatibility. Ti-6Al-4V, in particular, is an alpha-beta titanium alloy with superb specific strength, being historically employed in the military and civil aviation sectors. While this alloy remains valuable for the aerospace and defense industries [1], it has also become of interest to the automotive [2,3] and biomedical [4,5] sectors due to its wear and corrosion resistance. Yet, Ti-6Al-4V is an alloy that is difficult to process using traditional manufacturing methods. Its elevated melting point (1670 °C) and high chemical reactivity with oxygen and nitrogen make casting it challenging and costly [6,7]. Moreover, its relatively low modulus of elasticity and low thermal conductivity also create many challenges for conventional machining [8,9]. Nevertheless, the additive manufacturing (AM) technology of powder bed fusion (PBF) has proven to be very efficient for processing titanium alloys, creating parts with comparable and even superior mechanical properties [10].

The electron beam powder bed fusion (EB-PBF) process, defined by ISO/ASTM DIS 52900 [11], uses a scanning electron beam as the thermal energy source to melt metallic powders and create dense solid layers one at a time. In EB-PBF, each newly deposited layer of powder material is subjected to two scanning stages: the feedstock powder heating steps, known as preheating and post-heating, and the powder melting process per se. Besides ensuring a constant temperature profile across the powder bed, the powder heating stages loosely sinter the feedstock material to create conductivity paths for incident electrons and to avoid powder particle repulsion [12–14]. There are two consecutive preheating steps in EB-PBF: the first utilizes a fast-scanning defocused electron beam that raises the temperature of the entire powder bed homogeneously (Figure 1a), while the second step provides additional heating only to the regions where the melting process will take place next [15,16]. The melting process utilizes a focused electron beam to fuse the powder material by selectively scanning specific regions of the bed, constructing solid cross-sectional layers of the desired parts. This stage usually consists of two steps: contour and hatch scanning melting. The contour (or contouring) step melts the perimeters of the parts, which can be made of several concentric lines [13]. By default, the contouring in EB-PBF is performed with a spot-melting strategy known as MultiBeam, in which several active melt pools are formed along a line

(Figure 2a) for faster scanning and supposedly better surface quality [17]. However, the spot-melting strategy in EB-PBF was verified to produce parts with worse surface quality when compared to parts produced with continuous contour scanning strategies, though the latter displayed the worst dimensional accuracy [18,19]. The hatch (or hatching) scanning step melts the bulk of parts utilizing a fast and high-power electron beam in continuous scanning strategies (Figure 1c), most times performed in a rotating square pattern to avoid anisotropy [16,20]. Finally, after the melting stage, a post-heating step takes place to balance the temperature on the powder bed as a whole, either to heat up some areas of the bed or to allow them to cool down [13].

Figure 1. Preheating (a), contouring (b), and hatching (c) build sequences of an EB-PBF process [15]. Published under a Creative Commons Attribution-NonCommercial-NoDerivs 2.5 License.

The EB-PBF process offers a few advantages over the PBF processes with laser energy sources (L-PBF). EB-PBF, also known commercially as Electron Beam Melting (EBM), is carried out in a high-vacuum chamber to avoid deflection electrons, though this also ensures the chemical stability of reactive metals such as Ti-6Al-4V by maintaining an inert environment inside [21]. The absorption efficiency of lasers in metallic materials is dependent on the material's reflectivity, whereas, for electron beams, it is only marginally dependent on the density of the material, allowing EB-PBF to operate with higher scanning speeds and reduced power consumption compared to L-PBF [22]. In addition, the high temperatures kept inside the manufacturing chamber in EB-PBF significantly reduce the residual stresses in the final parts compared to L-PBF [23].

EB-PBF also shows great potential in producing high-performance Ti-6Al-4V parts. The geometric freedom AM technologies offer opens up many opportunities for lightweight part design for aerospace applications [24] and intricate designs optimized for biomedical uses [25]. However, one of the industry's impediments to the broader adoption of this particular manufacturing process is the intrinsic rough surface finish of EB-PBF parts. Generally speaking, the surface roughness levels found in EB-PBF parts are comparable to some sand casting and forging processes [26], with Ra roughness values up to 50 μm [27,28]. While surface roughness is often associated with undesirable effects on friction and wear of moving parts, its impact on the integrity of parts under dynamic loads is probably the most severe for EB-PBF parts. It has been demonstrated that the irregular surface morphology characteristic of EB-PBF parts promotes stress concentration and crack initiation points along the surface, significantly reducing fatigue performance [29–34]. While traditional and alternative surfacing methods have been shown to improve the fatigue life of Ti-6Al-4V parts by EB-PBF [35–39], besides the operational challenges of surface-processing complex geometry and internal regions, these additional processing steps can add substantial costs to an already expensive manufacturing process [40]. Still, rough surface finishes are not always undesirable in terms of functionality. The as-built roughness level of EB-PBF parts is known to positively affect cell proliferation, blood coagulation, and the osseointegration of Ti-6Al-4V orthopedic and dental implants [41–47].

According to the literature [48], the leading causes for the surface roughness generation in EB-PBF are: (1) the staircase effect, (2) the adhesion of partially melted powder particles, and (3) the irregular surface morphology created by melt pool instabilities and process deviation. The staircase effect refers to the dimensional and geometrical deviations of additively manufactured surfaces due to this process's layer-stacking nature. The severity of the staircase effect is highly dependent on the orientation of each surface during manufacturing [28,49–52], as illustrated in Figure 2. The top surfaces are built strictly parallel to the build platform and are not affected by the staircase effect. These surfaces display the best surface finishes overall, with Ra roughness values reported up to 13 μm [53] as they are only partially affected by powder particles' adhesion. The adhesion of partially melted powder particles is considered by many authors the primary mechanism behind surface roughness in EB-PBF [54,55] and is closely related to the thermal interactions that occur during processing. The significant temperature difference between the melted areas and the powder bed generates a high thermal gradient toward the enclosing unprocessed powder. The heat transferred to the surrounding area is enough to partially melt adjacent powder particles that attach to the solid surfaces [20,56,57]. This phenomenon generates surfaces covered by round protuberances of the same size magnitude as the feedstock powder particles (Figure 2). The irregular surface morphology created by the EB-PBF process is also closely related to its intrinsic thermal interactions, particularly by the hydrodynamic effects experienced by the molten material during phase changes [58]. Thermocapillary effects and melt pool instabilities can displace molten material that solidifies and form sharp protuberant structures on EB-PBF surfaces [29,50,59,60]. Other defects, such as lack-of-fusion irregularities, can occur when the thermal energy provided by the electron beam in a particular region is not enough to fully melt the powder particles, leading to the formation of elongated voids and pores in parts[12,61].

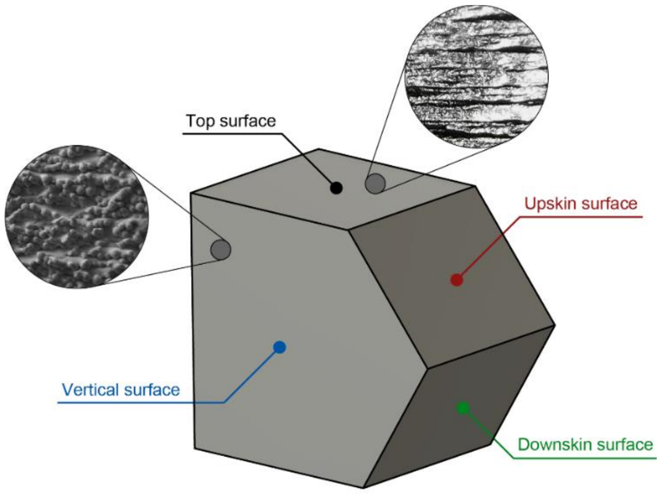

Figure 2. Illustration of an EB-PBF part with surfaces produced in different orientations.

It can be noted that the surface quality of EB-PBF parts is clearly related to the thermal interactions the material experiences. As such, all process parameters related to energy and heat transfer could potentially influence the surface topology parts. The electron beam parameters, such as beam current, focus offset, and scanning speeds, were all verified to influence the surface roughness of Ti-6Al-4V parts [19,54,62–66]. Other factors associated with heat transfer inside the build chamber were discovered to affect the surface roughness as well, including the arrangement of parts in the build chamber, which can create pockets of energy accumulation in the powder bed [67–70]. Accordingly, it would be expected that the geometry of parts would also influence the surface roughness to some extent, as it directly impacts the total energy required for melting the powder region and the subsequent cooling rates. While the build (or wall) thickness of parts was proved to affect the microstructure [71–73] and the mechanical properties of parts [74,75], the relationship between build thickness and surface roughness is not yet thoroughly understood.

Safdar et al. [54] verified the influence of build thickness and other process parameters on vertical surfaces (built at 90°) of Ti-6Al-4V specimens by EB-PBF. The results revealed a tendency of increasing surface roughness with increasing thickness, which the authors explained as being due to the higher energy required to melt and build thicker geometries. The higher energy density employed would then promote more surrounding powder particles to attach to the surfaces, creating rougher surfaces altogether. Karlsson Algardh et al. [76] evaluated the influence of build thickness and powder size distribution on the roughness of lateral surfaces built vertically. According to the authors, the Ra roughness of Ti-6Al-4V specimens with build thicknesses of 0.5, 1.0, 2.0, and 5.0 mm showed a trend slightly opposite to that of Safdar et al. [54], with thinner samples exhibiting higher roughness values instead. This trend was also observed by Razavi et al. [77], though with slightly different thickness levels (1.0, 3.0, and 5.0 mm). Besides evaluating the fatigue behavior of said specimens, Razavi et al. [77] also investigated the roughness of inclined surfaces built at 45°, both upskin and downskin according to Figure 2. According to the authors, these inclined surfaces seemed to follow the same trend as observed in the vertical surfaces. The authors claim that the reason for this is the reduced quantity of electron beam scan lines required for producing thinner geometries, which can lead to irregular surface morphology and surface build defects [77]. More recently, Segersäll et al. [78] also examined the influence of build thickness on the surface roughness and fatigue of EB-PBF parts. Ti-6Al-4V specimens of 1.5, 2.1, and 2.7 mm thicknesses were produced in different build orientations and had their surfaces measured and characterized by four different methods. However, according to the authors, the build thickness did not seem to influence the surface quality in the study.

The disparity between the results in these studies can be due to a number of factors. As already discussed, surface roughness in EB-PBF is highly dependent on the thermal interactions and the process parameters that control the electron beam and the scanning strategy; hence the use of different process parameters would evidently interfere with the results regarding the influence of build thickness. However, the process parameters utilized for specimen fabrication in each of the studies mentioned were not described in detail, making the assessment and comparison of the results impractical. The part arrangement inside the build chamber, which is also known to affect the surface roughness in EB-PBF, was also not sufficiently described in these studies or even reported whether it was considered for the experiment design. Moreover, the experiments of all the above studies were designed to explore other factors of EB-PBF, including the fatigue performance and the effects of other process variables on the resulting surface roughness, potentially introducing more variability in an already sensible manufacturing process.

Besides its relevancy in the functional performance of parts, the study of surface roughness in EB-PBF is also critical for better understanding this manufacturing process and helping improve parts' reliability and quality [79]. Recognizing the relationship between build thickness and surface roughness can also help researchers design better experiments since varying wall thickness was already reported to disrupt experimental studies in EB-PBF with surface roughness [51]. A deeper understanding of surface-related aspects in EB-PBF requires analyzing surfaces built in distinct orientations and with sufficient replicates to account for the high variability of this process. The present literature regarding the relationship between build thickness and surface roughness lacks both, with usually only one specimen per thickness analyzed and very few studies examining non-vertical surfaces. Considering the dissimilar results and lack of extensive analysis in the literature, this work aims to contribute to the understanding of the EB-PBF process by investigating the effects of varying build thicknesses on the surface roughness of Ti-6Al-4V. To that end, an experiment has been devised considering the various process variables affecting the surface quality of EB-PBF to evaluate vertical and inclined surfaces, producing sufficient replicates for statistical significance.

2. Materials and methods

2.1 Specimen design and fabrication

Two different specimens were designed for this experiment: one for vertical surface analysis (Figure 3a) and an inclined specimen for analyzing both upskin and downskin surfaces (Figure 3b). The inclined specimens were designed with a 65° slopping angle to ensure a successful build without requiring support structures, thus allowing the measurement and characterization of the downskin as-built surfaces. Both specimens were purposely dimensioned for tactile roughness measurements considering an evaluation length of 40 mm, according to the guidelines of ISO 4288 [80] for the expected range of Ra roughness. The specimens were produced with nominal thickness values of 0.5, 1.0, 2.0, 2.5, 3.0, and 4.0 mm, with four repetitions per thickness, totalizing 48 specimens (24 vertical and 24 inclined). The thickness levels were selected according to their verified influence on the mechanical properties of parts produced by EB-PBF [74,75] and to cover a wide range of values. The EB-PBF equipment employed in this experiment was the Arcam Q10plus machine by GE Additive (GE, USA). The Ti-6Al-4V feedstock powder utilized was also supplied by GE Additive, with a particle size distribution ranging from 45 to 105 μm.

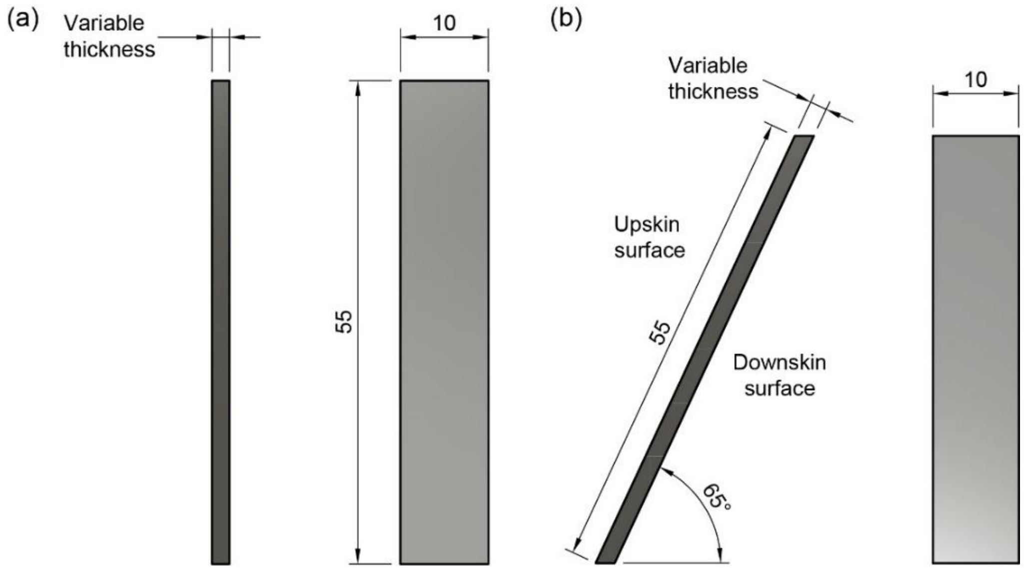

Figure 3. Vertical (a) and inclined (b) specimens designed for tactile surface measurement.

All specimens were produced using the EB-PBF machine's default theme for this material for a layer height of 50 μm (Ti6Al4V_Q10plus version 5.2.23). The most relevant process parameters for the preheating and melting stages are reported in Table 1, while the arrangement of specimens inside the build chamber is illustrated in Figure 4. The thicker samples were positioned closer to thinner ones in an attempt to avoid dissimilar thermal accumulation in the powder bed, and all specimens were positioned with equal distances between them to reduce and equalize the energy accumulation effects in the surface roughness [70] as much as possible.

Once produced, the unprocessed powder around the specimens was removed by an abrasive blasting process using Arcam's Powder Removal Station (PRS) system. Each specimen was then identified prior to removal to record the exact position it was produced in the build platform. No additional process was required to detach the specimens from the build platform since the contact area between them was minimal, and each part could be removed manually.

Table 1. Machine build parameters used for specimen fabrication.

Preheat	**Preheat**	Focus offset	44 mA
		Heating focus offset	100 mA
		Offset to part	4 mm
		Surface temperature	940 C
	Preheating I	Max beam current	16 mA
		Beam speed	18000 mm/s
		No. of repetitions	2
		Average current	0 mA
		Line order	20
		Line offset	0.4 mm
	Preheating II	Max beam current	19 mA
		Beam speed	18000 mm/s
		No. of repetitions	2
		Average current	5.4 mA
		Line order	20
		Line offset	0.4 mm
Melt	**Contours**	Number of contours	3
		Block offset	True
	Outer contour	Beam current	5 mA
		Max beam current	5 mA
		Speed	750 mm/s
		Line offset	0.22 mm
		Focus offset	5 mA
	Inner contour	Beam current	8 mA
		Max beam current	8 mA
		Speed	800 mm/s
		Line offset	0.135 mm
		Focus offset	5 mA
	Hatch	Use rotating hatch	True
		Linear current compensation	True
		Beam current	15 mA
		Max beam current	30 mA
		Manual speed	4530 mm/s
		Speed function	60
		Line offset	0.20 mm
		Focus Offset	36 mA

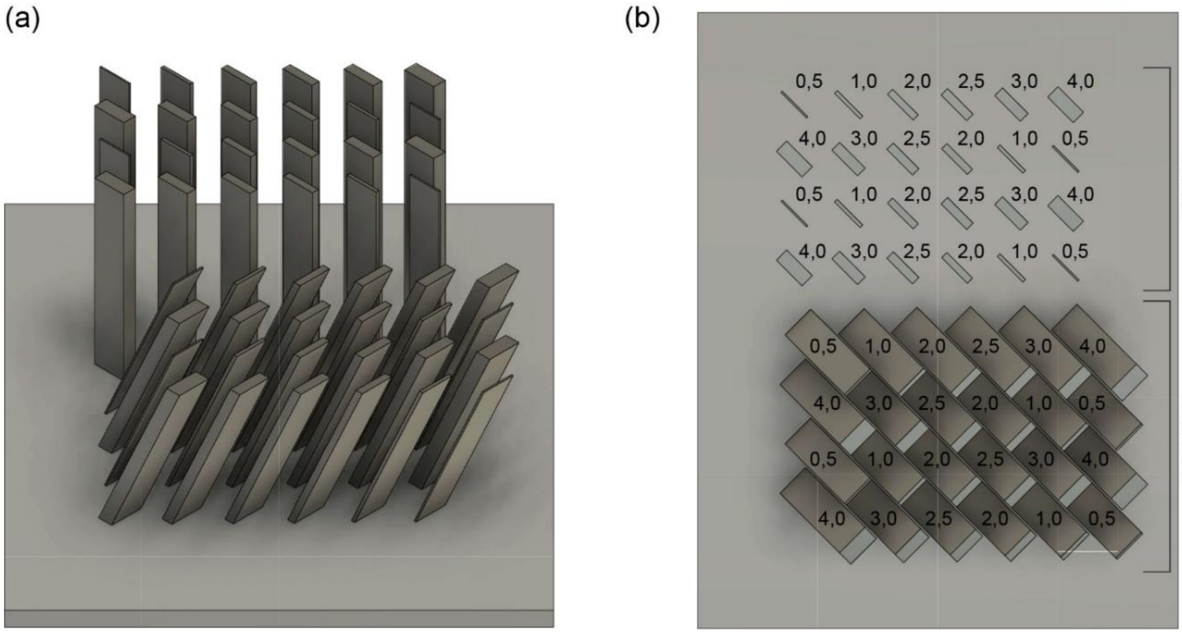

Figure 4. (a) Part arrangement for all 48 specimens fabricated and (b) distribution of specimens based on geometry and build thickness (in mm).

2.2 Surface measurement and characterization

The surfaces were measured with a Talysurf PGI 830 tactile profilometer (Taylor Hobson, UK) equipped with a 2.0 µm conical diamond tip. A sampling length of 50 mm was registered with a measurement speed of 0.5 mm/s, and three parallel measurements were taken for each surface in a direction perpendicular to the lay (Figure 5a) according to the recommendations in ISO/ASTM 52902 [81]. A total of 288 profile measurements were obtained from the 96 surfaces. The surface roughness characterization was performed using the Mountains® 9 software (Digital Surf, France). A cut-off filter of 8 mm was used according to ISO 4288 [80] for the expected Ra roughness values, with an evaluation length of 5 cut-offs (40 mm) with a half cut-off distance discarded from the start and end of each sampling length.

The roughness parameters used for the analysis were the arithmetic mean deviation (Ra), the root mean square deviation (Rq), the skewness (Rsk) and kurtosis (Rku) of the profile, as well as the peak parameters of the total height of the profile (Rt) and the maximum height of profile (Rz). The average roughness parameters Ra and Rq assess the profile's deviations about the mean line within an evaluation length, with Ra being the most common roughness parameter used by the industry. The profile's skewness (Rsk) gauge the even distribution of peaks and valleys in a given profile, whereas the Kurtosis (Rku) measures the profile's sharpness. The peak roughness parameters of Rt and Rz determine the maximum peak-to-valley distances in the profile. All these roughness parameters were selected according to their prevalence in the literature on surface roughness with EB-PBF [82] and according to the recommendations of ISO/ASTM 52902 [81]. The waviness component of the profiles was not analyzed as its contribution to the roughness investigation of EB-PBF appears to be minor [51]. All measured profiles were characterized individually, and the mean roughness parameters were calculated for each surface. Finally, some surfaces were also observed under a ZEISS EVO MA 15 (Zeiss, Germany) scanning electron microscope to investigate differences in surface morphology.

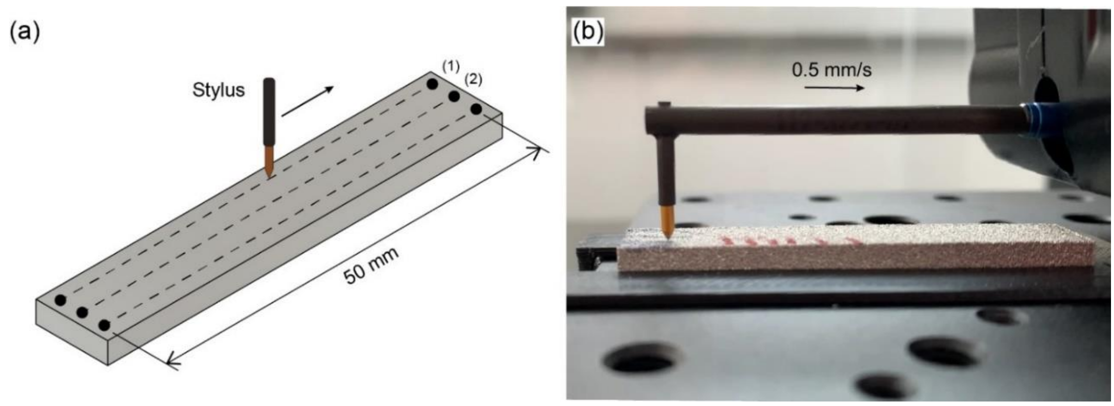

Figure 5. Procedure for surface roughness measurement via stylus profilometer.

2.3 Preliminary and statistical analysis

A preliminary analysis was performed to verify whether the position of the specimens in relation to the build chamber influenced their surface roughness. No significant variation in the average roughness parameters was found for same-thickness specimens built in different locations of the build platform, so they could be considered replicas for the subsequent analysis. A full factorial analysis was performed for the Ra values considering the prevalence of this parameter in the literature for surface roughness. The factorial analysis comprised two factors: the surface orientation (vertical, upskin, and downskin) and the build thickness levels (0.5, 1.0, 2.0, 2.5, 3.0, and 4.0 mm), with four replicates each. The remaining roughness parameters were also reported and plotted to support the analysis.

3. Results

All specimens displayed Ra values ranging from 21 to 35 μm, well within the expected range for EB-PBF with this alloy. Table 2 shows the numerical results for the full factorial analysis performed for Ra, and the interaction plots for orientation and build thickness can be seen in Figure 6. Other results from the factorial analysis are found in Appendix A. The build thickness affected the surface roughness of vertical, upskin, and downskin surfaces differently, and for this reason, the results for each type of surface will be presented and analyzed separately in the following sections.

Table 2. ANOVA results for the factorial analysis of Ra versus thickness and surface orientation.

Source	**DF**	**Adj SS**	**Adj MS**	**F-Value**	**P-Value**
Model	17	1022.44	60.143	64.25	0.0000
Linear	7	862.99	123.284	131.69	0.0000
Thickness	5	36.92	7.385	7.89	0.0000
Surface orientation	2	826.06	413.032	441.21	0.0000
2-Way Interactions	10	159.45	15.945	17.03	0.0000
Thickness*Surface orientation	10	159.45	15.945	17.03	0.0000
Error	54	50.55	0.936		
Total	71	1072.99			

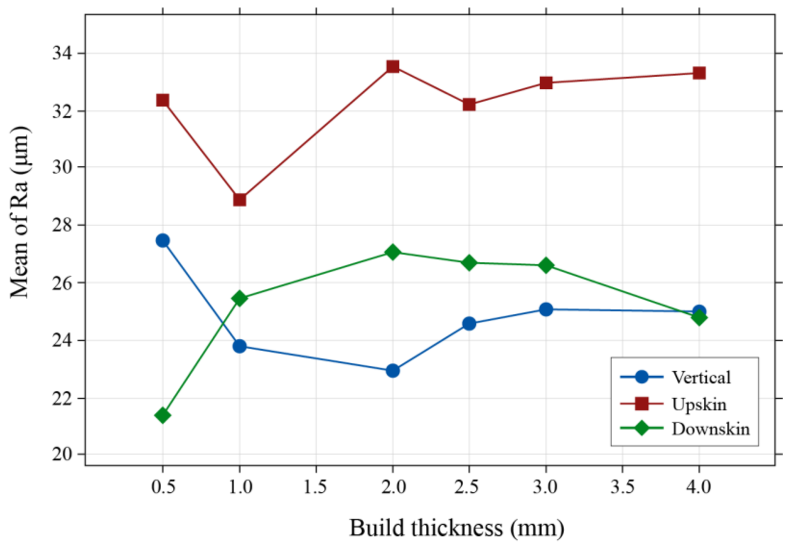

Figure 6. Interaction plot for Ra roughness versus build thickness and surface orientation.

3.1 Vertical surfaces

Table 3 shows the average values of the roughness parameters for each thickness level of the vertical specimens. The Ra values were in the range of 22 and 29 µm, which is consistent with the literature for this orientation [27,33,67]. The boxplot graphs for each roughness parameter are displayed in Figure 7. The 0.5 mm specimens consistently showed the highest surface roughness values across all parameters, with Ra ranging from 26.21 to 28.80 µm. The 1.0 and 2.0 mm specimens had the best overall surface quality, with the lowest recorded Ra of 21.90 µm belonging to a 2.0 mm specimen. The remaining specimens all displayed similar roughness levels among themselves, falling within the 24 – 25 µm range. The profile skewness (Rsk) values for the 0.5 mm specimens indicate a predominance of valleys in the surface morphology compared to other thickness levels. SEM images of vertical surfaces with the highest and lowest Ra values are displayed in Figure 8. It can be noted that both surfaces show comparable levels of adhered particles, although the underlying surface morphology of the 0.5 mm specimen displays deep valleys structures not observed in the 2.0 mm specimen.

Table 3. Mean values for the roughness parameters of vertical surfaces.

Thickness (mm)	Ra (µm)	Rq (µm)	Rz (µm)	Rt (µm)	Rsk	Rku
0.5	27.49	34.40	187.16	223.72	-0.1399	2.92
1.0	23.80	29.83	167.13	196.97	0.0063	2.93
2.0	22.96	28.91	163.45	199.21	0.0382	3.01
2.5	24.60	30.83	170.88	207.57	-0.0166	2.97
3.0	25.09	31.52	173.17	206.38	-0.0811	2.95
4.0	25.z02	31.43	176.97	208.44	-0.0727	2.97

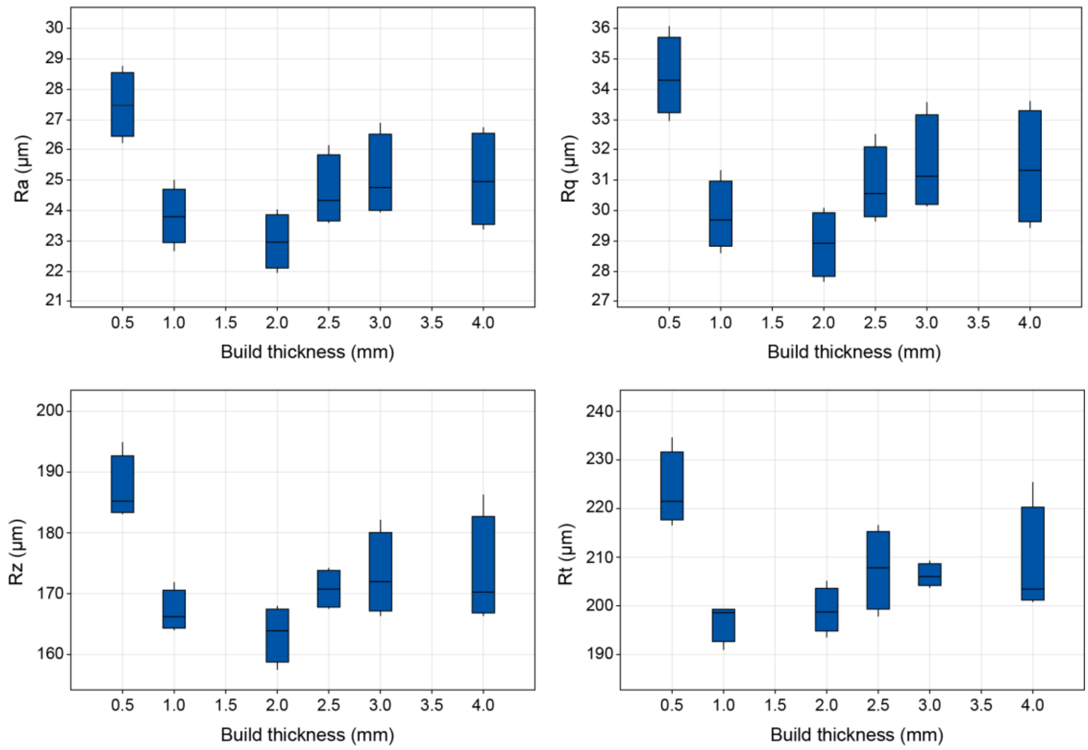

Figure 7. Boxplots graphs for Ra, Rq, Rz, and Rt roughness parameters of vertical surfaces.

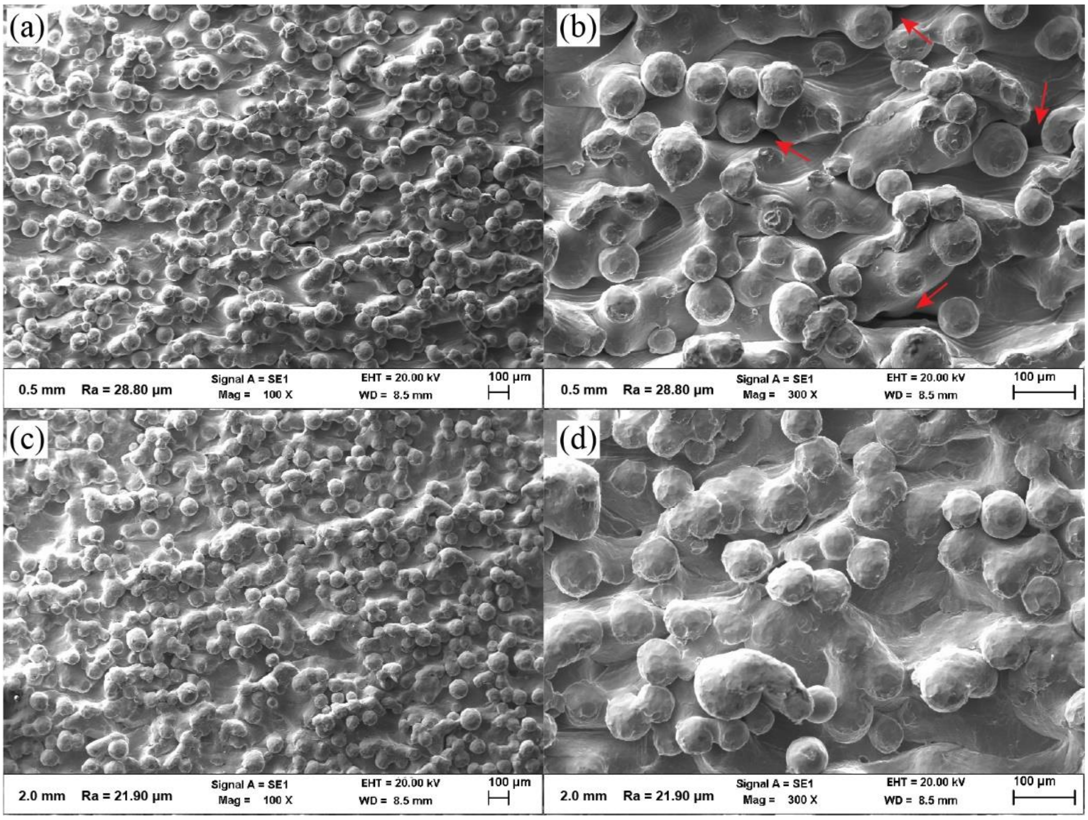

Figure 8. SEM micrographs for vertical surfaces with thicknesses of (a)(b) 0.5 mm (Ra = 28.80 µm) and (c)(d) 2.0 mm (Ra = 21.90 µm).

3.2 Upskin surfaces

Table 4 shows the roughness parameters for the thickness levels of the upskin surfaces, while the boxplot graphs are displayed in Figure 9. The surface roughness levels of the upskin surfaces were the highest among all surface orientations, with Ra values ranging from around 28 to 35 μm. The Ra and Rq roughness levels were very similar across nearly all specimens, with the exception of the 1.0 mm specimens at notably lower levels. Nevertheless, the Rt and Rz peak parameters found for the 0.5 mm specimens were comparatively lower than the 2.0 - 4.0 mm specimens, which agrees with the lower Rku values of these thinner specimens that indicate an absence of extreme peaks or valley structures. The 1.0 mm specimens also exhibited Rsk values closer to zero compared to all other thickness levels. This indicates a surface morphology with a similar peak-to-valley ratio for the 1.0 mm specimens rather than the predominant peak topology of all the other specimens. SEM images of a 0.5 and a 1.0 mm specimen are displayed in Figure 10. Both images reveal the distinct protuberant structures of upskin surfaces, but the 1.0 mm specimen (with the lowest Ra value recorded) appears to have more partially melted particles adhered to its surfaces, particularly under the protuberant structures.

Table 4. Mean values for average and peak roughness parameters of upskin surfaces.

Thickness (mm)	Ra (μm)	Rq (μm)	Rz (μm)	Rt (μm)	Rsk	Rku
0.5	32.42	39.86	201.76	233.89	0.2012	2.05
1.0	28.94	36.01	197.46	234.77	- 0.0205	2.87
2.0	33.58	41.64	222.93	265.10	0.0961	2.80
2.5	32.26	39.82	204.92	235.52	0.1701	2.73
3.0	33.03	40.86	214.29	249.94	0.2066	2.74
4.0	33.34	41.14	214.73	257.73	0.1238	2.85

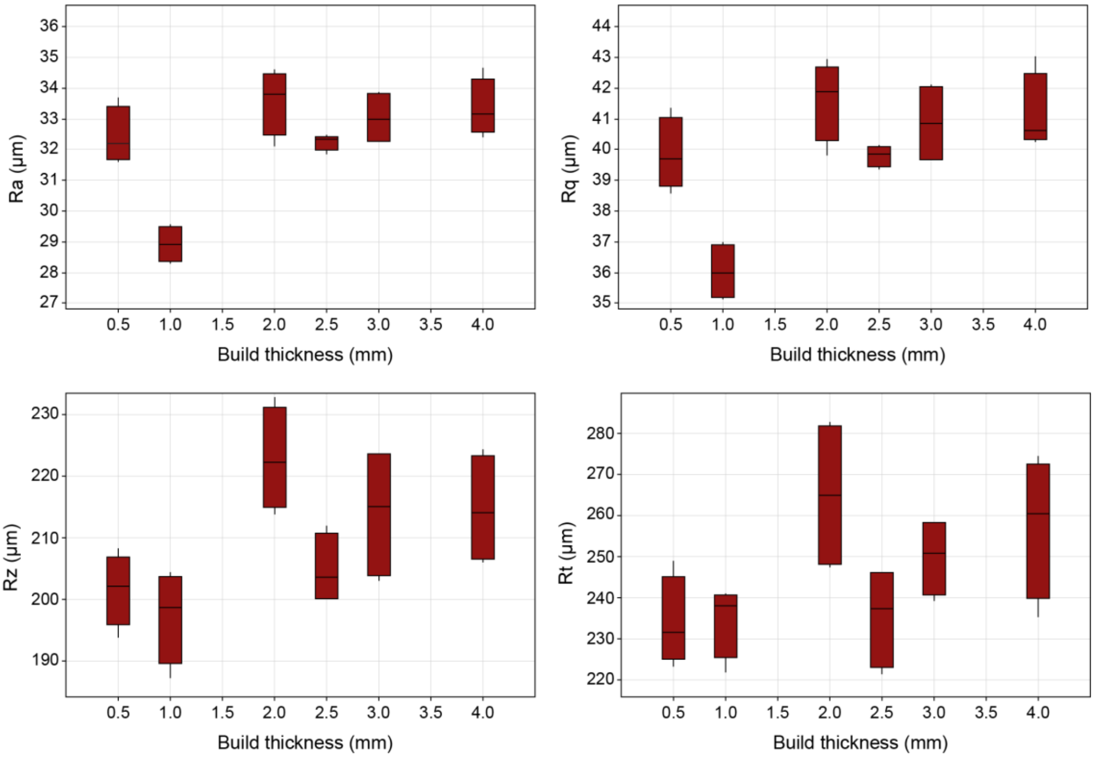

Figure 9. Boxplots graphs for Ra, Rq, Rz, and Rt roughness parameters of upskin surfaces.

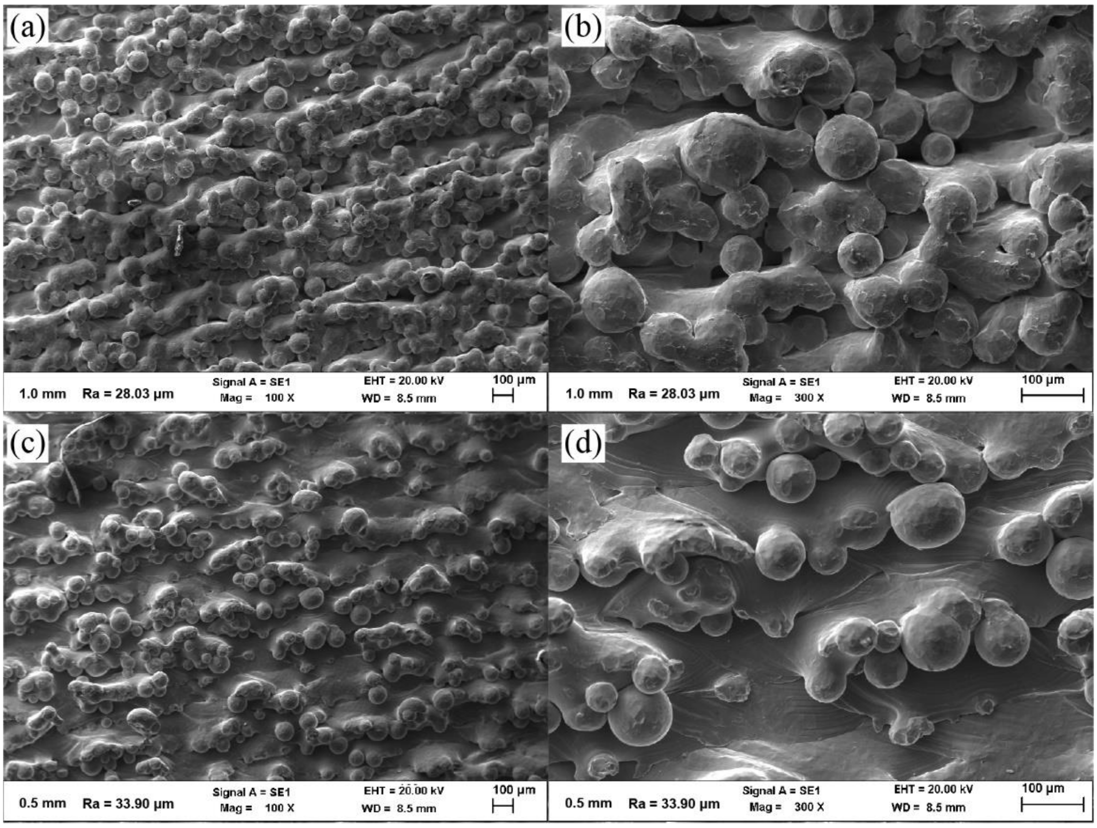

Figure 10. SEM micrographs for upskin surfaces with thickness of (a)(b) 1.0 mm (Ra = 28.03 µm) and (c)(d) 0.5 mm (Ra = 33.90 µm).

3.3 Downskin surfaces

The roughness parameters obtained from the downskin surfaces are displayed in Table 5, and the boxplot graphs are in Figure 11. Overall, the Ra values of downskin surfaces are comparable to vertical specimens. However, the roughness parameters of the 0.5 mm specimens were consistently lower than the other specimens, with Ra ranging between 20.77 and 21.99 µm, while the remaining thickness levels were around 24 to 28 µm. This is a novel result in the literature. The profile's skewness (Rsk) values of the downskin surfaces were typically positive, indicating a predominance of peaks in their surface profiles, except for the 0.5 and 4.0 mm specimens with Rsk much closer to zero, suggesting a more balanced surface morphology. Figure 12 shows SEM images of the downskin surfaces of a 0.5 mm and a 2.0 mm specimen. Both surfaces are characterized by protrusions and partially adhered particles, though the protrusions seem more apparent for the 2.0 mm specimen (Figure 12d).

Table 5. Mean values for average and peak roughness parameters of downskin surfaces.

Thickness (mm)	Ra (µm)	Rq (µm)	Rz (µm)	Rt (µm)	Rsk	Rku
0.5	21.37	26.87	154.99	186.35	0.0857	3.06
1.0	25.49	31.93	173.40	208.89	0.2879	3.01
2.0	27.10	34.02	187.03	234.36	0.2305	3.07
2.5	26.72	33.49	182.86	223.05	0.2352	2.96
3.0	26.63	33.23	181.33	223.16	0.2087	2.95
4.0	24.80	30.98	167.50	208.86	0.0268	2.91

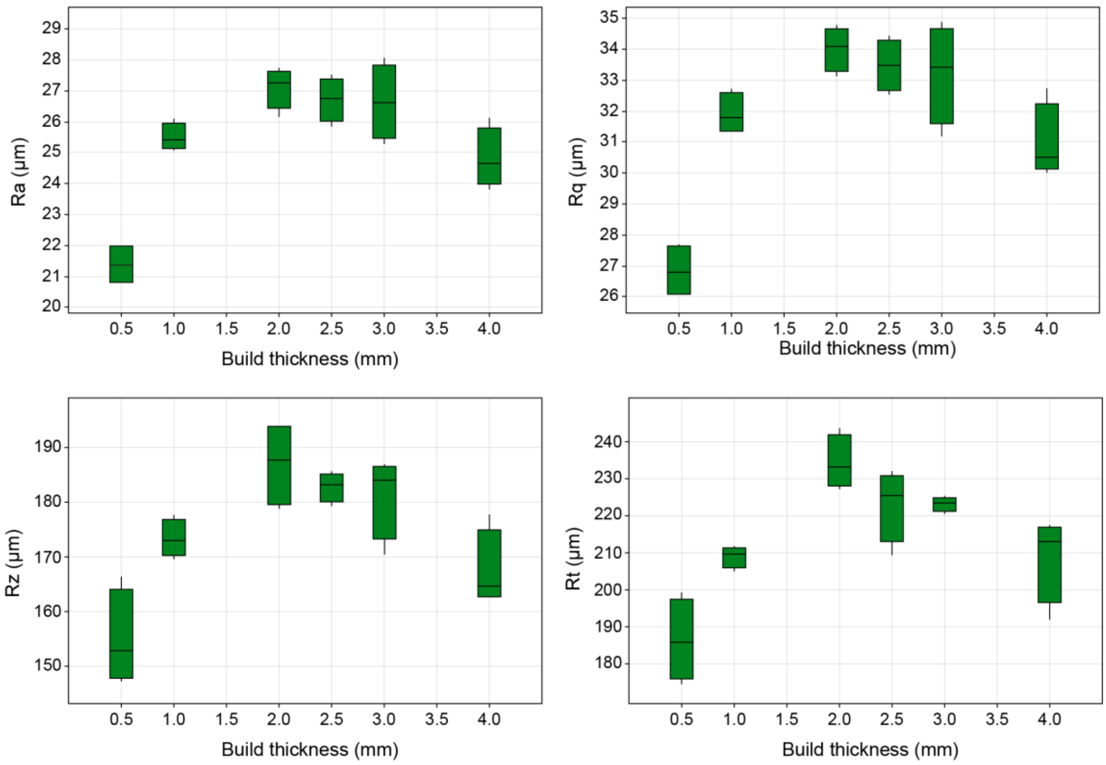

Figure 11. Boxplots graphs for Ra, Rq, Rz, and Rt roughness parameters of downskin surfaces.

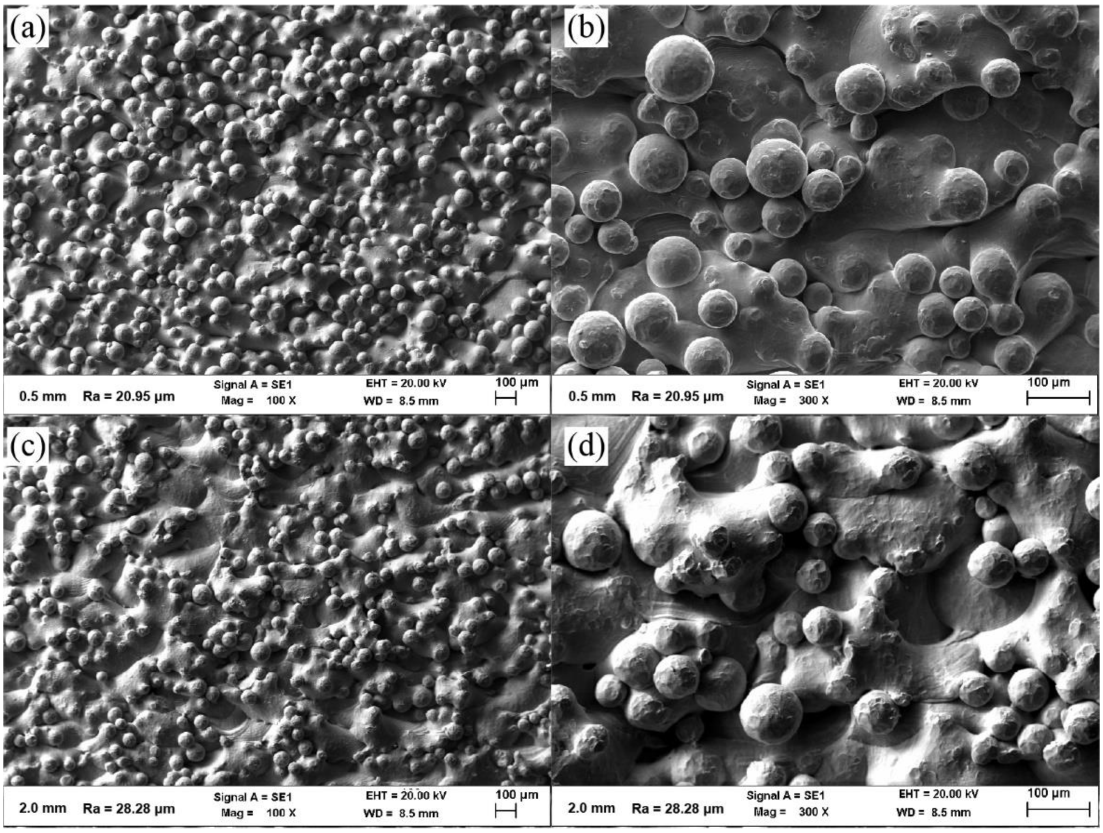

Figure 12. SEM micrographs for downskin surfaces with thickness of (a)(b) 0.5 mm (Ra = 20.95 µm) and (c)(d) 2.0 mm (Ra = 28.28 µm).

4. Discussion

Since the topology and the severity of mechanisms behind the surface roughness generation in PBF differ according to the orientation, it could be expected that the build thickness would affect vertical, upskin, and downskin surfaces differently. The results from the experiment confirm this hypothesis. To better interpret the results towards the influence of build thickness on the surface roughness, the discussion of the results will be done separately for each surface type. Still, some aspects of the experiment remain relevant for the analysis regardless of the surface orientation. Since all specimens were produced with the same feedstock powder, and the inclination angle of each specimen type was kept constant (90° for vertical surfaces and 65° for upskin and downskin surfaces), the influence of the staircase effect on the surface roughness can be considered minimal in this experiment. Therefore, the effects of build thicknesses on the final surface roughness should either be due to attached powder particles or irregular surface morphology generated by the process itself.

4.1 Vertical surfaces

The most unusual behavior observed in the results for the vertical surfaces is the consistently higher roughness parameters of the 0.5 mm specimens, a result similar to that of Karlsson et al. [76] (though with distinct Ra levels). To try and understand this behavior, one should consider the scanning strategy for melting differently sized cross-sectional layers during processing, illustrated in Figure 13. Larger cross-sections (Figures 13a and 13b) are built by the two melting steps described earlier: the contours are melted first with a spot-melting strategy, whereas the solid interior is melted with the hatch melting strategy. If a fixed number of contours is set for the entire build, then reducing the cross-sectional layer area would decrease the region built by hatch scannings until the layer is fully melted by contours only (Figure 13c). Further reductions in the cross-sectional area would trigger the "Block Offset" function, in which one single contour line is employed to melt a given region [83], as illustrated by Figure 13d.

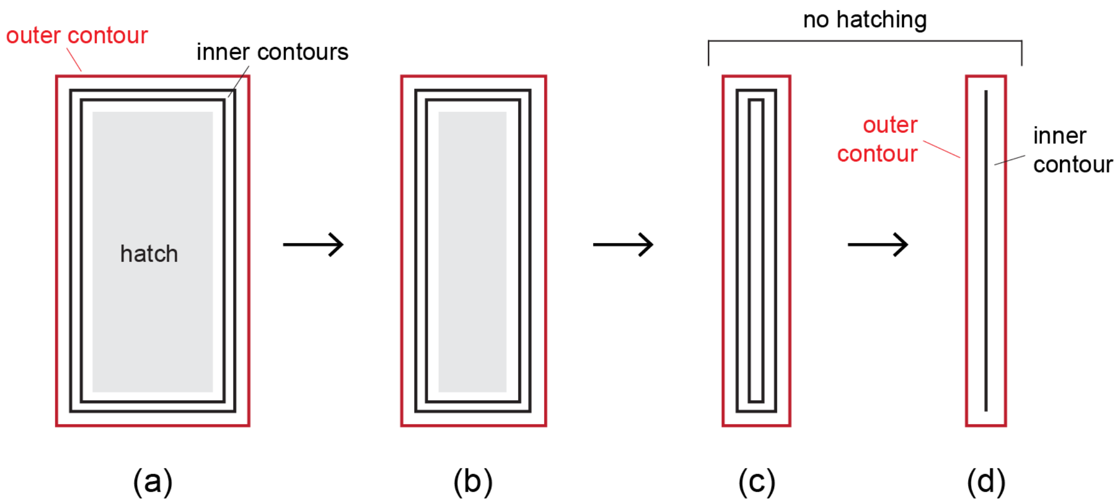

Figure 13. Scanning strategies for varying cross-sectional areas in EB-PBF.

The 0.5 mm vertical specimens had the smallest cross-sectional area of all specimens and were entirely built by low-power contour scans (Table 1), meaning that lower thermal energy was being provided to those particular regions. In order to keep a uniform temperature distribution in the powder bed, the post-heating step compensates for this difference by providing additional energy to cooler regions, such as those close to smaller cross-sectional areas [53]. According to Galati et al. [51], the extra energy provided to smaller cross-section areas during the post-heating step could elevate the temperatures in the surrounding powder bed region to a point where more powder particles could partially melt and attach to solid surfaces. This circumstance would be plausible to explain the higher roughness values of the vertical 0.5 mm specimens. However, by analyzing the SEM images in Figure 8, the quantity of partially melted particles in the 0.5 mm specimen (Ra = 28.27 µm) and the 2.0 mm specimen (Ra = 21.69 µm) appears to be very similar, suggesting that a different mechanism could be responsible for the contrasting surface quality.

Razavi et al. [77] claim that the fewer scan lines required to melt smaller cross-sectional areas could result in insufficient melting and, therefore, the creation of irregular surface structures and open defects that contribute to a rougher surface finish. While this could explain the behavior observed for the vertical surfaces in the present study, the reasons might also be due to the process parameters employed for melting reduced cross-sections. In EB-PBF, the outer contours are usually melted using a low-powered electron beam to purposively not induce surrounding powder particles to melt and attach to surfaces. This is how the specimens were produced in this experiment, as Table 1 shows the reduced beam current parameter of 5 mA for outer contours compared to 8 mA for inner contours. Considering the line offset values set for the contours (Table 1), it can be agreed that the 0.5 mm specimens were primarily built using the outer contours scannings. Creating entire parts with low-power electron beams via a spot-melting scanning strategy could lead to inadequate melting and lack-of-fusion surface defects characterized by open cavities and deep recesses in the surface [84]. The negative skewness values found for the 0.5 mm specimens (that indicates the predominance of valleys over peaks) and the deep recesses observed in Figure 8b could be associated with lack-of-fusion defects, a condition that the 2.0 mm surface (Figure 8d) does not show.

4.2 Upskin surfaces

The upskin surfaces had the highest roughness parameters among all surface orientations in this study. While many authors claim upskin surfaces exhibit a better surface quality compared to vertical and downskin surfaces, this is only true for more shallow inclination angles [51]. Triantaphyllou et al. [28] observed that, for a 60° inclination angle, the upskin surfaces of Ti-6Al-4V specimens showed higher Ra roughness values than both the vertical and correspondent downskin surfaces, the same behavior observed for the inclined specimens at built 65° in this study.

The upskin surfaces of 0.5 mm specimens did not follow the same behavior observed for the vertical surfaces, with Ra and Rq values comparable to the 2.0 to 4.0 mm specimens. Besides the fact that surfaces built with different orientations are affected differently by the roughness generation mechanisms, the slightly larger cross-sectional area of inclined specimens may also have played a role in this case. The diagram in Figure 14 shows that, for an inclination angle of 65°, the cross-sectional area of inclined specimens is approximately 10% larger than the cross-section of vertical specimens of the same thickness. While this 10% increase could seem minor, it could be enough to allow more inner contour scans to be performed, increasing the total amount of energy provided to the area and possibly reducing the defects induced by insufficient melting. The study by Brown et al. [63] with L-PBF and 304L shows that a slight increase in the hatching area percentage can be enough to almost completely remove surface lack-of-fusion defects in thin-walled parts. While this is not strictly the case here since no hatch scans were used to build the 0.5 mm specimens, it is indicative that higher-powered scans can reduce the lack-of-fusion defects, especially for the thinner parts.

The 1.0 mm specimens displayed the lowest roughness parameters among all upskin surfaces, and the reason for this behavior is yet to be understood. The SEM images in Figure 10a and Figure 10b show a 1.0 mm specimen surface with a seemly higher number of adhered particles than the 0.5 mm specimen, which can be counter-intuitive considering the lower roughness levels of the 1.0 mm upskin surface. It should not be discarded that the presence of partially melted particles in between the peak structures could lessen the overall height of the profile during measurement with a profilometer. This could also explain the distinct skewness values for the 1.0 mm upskin surfaces that indicate a more balanced peak and valley ratio when compared to the remaining specimens. Additional surface analysis would be required to explain this behavior, either with optical equipment or x-ray computer tomography (XCT) technologies.

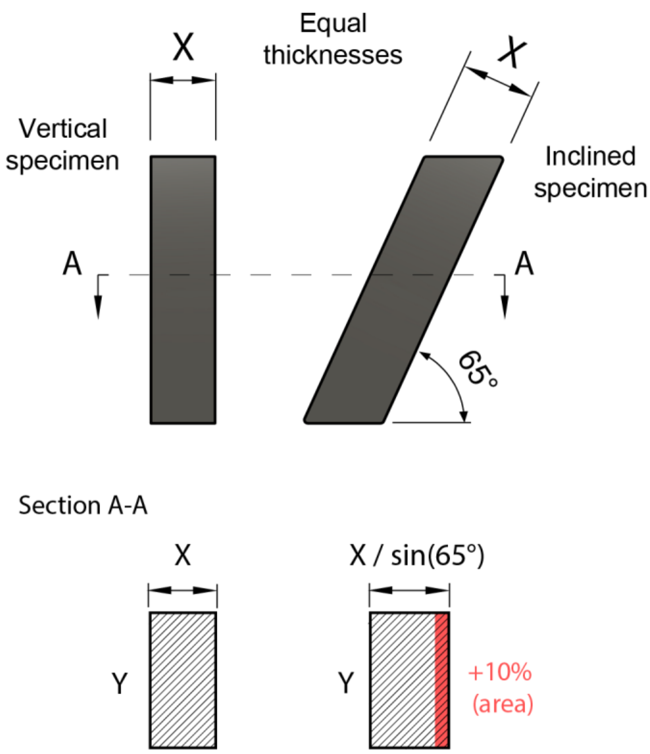

Figure 14. Horizontal cross-sectional areas of vertical and inclined specimens.

4.3 Downskin surfaces

The results for the downskin surfaces reveal a behavior that is novel to the literature, in which thinner 0.5 mm specimens display better surface quality compared to the 1.0 - 4.0 mm ones. In fact, the downskin surfaces of 0.5 mm specimens had the lowest roughness parameters of this entire experiment. According to the literature [51, 53], the surface morphology of downskin surfaces is dominated by partially melted attached particles and irregular surface structures. The latter are created by unsupported molten material in the melt pool pulled by gravity that penetrates the powder bed underneath [85], creating protrusions typical of downskin surfaces. This vertical displacement of molten material is aggravated by deeper melt pools generated by higher levels of accumulated thermal energy [86]. These distinct structures can be observed in the SEM images in Figure 12, being inherently different from the protrusions observed in the upskin surfaces (Figure 10), which in turn are created by overflown material from lateral movement of the melt pool instead.

Considering that the 0.5 mm specimens are primarily built with low-powered contour scans compared to the thicker specimens, perhaps the relatively lower energy provided during melting can positively affect the roughness of downskin surfaces. Shallower melt pools alleviate the vertical displacement of molten material and therefore reduce the extent of the protrusions characteristic of downskin surfaces. The SEM images in Figure 12 also seem to support this argument. While both surfaces are covered by a comparable number of partially melted particles, the downskin protrusions are more apparent in the 2.0 mm specimen (Figure 12d) than in the 0.5 mm specimen (Figure 12b).

5. Conclusion

In this study, an experiment was designed to evaluate the relationship between build thickness and surface roughness of Ti-6Al-4V specimens produced by EB-PBF. All the process variables known to affect the final roughness in EB-PBF were considered in the experimental design to reduce the interference of external factors. The experiment was also designed to include a sufficient number of replicates for statistical significance. The profiles of surfaces built in three different orientations were measured and characterized strictly according to ISO 4288 [80] and ISO/ASTM 52902 [81] The main findings of this study can be summarized as follows:

- The specimen build thickness affects the surface roughness, particularly for thicknesses lower than 1.0 mm. The build thickness was also verified to have different effects on surfaces depending on their build orientation.
- For vertical (90°) surfaces, 0.5 mm-thick specimens displayed the highest roughness parameters compared to thicker specimens ranging from 1.0 to 4.0 mm.
- For upskin surfaces built at 65°, the 1.0 mm specimens showed the best surface quality overall, with the thinner 0.5 mm specimens having Ra roughness values comparable to the 2.0 - 4.0 mm specimens.
- For downskin surfaces built at 65°, the 0.5 mm specimens showed significantly lower surface roughness parameters, a novel result to the literature.
- The causes for these different behaviors may be associated with the scanning strategy and electron beam parameters used for melting reduced cross-sectional areas.

Funding

This study was financed in part by the Coordenação de Aperfeiçoamento de Pessoal de Nível Superior – Brasil (CAPES) – Finance Code 001.

Acknowledgments

This research was performed in part thanks to the resources and facilities of LAprint at the Information Technology Center Renato Archer under the Brazilian Ministry of Science and Technology.

Appendix A. Supplementary data

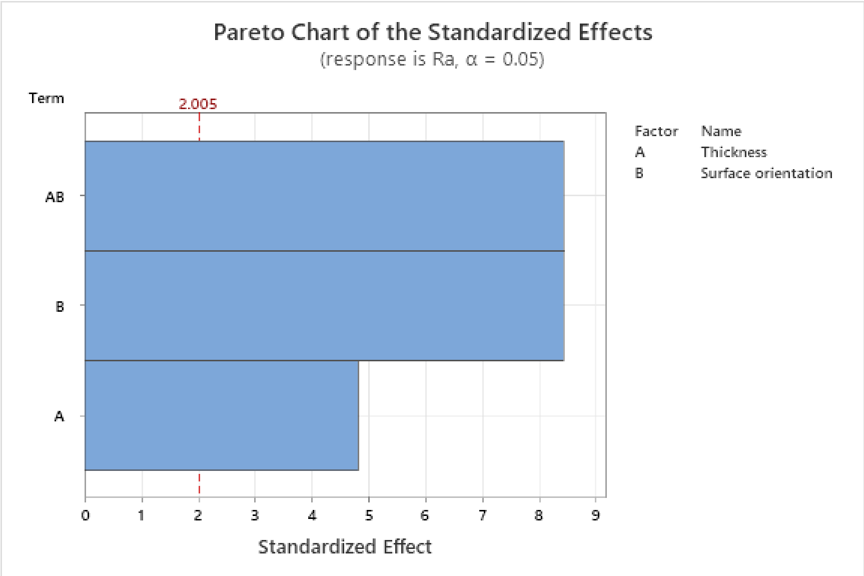

Figure A.1. Pareto chart for the full factorial analysis.

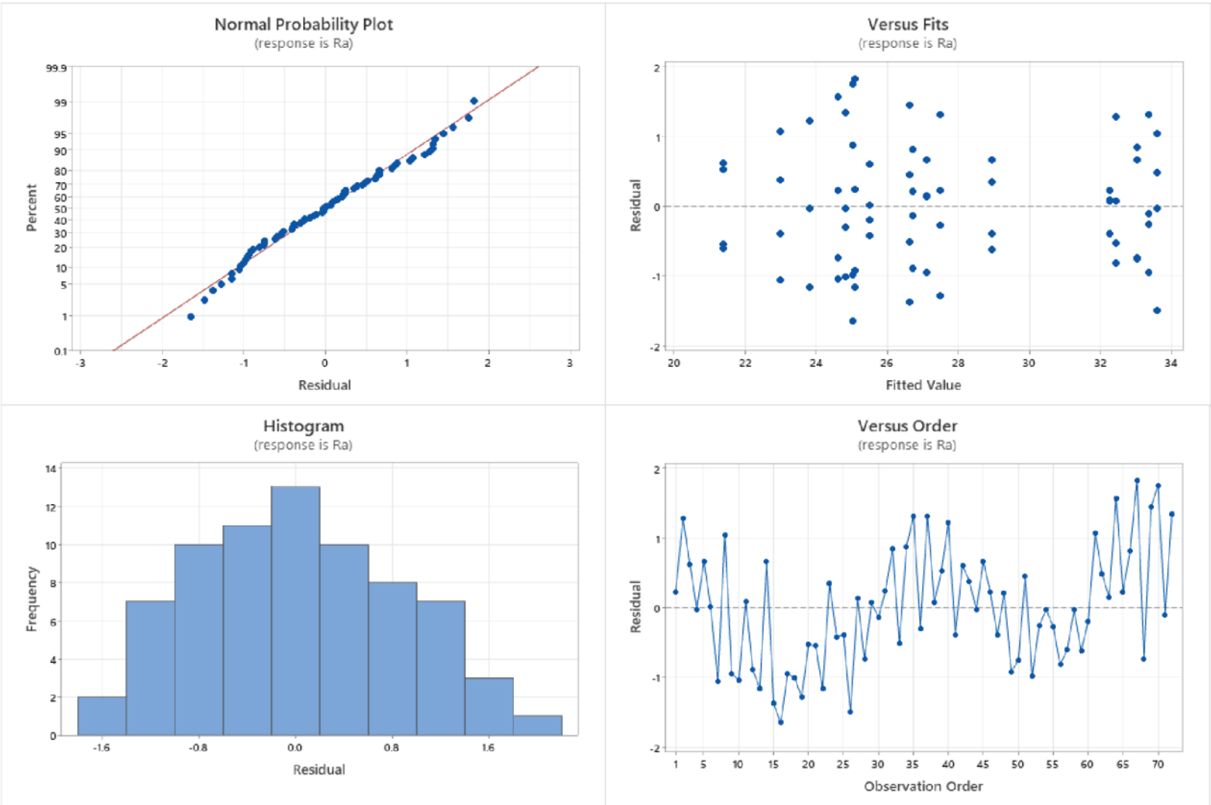

Figure A.2. Residual and histogram charts from the full factorial analysis.

References

[1] J.C. Williams, R.R. Boyer, Opportunities and issues in the application of titanium alloys for aerospace components, Metals (Basel). 10 (2020). https://doi.org/10.3390/met10060705.

[2] H. Fujii, K. Takahashi, Y. Yamashita, Application of titanium and its alloys for automobile parts, Nippon Steel Tech. Rep. 02003 (2003) 70–75. https://doi.org/10.1051/matecconf/202032102003.

[3] T. Furuta, Chapter 4 - Automobile applications of titanium, in: F. Froes, M. Qian, M. Niinomi (Eds.), Titan. Consum. Appl., Elsevier, 2019: pp. 77–90. https://doi.org/https://doi.org/10.1016/B978-0-12-815820-3.00006-X.

[4] M. Kaur, K. Singh, Review on titanium and titanium based alloys as biomaterials for orthopaedic applications, Mater. Sci. Eng. C. 102 (2019) 844–862. https://doi.org/10.1016/j.msec.2019.04.064.

[5] J. W. Nicholson, Titanium Alloys for Dental Implants: A Review, Prosthesis. 2 (2020) 100–116. https://doi.org/10.3390/prosthesis2020011.

[6] J.R.D.O. Bauer, Propriedades mecânicas do titânio comercialmente puro e da liga Ti-6Al-4V fundidos em diferentes ambientes, Doctoral dissertation, University of São Paulo, (2007). http://www.teses.usp.br/teses/disponiveis/23/23140/tde-02012008-153128/.

[7] L. Nastac, M.N. Gungor, I. Ucok, K.L. Klug, W.T. Tack, Advances in investment casting of Ti–6Al–4V alloy: a review, Int. J. Cast Met. Res. 19 (2006) 73–93. https://doi.org/10.1179/136404605225023225.

[8] A.S. Patil, S. V. Ingle, Y.S. More, M.S. Mathe, Machining Challenges in Ti-6Al-4V . - A Review, Int. J. Innov. Eng. Technol. 5 (2015) 6–23. ijiet.com/wp-

content/uploads/2015/08/2.pdf.

[9] S. Pradhan, S. Singh, C. Prakash, G. Królczyk, A. Pramanik, C.I. Pruncu, Investigation of machining characteristics of hard-to-machine Ti-6Al-4V-ELI alloy for biomedical applications, J. Mater. Res. Technol. 8 (2019) 4849–4862. https://doi.org/10.1016/j.jmrt.2019.08.033.

[10] X. Gong, T. Anderson, K. Chou, Review on powder-based electron beam additive manufacturing Technology, Manuf. Rev. 1 (2014). https://doi.org/10.1051/mfreview/2014001.

[11] ISO/ASTM 52900:2015 Additive Manufacturing - General Principles - Terminology, ASTM and International Organization for Standardization ISO, 2015.

[12] M. Galati, O. Di Mauro, L. Iuliano, Finite element simulation of multilayer electron beam melting for the improvement of build quality, Crystals. 10 (2020) 1–18. https://doi.org/10.3390/cryst10060532.

[13] T.R Mahale, Electron Beam Melting of Advanced Materials and Structures, Doctoral dissertation, NC State University, (2019). http://www.lib.ncsu.edu/resolver/1840.16/4943.

[14] J. Milberg, M. Sigl, Electron beam sintering of metal powder, Prod. Eng. 2 (2008) 117–122. https://doi.org/10.1007/s11740-008-0088-2.

[15] E. Hernández-Nava, A study on the mechanical properties of micro-truss Ti-6Al-4V materials fabricated by Electron Beam Melting, Doctoral dissertation, University of Sheffield, UK, (2016) 1–132. https://etheses.whiterose.ac.uk/15488/.

[16] S. Tammas-Williams, H. Zhao, F. Leonard, F. Derguti, I. Todd, P.B. Prangnell, XCT analysis of the influence of melt strategies on defect population in Ti-6Al-4V components manufactured by Selective Electron Beam Melting, Mater. Charact. 102

(2015) 47–61. https://doi.org/10.1016/j.matchar.2015.02.008.

[17] M. Svensson, U. Ackelid, Additive manufacturing with multibeam technology, Aeromat 21 Conf. Expo. Am. Soc. Met. (2010). https://asm.confex.com/asm/aero10/webprogram/Paper26575.html.

[18] P. Karimi, C. Schnur, E. Sadeghi, J. Andersson, Contour design to improve topographical and microstructural characteristics of Alloy 718 manufactured by electron beam-powder bed fusion technique, Addit. Manuf. 32 (2020) 101014. https://doi.org/10.1016/j.addma.2019.101014.

[19] P. Wang, W.J. Sin, M.L.S. Nai, J. Wei, Effects of processing parameters on surface roughness of additive manufactured Ti-6Al-4V via electron beam melting, Materials (Basel). 10 (2017) 8–14. https://doi.org/10.3390/ma10101121.

[20] M. Galati, Chapter 8 - Electron beam melting process: a general overview, in: J. Pou, A. Riveiro, J.P. Davim (Eds.), Addit. Manuf., Elsevier, 2021: pp. 277–301. https://doi.org/https://doi.org/10.1016/B978-0-12-818411-0.00014-8.

[21] L.C. Zhang, Y. Liu, S. Li, Y. Hao, Additive Manufacturing of Titanium Alloys by Electron Beam Melting: A Review, Adv. Eng. Mater. 20 (2018) 1–16. https://doi.org/10.1002/adem.201700842.

[22] GE Additive, Inside Electron Beam Melting, White Paper. https://www.ge.com/additive/download-ebm-white-paper (accessed 11 October 2022).

[23] L.M. Sochalski-Kolbus, E.A. Payzant, P.A. Cornwell, T.R. Watkins, S.S. Babu, R.R. Dehoff, M. Lorenz, O. Ovchinnikova, C. Duty, Comparison of Residual Stresses in Inconel 718 Simple Parts Made by Electron Beam Melting and Direct Laser Metal Sintering, Metall. Mater. Trans. A Phys. Metall. Mater. Sci. 46 (2015) 1419–1432. https://doi.org/10.1007/s11661-014-2722-2.

[24] B. Blakey-Milner, P. Gradl, G. Snedden, M. Brooks, J. Pitot, E. Lopez, M. Leary, F. Berto, A. du Plessis, Metal additive manufacturing in aerospace: A review, Mater. Des. 209 (2021) 110008. https://doi.org/10.1016/j.matdes.2021.110008.

[25] L. Zumofen, K.S. Kopanska, E. Bono, A. Kirchheim, E.B. De Haller, U. Graf-Hausner, Properties of Additive-Manufactured Open Porous Titanium Structures for Patient-Specific Load-Bearing Implants, Front. Mech. Eng. 7 (2022) 1–12. https://doi.org/10.3389/fmech.2021.830126.

[26] T.V. Vorbuguer, Surface finish metrology tutorial, Natl. Inst. Stand. Technol. (1990) 1–159. https://www.nist.gov/system/files/documents/calibrations/89-4088.pdf.

[27] G. Nicoletto, R. Konečná, M. Frkáň, E. Riva, Surface roughness and directional fatigue behavior of as-built EBM and DMLS Ti6Al4V, Int. J. Fatigue. 116 (2018) 140–148. https://doi.org/10.1016/j.ijfatigue.2018.06.011.

[28] A. Triantaphyllou, C.L. Giusca, G.D. Macaulay, F. Roerig, M. Hoebel, R.K. Leach, B. Tomita, K.A. Milne, Surface texture measurement for additive manufacturing, Surf. Topogr. Prop. 3 (2015). https://doi.org/10.1088/2051-672X/3/2/024002.

[29] M. Fousová, D. Vojtěch, K. Doubrava, M. Daniel, C.F. Lin, Influence of inherent surface and internal defects on mechanical properties of additively manufactured Ti6Al4V alloy: Comparison between selective laser melting and electron beam melting, Materials (Basel). 11 (2018). https://doi.org/10.3390/ma11040537.

[30] M. Kahlin, H. Ansell, J.J. Moverare, Fatigue behaviour of notched additive manufactured Ti6Al4V with as-built surfaces, Int. J. Fatigue. 101 (2017) 51–60. https://doi.org/10.1016/j.ijfatigue.2017.04.009.

[31] R. Schur, S. Ghods, E. Schultz, C. Wisdom, R. Pahuja, A. Montelione, D. Arola, M. Ramulu, A Fractographic Analysis of Additively Manufactured Ti6Al4V by Electron Beam Melting: Effects of Powder Reuse, J. Fail. Anal. Prev. 20 (2020) 794–803.

https://doi.org/10.1007/s11668-020-00875-0.

[32] K.S. Chan, Characterization and analysis of surface notches on Ti-alloy plates fabricated by additive manufacturing techniques, Surf. Topogr. Metrol. Prop. 3 (2015) 44006. https://doi.org/10.1088/2051-672X/3/4/044006.

[33] D. Greitemeier, C. Dalle Donne, F. Syassen, J. Eufinger, T. Melz, Effect of surface roughness on fatigue performance of additive manufactured Ti–6Al–4V, Mater. Sci. Technol. 32 (2016) 629–634. https://doi.org/10.1179/1743284715Y.0000000053.

[34] R. Jones, J.G. Michopoulos, A.P. Iliopoulos, R.K.S. Raman, N. Phan, T. Nguyen, Representing crack growth in additively manufactured Ti-6Al-4V, Int. J. Fatigue. 116 (2018) 610–622. https://doi.org/10.1016/j.ijfatigue.2018.07.019.

[35] B. Vayssette, N. Saintier, C. Brugger, M. El May, Surface roughness effect of SLM and EBM Ti-6Al-4V on multiaxial high cycle fatigue, Theor. Appl. Fract. Mech. 108 (2020) 102581. https://doi.org/10.1016/j.tafmec.2020.102581.

[36] V. Chastand, P. Quaegebeur, W. Maia, E. Charkaluk, Comparative study of fatigue properties of Ti-6Al-4V specimens built by electron beam melting (EBM) and selective laser melting (SLM), Mater. Charact. 143 (2018) 76–81. https://doi.org/10.1016/j.matchar.2018.03.028.

[37] M. Kahlin, H. Ansell, D. Basu, A. Kerwin, L. Newton, B. Smith, J.J. Moverare, Improved fatigue strength of additively manufactured Ti6Al4V by surface post processing, Int. J. Fatigue. 134 (2020). https://doi.org/10.1016/j.ijfatigue.2020.105497.

[38] Y.Y. Sun, S.L. Lu, S. Gulizia, C.H. Oh, D. Fraser, M. Leary, M. Qian, Fatigue Performance of Additively Manufactured Ti-6Al-4V: Surface Condition vs. Internal Defects, Jom. 72 (2020) 1022–1030. https://doi.org/10.1007/s11837-020-04025-7.

[39] H. Soyama, F. Takeo, Effect of Various Peening Methods on the Fatigue Properties of

Titanium Alloy Ti6Al4V Manufactured by Direct Metal Laser Sintering and Electron Beam Melting, Materials (Basel). 13 (2020). https://doi.org/10.3390/ma13102216.

[40] P.C. Priarone, M. Robiglio, G. Ingarao, L. Settineri, Assessment of Cost and Energy Requirements of Electron Beam Melting (EBM) and Machining Processes, in: Campana, G and Howlett, RJ and Setchi, R and Cimatti, B (Ed.), Sustain. Des. Manuf. 2017, 2017: pp. 723–735. https://doi.org/10.1007/978-3-319-57078-5_68.

[41] P. Thomsen, J. Malmström, L. Emanuelsson, M. René, A. Snis, Electron beam-melted, free-form-fabricated titanium alloy implants: Material surface characterization and early bone response in rabbits, J. Biomed. Mater. Res. - Part B Appl. Biomater. 90 B (2009) 35–44. https://doi.org/10.1002/jbm.b.31250.

[42] V. Weissmann, P. Drescher, H. Seitz, H. Hansmann, R. Bader, A. Seyfarth, A. Klinder, A. Jonitz-Heincke, Effects of Build Orientation on Surface Morphology and Bone Cell Activity of Additively Manufactured Ti6Al4V Specimens, Materials (Basel). 11 (2018). https://doi.org/10.3390/ma11060915.

[43] B.-S. Lee, H.-J. Lee, K.-S. Lee, H.G. Kim, G.-H. Kim, C.-W. Lee, Enhanced osseointegration of Ti6Al4V ELI screws built-up by electron beam additive manufacturing: An experimental study in rabbits, Appl. Surf. Sci. 508 (2020). https://doi.org/10.1016/j.apsusc.2019.145160.

[44] D.S. Ruppert, O.L.A. Harrysson, D.J. Marcellin-Little, S. Abumoussa, L.E. Dahners, P.S. Weinhold, Osseointegration of Coarse and Fine Textured Implants Manufactured by Electron Beam Melting and Direct Metal Laser Sintering, 3D Print. Addit. Manuf. 4 (2017) 91–97. https://doi.org/10.1089/3dp.2017.0008.

[45] A.A. Al-Tamimi, M.A. Hernandez, A. Omar, D.F. Morales-Aldana, C. Peach, P. Bartolo, Mechanical, biological and tribological behaviour of fixation plates 3D printed by electron beam and selective laser melting, Int. J. Adv. Manuf. Technol. 109 (2020) 673–688. https://doi.org/10.1007/s00170-020-05676-1.

[46] R. Klingvall Ek, J. Hong, A. Thor, M. Bäckström, L.-E. Rännar, Micro- to Macroroughness of Additively Manufactured Titanium Implants in Terms of Coagulation and Contact Activation, Int. J. Oral Maxillofac. Implants. 32 (2017) 565–574. https://doi.org/10.11607/jomi.5357.

[47] C. Lindsay, D. Ruppert, S. Abumoussa, L. Dahners, P. Weinhold, Benefits of additive manufacturing and micro and nano surface texture modifications on mechanical strength and infection resistance of skin-implant interfaces in rats, J. Biomater. Appl. 34 (2020) 1193–1200. https://doi.org/10.1177/0885328220903961.

[48] L. C. B. Carolo, R.E. Cooper O., A review on the influence of process variables on the surface roughness of Ti-6Al-4V by electron beam powder bed fusion, Addit. Manuf. 59 (2022) 103103. https://doi.org/https://doi.org/10.1016/j.addma.2022.103103.

[49] A.T. Sidambe, Three dimensional surface topography characterization of the electron beam melted Ti6Al4V, Met. Powder Rep. 72 (2017) 200–205. https://doi.org/10.1016/j.mprp.2017.02.003.

[50] T. Persenot, A. Burr, G. Martin, J.Y. Buffiere, R. Dendievel, E. Maire, Effect of build orientation on the fatigue properties of as-built Electron Beam Melted Ti-6Al-4V alloy, Int. J. Fatigue. 118 (2019) 65–76. https://doi.org/10.1016/j.ijfatigue.2018.08.006.

[51] M. Galati, G. Rizza, S. Defanti, L. Denti, Surface roughness prediction model for Electron Beam Melting (EBM) processing Ti6Al4V, Precis. Eng. 69 (2021) 19–28. https://doi.org/https://doi.org/10.1016/j.precisioneng.2021.01.002.

[52] T. Grimm, G. Wiora, G. Witt, Characterization of typical surface effects in additive manufacturing with confocal microscopy, Surf. Topogr. Metrol. Prop. 3 (2015). https://doi.org/10.1088/2051-672X/3/1/014001.

[53] M. Galati, P. Minetola, G. Rizza, Surface roughness characterisation and analysis of the

Electron Beam Melting (EBM) process, Materials (Basel). 12 (2019). https://doi.org/10.3390/ma12132211.

[54] A. Safdar, H.Z. He, L.Y. Wei, A. Snis, L.E. Chavez De Paz, Effect of process parameters settings and thickness on surface roughness of EBM produced Ti-6Al-4V, Rapid Prototyp. J. 18 (2012) 401–408. https://doi.org/10.1108/13552541211250391.

[55] W. Everhart, E. Sawyer, T. Neidt, J. Dinardo, B. Brown, The effect of surface finish on tensile behavior of additively manufactured tensile bars, J. Mater. Sci. 51 (2016) 3836–3845. https://doi.org/10.1007/s10853-015-9702-9.

[56] I. Gibson, D. Rosen, Stucker, Additive Manufacturing Technologies, Second Edi, Springer New York, NY, 2015. https://doi.org/10.1007/978-1-4939-2113-3.

[57] R.K. Leach, D. Bourell, S. Carmignato, A. Donmez, N. Senin, W. Dewulf, Geometrical metrology for metal additive manufacturing, CIRP Ann. Technol. 68 (2019) 677–700. https://doi.org/10.1016/j.cirp.2019.05.004.

[58] C. Körner, A. Bauereiß, E. Attar, Fundamental consolidation mechanisms during selective beam melting of powders, Model. Simul. Mater. Sci. Eng. 21 (2013). https://doi.org/10.1088/0965-0393/21/8/085011.

[59] P. Lhuissier, C. de Formanoir, G. Martin, R. Dendievel, S. Godet, Geometrical control of lattice structures produced by EBM through chemical etching: Investigations at the scale of individual struts, Mater. \& Des. 110 (2016) 485–493. https://doi.org/10.1016/j.matdes.2016.08.029.

[60] M. Suard, G. Martin, P. Lhuissier, R. Dendievel, F. Vignat, J.J. Blandin, F. Villeneuve, Mechanical equivalent diameter of single struts for the stiffness prediction of lattice structures produced by Electron Beam Melting, Addit. Manuf. 8 (2015) 124–131. https://doi.org/10.1016/j.addma.2015.10.002.

[61] N. Sanaei, A. Fatemi, Defects in additive manufactured metals and their effect on fatigue performance: A state-of-the-art review, Prog. Mater. Sci. 117 (2021) 100724. https://doi.org/10.1016/j.pmatsci.2020.100724.

[62] S. Shrestha, Y.K. Chou, Process effect on part surface roughness in powder-bed electron beam additive manufacturing, ASME 2017 12th Int. Manuf. Sci. Eng. Conf. MSEC 2017 Collocated with JSME/ASME 2017 6th Int. Conf. Mater. Process. 2 (2017). https://doi.org/10.1115/MSEC2017-3015.

[63] U. Prisco, A. Astarita, A. El Hassanin, S. Franchitti, Influence of processing parameters on microstructure and roughness of electron beam melted Ti-6Al-4V titanium alloy, Mater. Manuf. Process. 34 (2019) 1753–1760. https://doi.org/10.1080/10426914.2019.1683576.

[64] A.T. Silvestri, S. Foglia, R. Borrelli, S. Franchitti, C. Pirozzi, A. Astarita, Electron beam melting of Ti6Al4V: Role of the process parameters under the same energy density, J. Manuf. Process. 60 (2020) 162–179. https://doi.org/10.1016/j.jmapro.2020.10.065.

[65] T. Scharowsky, A. Bauereiss, C. Koerner, Influence of the hatching strategy on consolidation during selective electron beam melting of Ti-6Al-4V, Int. J. Adv. Manuf. Technol. 92 (2017) 2809–2818. https://doi.org/10.1007/s00170-017-0375-1.

[66] R.K. Ek, L.-E. Rannar, M. Backstom, P. Carlsson, The effect of EBM process parameters upon surface roughness, RAPID Prototyp. J. 22 (2016) 495–503. https://doi.org/10.1108/RPJ-10-2013-0102.

[67] R. Borrelli, S. Franchitti, C. Pirozzi, L. Carrino, L. Nele, W. Polini, L. Sorrentino, A. Corrado, Ti6Al4V Parts Produced by Electron Beam Melting: Analysis of Dimensional Accuracy and Surface Roughness, J. Adv. Manuf. Syst. 19 (2020) 107–130. https://doi.org/10.1142/S0219686720500067.

[68] M. Galati, A. Snis, L. Iuliano, Experimental validation of a numerical thermal model of the EBM process for Ti6Al4V, Comput. Math. with Appl. 78 (2019) 2417–2427. https://doi.org/10.1016/j.camwa.2018.07.020.

[69] D. Kotzem, A. Höffgen, R. Raveendran, F. Stern, K. Möhring, F. Walther, Position-dependent mechanical characterization of the PBF-EB-manufactured Ti6Al4V alloy, Prog. Addit. Manuf. (2021). https://doi.org/10.1007/s40964-021-00228-9.

[70] M. Jamshidinia, R. Kovacevic, The influence of heat accumulation on the surface roughness in powder-bed additive manufacturing, Surf. Topogr. Metrol. Prop. 3 (2015). https://doi.org/10.1088/2051-672X/3/1/014003.

[71] X. Tan, Y. Kok, Y.J. Tan, G. Vastola, Q.X. Pei, G. Zhang, Y.-W. Zhang, S.B. Tor, K.F. Leong, C.K. Chua, An experimental and simulation study on build thickness dependent microstructure for electron beam melted Ti-6Al-4V, J. Alloys Compd. 646 (2015) 303–309. https://doi.org/10.1016/j.jallcom.2015.05.178.

[72] W.Q. Toh, P. Wang, X. Tan, M.L.S. Nai, E. Liu, S.B. Tor, Microstructure and Wear Properties of Electron Beam Melted Ti-6Al-4V Parts: A Comparison Study against As-Cast Form, Metals (Basel). 6 (2016). https://doi.org/10.3390/met6110284.

[73] Y.H. Kok, X.P. Tan, N.H. Loh, S.B. Tor, C.K. Chua, Geometry dependence of microstructure and microhardness for selective electron beam-melted Ti-6Al-4V parts, VIRTUAL Phys. Prototyp. 11 (2016) 183–191. https://doi.org/10.1080/17452759.2016.1210483.

[74] B. Brown, W. Everhart, J. Dinardo, Characterization of bulk to thin wall mechanical response transition in powder bed AM, Rapid Prototyp. J. 22 (2016) 801–809. https://doi.org/10.1108/RPJ-10-2015-0146.

[75] R. Sepe, S. Franchitti, R. Borrelli, F. Di Caprio, E. Armentani, F. Caputo, Correlation between real geometry and tensile mechanical behaviour for Ti6Al4V electron beam

melted thin specimens, Theor. Appl. Fract. Mech. 107 (2020). https://doi.org/10.1016/j.tafmec.2020.102519.

[76] J.K. Algardh, T. Horn, H. West, R. Aman, A. Snis, H. Engqvist, J. Lausmaa, O. Harrysson, Thickness dependency of mechanical properties for thin-walled titanium parts manufactured by Electron Beam Melting (EBM) ®, Addit. Manuf. 12 (2016) 45–50. https://doi.org/10.1016/j.addma.2016.06.009.

[77] S.M.J. Razavi, B. Van Hooreweder, F. Berto, Effect of build thickness and geometry on quasi-static and fatigue behavior of Ti-6Al-4V produced by Electron Beam Melting, Addit. Manuf. 36 (2020) 101426. https://doi.org/10.1016/j.addma.2020.101426.

[78] M. Segersäll, A. Kerwin, A. Hardaker, M. Kahlin, J. Moverare, Fatigue response dependence of thickness measurement methods for additively manufactured E-PBF Ti-6Al-4 V, Fatigue Fract. Eng. Mater. Struct. 44 (2021) 1931–1943. https://doi.org/10.1111/ffe.13461.

[79] W.J. Sames, F.A. List, S. Pannala, R.R. Dehoff, S.S. Babu, The metallurgy and processing science of metal additive manufacturing, Int. Mater. Rev. 61 (2016) 315–360. https://doi.org/10.1080/09506608.2015.1116649.

[80] ABNT NBR ISO 4288:2008 Geometrical Product Specifications (GPS) — Surface texture: Profile method — Rules and procedures for the assessment of surface texture. Associação Brasileira de Normas Técnicas (ABNT) and International Organization for Standardization ISO, 2008.

[81] ISO/ASTM 52902:2019 Additive manufacturing - Test artifacts - Geometric capability assessment of additive manufacturing systems, ASTM and International Organization for Standardization ISO, 2019.

[82] A. Townsend, N. Senin, L. Blunt, R.K. Leach, J.S. Taylor, Surface texture metrology for metal additive manufacturing: a review, Precis. Eng. 46 (2016) 34–47.

https://doi.org/10.1016/j.precisioneng.2016.06.001.

[83] S. Roos, C. Botero, J. Danvind, A. Koptioug, L.-E. Rännar, Macro- and Micromechanical Behavior of 316LN Lattice Structures Manufactured by Electron Beam Melting, J. Mater. Eng. Perform. 28 (2019) 7290–7301. https://doi.org/10.1007/s11665-019-04484-3.

[84] C. Guo, W. Ge, F. Lin, Effects of scanning parameters on material deposition during Electron Beam Selective Melting of Ti-6Al-4V powder, J. Mater. Process. Technol. 217 (2015) 148–157. https://doi.org/10.1016/j.jmatprotec.2014.11.010.

[85] S. Evsevleev, T. Mishurova, D. Khrapov, A. Paveleva, D. Meinel, R. Surmenev, M. Surmeneva, A. Koptyug, G. Bruno, X-ray computed tomography procedures to quantitatively characterize the morphological features of triply periodic minimal surface structures, Materials (Basel). 14 (2021). https://doi.org/10.3390/ma14113002.

[86] J.C. Snyder, K.A. Thole, Understanding Laser Powder Bed Fusion Surface Roughness, J. Manuf. Sci. Eng. ASME. 142 (2020). https://doi.org/10.1115/1.4046504.

3 DISCUSSÃO

Os resultados deste estudo podem ser relacionados com cada um dos objetivos específicos definidos, que por sua vez estão vinculados com cada um dos três artigos elaborados. O primeiro artigo, intitulado “*Defects in Electron Beam Melting: a bibliometric analysis*”, atende ao primeiro objetivo específicos, enquanto o segundo (“*A review on the influence of process variables on the surface roughness of Ti-6Al-4V by electron beam powder bed fusion*”) cumpre o segundo objetivo específico. Da mesma forma, o terceiro artigo submetido a publicação (“*The effects of varying build thickness on the surface roughness of Ti-6Al-4V by electron beam powder bed fusion*”) atende ao terceiro e último objetivo específico.

Os resultados obtidos pelo primeiro artigo revelam a relevância do tema da qualidade no processo de fusão em leito de pó por feixe de elétrons visto o aumento do número de publicações no tema nos últimos 10 anos. Conforme apontado pelo estudo, esse aumento parece acompanhar o de gastos relacionados a fabricação de peças de uso final por processos de manufatura aditiva. A análise das palavras-chave das publicações no tema também indica que o tópico da rugosidade superficial possui um foco maior até do que o da porosidade, principalmente quando associado aos seus efeitos na vida em fadiga. A liga Ti-6Al-4V também se mostrou o material prevalente em estudos no tema de qualidade de peças produzidas por EB-PBF. Com isso, pode-se dizer que a motivação deste trabalho é válida considerando o grande interesse da comunidade acadêmica na rugosidade superficial e nessa liga, além do fato de que o tema de mitigação e controle de rugosidade através de variáveis de processo estar muito presente nos estudos com maior número de citações.

A revisão sistemática da literatura apresentada no segundo artigo do Capítulo 2 também se mostrou de grande utilidade no contexto deste trabalho. Os resultados obtidos nessa etapa foram cruciais para o desenvolvimento e planejamento do experimento, de forma a excluir ao máximo qualquer interferência de outros fatores na rugosidade superficial que não fosse relativa àquela da espessura de parede. Apenas considerando-se todas as variáveis de processo que afetam a qualidade superficial em EB-PBF foi possível obter resultados inéditos e com significância estatística na etapa experimental deste trabalho. A revisão da bibliografia também revelou as dificuldades em se comparar pesquisas e resultados de artigos nessa área devido a forma como eles são reportados em suas publicações. Esse artigo por si só já contribui para a área de conhecimento ao fazer recomendações de normas técnicas a qual pesquisadores devem seguir caso queriam que seus resultados contribuam ainda mais para o avanço da pesquisa na área.

A pesquisa experimental foi bem-sucedida em verificar a relação entre espessura de parede e a rugosidade superficial de Ti-6Al-4V por EB-PBF, e por isso pode-se dizer que o presente trabalho contribui tanto para o maior entendimento do processo com feixe de elétrons como forma bases para que estudos mais aprofundados no tema sejam realizados. O fato de ter se verificado uma relação entre a espessura e a rugosidade deve ser notado por pesquisadores da área a fim de que seja considerado em experimentos futuros. Mesmo com as limitações deste estudo – as geometrias simples dos corpos-de-prova e a medição de rugosidade por um equipamento táctil – foi possível verificar comportamentos inéditos no quesito de espessura e rugosidade superficial. Embora esse trabalho tivesse como escopo apenas a verificação da relação entre as variáveis, o uso de outras tecnologias de medição de superfícies pode se mostrar útil para entendimento mais aprofundados dos resultados aqui observados. Nesse contexto, o uso de modelos e simulações matemáticas também deve contribuir na compreensão dos mecanismos que levaram aos comportamos aqui observados.

4 CONCLUSÃO

A questão da qualidade superficial em processos de fusão em leito de pó metálico possui um papel importantíssimo devido aos efeitos na performance mecânica e em quesitos biomédicos. Os resultados obtidos neste trabalho contribuem para a maior compreensão do processo com feixe de elétrons ao suprir uma lacuna de pesquisa e evidenciar comportamentos inéditos entre a espessura de parede e rugosidade superficial da liga Ti-6Al-4V. Uma análise bibliométrica para validação da motivação do estudo e da escolha da liga foi realizada, enquanto a revisão sistemática da bibliografia permitiu o que o experimento para investigação dos efeitos da espessura de parede na rugosidade superficial fosse bem-sucedido e reportado de forma a contribuir com trabalhos futuros.

Tanto os resultados já publicados na revisão bibliográfica como aqueles obtidos na etapa experimental deste trabalho são pertinentes para o desenvolvimento de futuras pesquisas na área. O primeiro condensa grande parte da literatura no tema e propõe recomendações de normas internacionais para a medição, caracterização, e publicação de resultados, enquanto a pesquisa experimental evidencia uma relação que deverá ser explorada com maior profundidade e considerada em planejamentos experimental no tema.

Trabalhos futuros podem focar tanto no entendimento aprofundado dos comportamentos observados neste trabalho, como também avaliar se tais comportamentos também são vistos em espécimes com formas curvilíneas ou geometrias intricadas. Também pode ser explorada se a variação do ângulo de inclinação dos corpos-de-prova influenciaria na forma pela qual a espessura afeta a rugosidade.

REFERÊNCIAS

ASSOCIAÇÃO BRASILEIRA DE NORMAS TÉCNICAS. **ABNT NBR ISO 4288:2008** Especificações geométricas de produto (GPS) - Rugosidade: Método do perfil - Regras e procedimentos para avaliação de rugosidade, 2008.

GE ADDITIVE. **Additive at Scale: Avio Aero Flies Into the Future**. Disponível em: https://www.ge.com/additive/stories/additive-at-scale-avio-aero. Acesso em: 4 out. 2022.

BAE, Chang-Jun; DIGGS, Alisha B; RAMACHANDRAN, Arathi. **Quantification and certification of additive manufacturing materials and processes**. Butterworth-Heinemann, 2018. *E-book*. Disponível em: https://doi.org/10.1016/B978-0-12-812155-9.00006-2.

BAGHERIFARD, Sara; GUAGLIANO, Mario. 12 - Post-processing, In **Additive Manufacturing Materials and Technologies, Fundamentals of Laser Powder Bed Fusion of Metals**, Elsevier, 2021, p. 327-348, *E-book*. Disponível em: http://dx.doi.org/10.1016/B978-0-12-824090-8.00001-9.

BEN-NER, Avner; SIEMSEN, Enno. Decentralization and Localization of Production: The Organizational and Economic Consequences of Additive Manufacturing (3D Printing). **California Management Review**, v.59, n.2, p. 5–23, 2017. Disponível em https://journals.sagepub.com/doi/10.1177/0008125617695284.

DIEGEL, Olaf; NORDIN, Axel; DAMIEN, Motte. Additive Manufacturing Technologies. In: **A Practical Guide to Design for Additive Manufacturing. Springer Series in Advanced Manufacturing**. Springer, Singapore. 2019. *E-book*. Disponível em: https://doi.org/10.1007/978-981-13-8281-9_2.

GIBSON, Ian; ROSEN, David; STUCKER. **Additive Manufacturing Technologies**. Second Edition, Springer New York, NY, 2015. *E-book*. Disponível em: https://doi.org/10.1007/978-1-4939-2113-3.

GIL, Antonio Carlos. **Como elaborar projetos de pesquisa**. 5. ed. São Paulo, Atlas, 2017.

HUBS. **Additive Manufacturing Trend Report – 2021**. p. 1–16, 2021. Disponível em: https://f.hubspotusercontent10.net/hubfs/4075618/Additive manufacturing trend report 2021.pdf?utm_campaign=Gated Content Downloads&utm_medium=email&_hsmi=82605589&_hsenc=p2ANqtz-

9pM5X9Hu5jL_49jLKLdBARaGb5PVPhM3kYwzk2c36z2bmdpMZRLJiSd4n5ZKSZOJoCbPnSwFXfi64.

INTERNATIONAL ORGANIZATION FOR STANDARIZATION. **ISO/ASTM 52900:2015** Additive Manufacturing - General Principles - Terminology, 2015.

JARDINI, André Luiz; LAROSA, Maria Aparecida; LONGHITANO, Guilherme Arthur; BINELLI, Aulus Roberto Romão; ZAVAGLIA, Cecília Amélia de Carvalho; SILVA, Jorge Vicente Lopes. Processos de AM por fusão de leito de pó metálico. *Em*: **MANUFATURA ADITIVIA**, Blucher, São Paulo, 2017. p. 247–269.

MOLITCH-HOU, Michael. Overview of additive manufacturing process. *In*: **Additive Manufacturing**, Butterworth-Heinemann, 2018. p. 1–38. *E-book*. Disponível em: https://doi.org/10.1016/B978-0-12-812155-9.00001-3.

REEVES, Phil; TUCK, Chris; HAGUE, Richard. Additive Manufacturing for Mass Customization. *In*: **Mass Customization**. Springer, London, 2011. p. 275–289. *E-book*. Disponível em: https://doi.org/10.1007/978-1-84996-489-0_13.

SAUERWEIN, Marita; DOUBROVSKI, Eugeni; BALKENENDE, Ruud; BAKKER, Conny. Exploring the potential of additive manufacturing for product design in a circular economy. **Journal of Cleaner Production**, v.226, p. 1138–1149, 2019. Disponível em: https://doi.org/10.1016/j.jclepro.2019.04.108.

SAMES, W.J.; LIST, F.A.; PANNALA, S.; DEHOFF, R.R.; BABU, S.S. The metallurgy and processing science of metal additive manufacturing, Int. **Mater. Rev. 61** (2016) 315–360. Disponível em: https://doi.org/10.1080/09506608.2015.1116649.

VANMEENSEL, Kim; LIETAERT, Karel; VRANCKEN, Bey; DADBAKHSH, Sasan; LI, Xiaopeng; KRUTH, Jean-Pierre; KRAKHMALEV, Pavel; YADROITSEV, Igor; HUMBEECK, Jan Van. **Additively manufactured metals for medical applications**. Elsevier Inc., 2018. *E-book*. Disponível em: http://dx.doi.org/10.1016/B978-0-12-812155-9/00008-6.

WAKEFIELD, Edward. **General Motors 3D prints 60,000 seals in five weeks using HP printers**, 2022. Disponível em: https://www.3dprintingmedia.network/general-motors-prints-60000-seals-in-five-weeks-using-hp-printers/.

WOHLERS ASSOCIATES. **Wohlers Report 2021**. Disponível em: https://wohlersassociates.com/product/wohlers-report-2021/

ANEXO A – AUTORIZAÇÃO DE USO DOS ARTIGOS PUBLICADOS

Abaixo são apresentadas as autorizações para que os artigos já publicados fossem apresentados nesse trabalho e o comprovante de submissão do artigo. O primeiro artigo possui autorização explicita da comissão organizadora do Congresso Brasileiro de Manufatura Aditiva. O segundo artigo, publicado na revista *Additive Manufacturing*, segue as regras gerais para reprodução da editora Elsevier. Os termos de copyright da editora garantem aos autores a reprodução do conteúdo em teses e dissertações acadêmicas contanto que não tenham fins comerciais. A Elsevier também garante à instituição (UNICAMP) a publicação de dissertações que contenham manuscritos e artigos por ela publicada contanto que sejam explicitados os links (DOI) para a publicação da editora. Por fim, a última imagem traz uma captura de tela da plataforma da revista Additive Manufacturing com o título e data da submissão do artigo em questão.

CONGRESSE.ME

Declaração - Congresso Brasileiro De Manufatura Aditiva CBMADI

Em nome da comissão organizadora do Congresso Brasileiro De Manufatura Aditiva CBMADI 1ª edição - realizado no período de 30/11/2020 a 01/12/2020, autorizo, para os devidos fins, o uso do artigo intitulado "DEFECTS IN ELECTRON BEAM MELTING: A BIBLIOMETRIC ANALYSIS", autoria de CAROLO; Lucas de Campos , ORDOÑEZ; Robert Eduardo Cooper, publicado nos Anais do evento acima citado.

Disponível https://eventos.congresse.me/cbmadi/resumos/7595.pdf?version=original

Sem mais para o momento,

Macaé/RJ, 29 de setembro de 2022.

Luiz Gustavo Borges
CEO Congresse.me

Author rights in Elsevier's proprietary journals	Published open access	Published subscription
Retain patent and trademark rights	√	√
Retain the rights to use their research data freely without any restriction	√	√
Receive proper attribution and credit for their published work	√	√
Re-use their own material in new works without permission or payment (with full acknowledgement of the original article): 1. Extend an article to book length 2. Include an article in a subsequent compilation of their own work 3. Re-use portions, excerpts, and their own figures or tables in other works.	√	√
Use and share their works for scholarly purposes (with full acknowledgement of the original article): 1. In their own classroom teaching. Electronic and physical distribution of copies is permitted 2. If an author is speaking at a conference, they can present the article and distribute copies to the attendees 3. Distribute the article, including by email, to their students and to research colleagues who they know for their personal use 4. Share and publicize the article via Share Links, which offers 50 days' free access for anyone, without signup or registration 5. Include in a thesis or dissertation (provided this is not published commercially) 6. Share copies of their article privately as part of an invitation-only work group on commercial sites with which the publisher has a hosting agreement	√	√
Publicly share the preprint on any website or repository at any time.	√	√

Disponível em: https://www.elsevier.com/about/policies/copyright. Acessado em 06/10/2022.

Institution rights

Regardless of how the author chooses to publish with Elsevier, their institution has the right to use articles for classroom teaching and internal training. Articles can be used for these purposes throughout the author's institution, not just by the author:

Institution rights in Elsevier's proprietary journals (providing full acknowledgement of the original article is given)	**All articles**
Copies can be distributed electronically as well as in physical form for classroom teaching and internal training purposes	√
Material can be included in coursework and courseware programs for use within the institution (but not in Massive Open Online Courses)	√
Articles can be included in applications for grant funding	√
Theses and dissertations which contain embedded final published articles as part of the formal submission can be posted publicly by the awarding institution with DOI links back to the formal publication on ScienceDirect	√

Disponível em: https://www.elsevier.com/about/policies/copyright. Acessado em 06/10/2022.

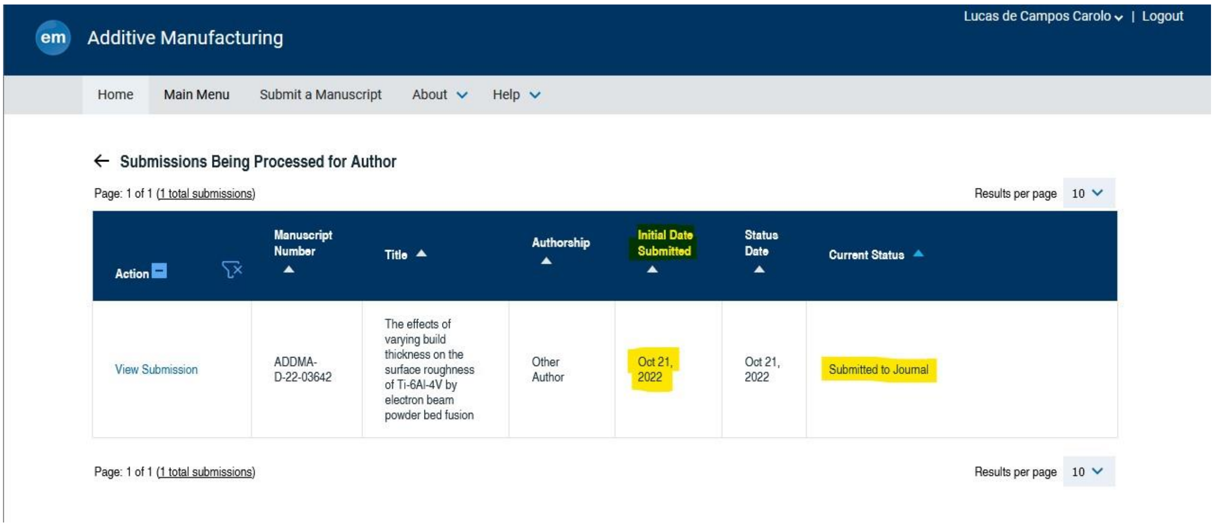

Captura de tela da plataforma da revista *Additive Manufacturing* com a data de submissão formal do artigo intitulado "*The effects of varying build thickness on the surface roughness of Ti-6Al-4V by electron beam powder bed fusion*".